17 0563

no: 3741

Promotor: Prof. Dr. Ir. R.M.Boom
Hoogleraar levensmiddelenproceskunde, Wageningen Universiteit

Copromotor: Dr.Ir. A.J. van der Goot
Universitair docent, sectie proceskunde, Wageningen Universiteit

Promotiecommissie: Prof. Dr. Ir J. Tramper
Wageningen Universiteit

Prof. Dr.Ir. F Voragen
Wageningen Universiteit

Prof. Dr. Ir. L.P.B.M.Janssen
Rijks Universiteit Groningen

Dr.Ir. J.W.G. DeMeester
Cerestar

Towards Intensification of Starch Processing

Mark van der Veen

17

Mark van der Veen

Towards Intensification of Starch Processing

Proefschrift
Ter verkrijging van de graad van doctor
op gezag van de rector magnificus
van Wageningen Universiteit,
Prof. Dr. Ir.L.Speelman
In het openbaar te verdedigen
op dinsdag 3 mei 2005
des namiddags te vier uur in de aula.

Propositions

1. Inactivation of the micro-organisms by means of selective heating using microwave technology is unlikely to occur
   (Chapter 2 of this thesis)

2. Shear forces should be regarded as process design parameter
   (Chapter5 of this thesis)

3. Process development, based on existing unit-operations never results in radical process innovations

4. Energy can be classified as 'green', when the exergy of the total process lower is than efficiently generated with fossil fuels

5. The fact that journals actively ask for a list of potential reviewers with submission of papers, can potentially lead to a less critical review climate

6. Justice and the feeling of justice contravene in some cases

7. If anybody wants to keep creating they have to be about change
   (Miles Davis, Birth of the Cool)

Propositions belonging to the thesis:
Towards Intensification of Starch Processing

Mark van der Veen
3 May 2005

Stellingen

1. Inactivering van micro-organismen door middel van selectieve verwarming met behulp van magnetron technologie is onwaarschijnlijk
   (Hoofdstuk 2 van dit proefschrift)

2. Afschuifkrachten zouden beschouwd moeten worden als ontwerp-parameter
   (Hoofdstuk 5 van dit proefschrift)

3. Procesontwikkeling, gebaseerd op bestaande unit-operaties zal nooit tot radicale procesinnovaties leiden.

4. Energie zou slechts geclassificeerd moeten worden als 'groen', wanneer de exergie van het totale opwekkingsproces lager is dan van efficiënte opwekking uit fossiele brandstoffen.

5. Het feit dat wetenschappelijke tijdschriften de auteurs actief vragen voor potentiële reviewers van het artikel, zou kunnen leiden tot de ontwikkeling van een minder kritisch review-klimaat

6. Recht en het gevoel voor rechtvaardigheid staan soms lijnrecht tegenover elkaar

7. Als iemand iets wil creëren, moet men open staan voor veranderingen
   (Miles Davis, Birth of the Cool)

Stellingen behorende bij het proefschrift:
Towards Intensification of Starch Processing

Mark van der Veen
3 mei 2005

Stellingen

1. Inactivering van micro-organismen door middel van selectieve verwarming met behulp van magnetron technologie is onwaarschijnlijk
   (Hoofdstuk 2 van dit proefschrift)

2. Afschuifkrachten zouden beschouwd moeten worden als ontwerp-parameter
   (Hoofdstuk 5 van dit proefschrift)

3. Procesontwikkeling, gebaseerd op bestaande unit-operaties zal nooit tot radicale procesinnovaties leiden.

4. Energie zou slechts geclassificeerd moeten worden als 'groen', wanneer de exergie van het totale opwekkingsproces lager is dan van efficiënte opwekking uit fossiele brandstoffen.

5. Het feit dat wetenschappelijke tijdschriften de auteurs actief vragen voor potentiële reviewers van het artikel, zou kunnen leiden tot de ontwikkeling van een minder kritisch review-klimaat

6. Recht en het gevoel voor rechtvaardigheid staan soms lijnrecht tegenover elkaar

7. Als iemand iets wil creëren, moet men open staan voor veranderingen
   (Miles Davis, Birth of the Cool)

Stellingen behorende bij het proefschrift:
Towards Intensification of Starch Processing

Mark van der Veen
3 mei 2005

Propositions

1. Inactivation of the micro-organisms by means of selective heating using microwave technology is unlikely to occur
   (Chapter 2 of this thesis)

2. Shear forces should be regarded as process design parameter
   (Chapter5 of this thesis)

3. Process development, based on existing unit-operations never results in radical process innovations

4. Energy can be classified as 'green', when the exergy of the total process lower is than efficiently generated with fossil fuels

5. The fact that journals actively ask for a list of potential reviewers with submission of papers, can potentially lead to a less critical review climate

6. Justice and the feeling of justice contravene in some cases

7. If anybody wants to keep creating they have to be about change
   (Miles Davis, Birth of the Cool)

Abstract

Towards Process Intensification of Starch Processing, Mark van der Veen
PhD Thesis, Wageningen University, The Netherlands, 2005

This thesis covers two topics, both aimed at improving process efficiency and product quality in starch processing.

The first topic covers the potential of microwave heating as means for mild preservation of heterogeneous food media. It has been postulated that if micro-organisms are present in domains that contain more moisture, it should be possible to selectively heat those areas and thus achieve the microbial inactivation with a lower overall thermal load onto the product. This concept of selective heating was investigated by an analysis of the dissipation of microwave energy and heat transfer phenomena in heterogeneous systems. The results presented in this thesis indicate that for domains sizes of millimetres or larger, temperature differences >10K can be established. For smaller domains, large temperature differences are not possible with currently available microwave technology.

The second topic focussed starch hydrolysis under low water conditions, with emphasis on the liquefaction and saccharification process steps. The results presented in this thesis showed that it is possible to hydrolyse starch in conditions of up to 65% dry matter. Two conceptual process designs were developed to liquefy starch in conditions with maximally 60% dry matter (single stage process) and higher dry solid conditions (two stage process) by means of a thermo-mechanical treatment. The effects of shear forces on α–amylase was measured and could be quantitatively described with a relative simple model, incorporating the effect of time, temperature and shear stress. Furthermore, it was reported that saccharification with glucoamylase is possible at very high dry matter concentrations, while hardly any additional inhibition of the enzyme was observed under those conditions. The rate of reaction was found to decrease with increasing dry matter concentration. Simulations showed that at conditions with 70% dry matter initially, still a product of 90 DE could be produced.

The results were concluded in a process model showing that increasing the dry matter concentration of 35% to 65% resulted in a decrease in water consumption of 87% for a given glucose production, while the reactor productivity was calculated to increase with 17%. Although several aspects have to be studied in more detail before successful implementation of the process, the study reported here reveals that there is clear potential for making the production of glucose from starch more efficient in terms of energy and water consumption.

Contents

1 Introduction

1. Starch Hydrolysis

1.1 Starch

Starch is the main carbohydrate energy storage in almost all green plants and as such is an important component in the human diet. The majority of the starch is isolated at industrial scale and used as raw material in the food, paper, textile and other industries [1]. Worldwide, the main sources of starch are corn, wheat, potato and cassava (from which tapioca is derived), from which corn makes up to 80% of the global annual production (see figure 1.1) [2]. More than 60% of corn starch is produced in the United States (US). Wheat and potato starch are mainly produced in the European Union, while tapioca is mainly produced in Asia. The global annual starch production is about 48.5 million tons (in 2000). The global starch demand is expected to grow with 50% from 2000 to 2010. Approximately 44% of the starch production is used as native starch, 15% is modified (chemically/physically) and 41% is used for starch hydrolysates. Native and modified starch products are widely used in food-processing and paper industry (see table 1.1). In the food industry, native starch is used in products for structuring purposes, e.g. such as crisps and chips. A significant part of starch is modified, to broaden the range of applications of starch. In these modifications, the starch is partly gelatinised, hydrolysed or functional groups are added. Most of these modifications improve the swelling solubility of starch, which makes them suitable as thickening or structuring agents. Starch can be modified mechanically, chemically or enzymatically. Mechanically and chemically modified starches are applied in the food industry and are commonly used in the paper and adhesives industry as well. Another class of modification reactions is hydrolysis, in which the long chains are broken into small chains, called maltodextrins, or even completely hydrolysed into glucose and maltose or fructose. These products are widely used as sweeteners in beverages, candy and bakery products or as feedstock for fermentation processes. In the US, more than 85% of the starch is hydrolyzed (see figure 1.2). The main products are high fructose syrups (applied in the beverages

industry) and feedstock for bio-ethanol production. In 2000, more than 40% of the starch in the EU was hydrolysed, mainly for glucose syrups (beverage industry). Bio-ethanol has been recognized as 'green fuel' for cars in the EU and will replace a part of the fossil fuel in the near future. The market share of starch hydrolysates will therefore grow rapidly, to satisfy the rapid growing demand for bio-ethanol.
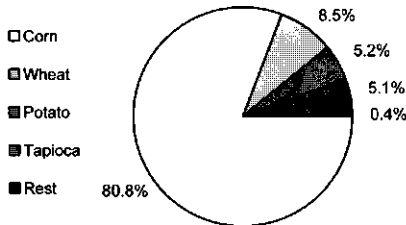

Figure 1.1: Global annual production of starch per crop in 2000 (source: LMC international Ltd (2002)) [2]
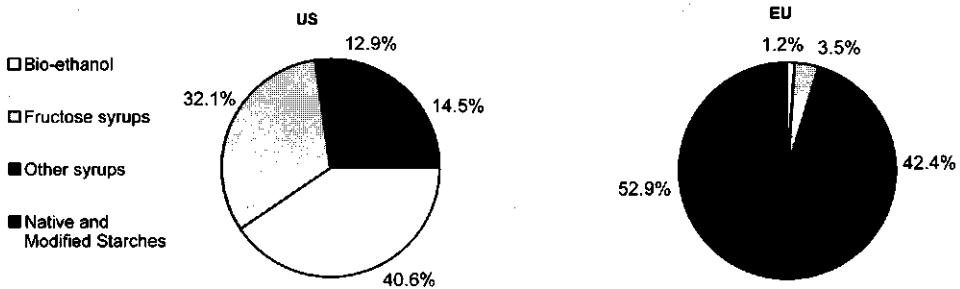

Figure 1.2: Production of starch products in the United States and European Union in 2000 (source: LMC international Ltd (2002)) [2]

Starch consists of small granular particles of in the range of 10 μm (corn) to 40 μm (potato). These granules swell, but do not dissolve in water [3]. Starch consists of 2 polymers, amylose and amylopectin. Amylose is a linear polymer of glucose, with a degree of polymerization (DP) of a few hundred to 10^4 glucose units, which are linked via α-1,4 glucosidic bonds. The molecular weight of amylose is typically 10^4 to 10^6 Da. Amylopectin is a molecule that consists of short linear glucosidic chains comprising 10 to 60 glucose units (average 22), which are linked by α-1,4 bonds (see figure 1.3). These short chains are connected through α-1,6 bonds, leading to an overall highly branched structure. Amylopectin typically contains about 10^6 glucose units, resulting in a molecular weight of 10^8 Da. Corn and wheat starch contain about 25% amylose and 75% amylopectin[1].
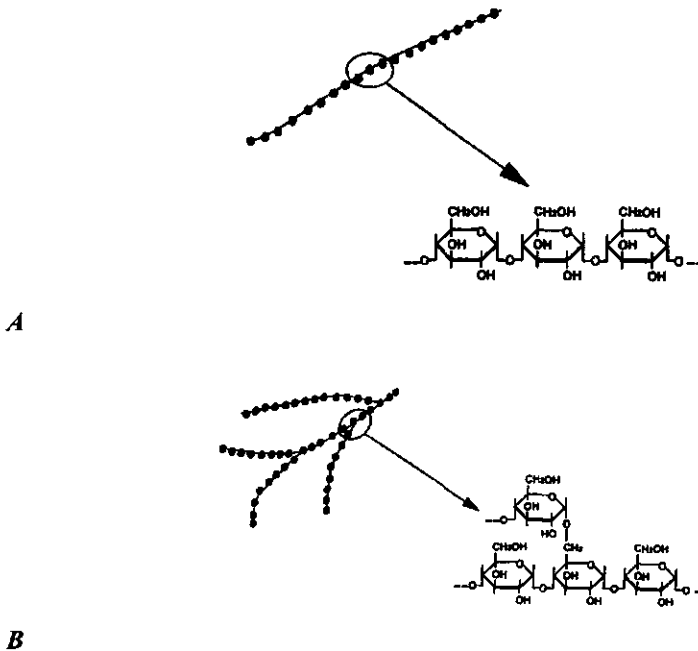
A

B

Figuur1.3: Schematic picture of a linear amylose molecule with α-1-4 linkages (A) and a branched amylopectin molecule with α-1,4 and α-1,6 linkages (B) (Source: Cargill Internal Report)

1.2 Starch hydrolysates

Starch hydrolysis is carried out in the presence of a catalyst [4]. Initially, hydrochloric acid was used as catalyst and this was commercialized in the late 19th century. Acidified starch slurry was heated to 140-160 °C for 15 to 20 minutes, yielding a product with a dextrose equivalent (DE) of 42-45 (which is equivalent do a degree of polymerisation of approximately 2.5) [5]. Hydrolysis catalysed by acid takes place randomly, leading to a complex mixture [6]. Although the process is fast and the product mixture obtained can be quite reproducible, it is difficult to influence its composition. This, combined with a relatively low yield and high levels of impurities that are obtained, made the acid catalysed process less than ideal.

Table 1.1: overview of starch properties and their application

Starch	Way of production	Reason for application	Application
Native	Isolation from various crops, tubes and cereals, e.g. corn, wheat, potato, cassava	Solid, high-calorie raw material, High viscosity	Structuring purposes (e.g. snacks/crisps) Adhesives (e.g. corrugated board) Thickening agents
Modified			
- Pre-gelatinisation	Dry heating	Improved cold water dispersibility	Adhesives (e.g. paper industry)
- Partial hydrolysis	Partial hydrolysis (catalysed by acid)	Reduced viscosity (rel. to native starch)	Binders (e.g. confectionary)
- Cross-linking	Cross linking	Modified cooking properties	Thickening agents (e.g. Soups/Sauces/Desserts/Bakery products)
- Introduction of functional groups	Esterification / Etherification	Improved viscosity stability	
Hydrolysates	Catalysed by Acid	Structurant	Maltodextrins (e.g. filler in food products/ sweetness reducer)
	Acid / Enzyme catalysed Enzyme / Enzyme catalysed	Sweet taste	Sweeteners (low MW sugars) Beverages/ bakery products/ Candy
		Nutrient for micro-organisms	Feed stock for fermentation
	Enzymatic	Isomerised into mixtures of isomers	Fructose (e.g. Beverages)

The yield of the hydrolysis process and the quality of the product was improved by the introduction of enzymes as catalyst [7]. Initially, fungal α-amylase and bacterial glucoamylase were used as an additional treatment (saccharification) to the acid hydrolyzed starch, resulting in a purer product with a DE of maximally 65 (equivalent to a degree of polymerisation (DP) of approximately 1.5), combined with higher yield. The main step forward was the introduction of thermo-stable α-amylase, which replaced hydrochloric acid as liquefying catalyst [7]. Combination of this liquefaction step with the former process of saccharification led to the enzyme/enzyme process. With this technology, products could be made with a DE of up to 95 (DP approximately 1.05), with high purity and high yields. Due to the further development of saccharification enzymes, it is possible to control the product composition over a broad range of products, through the right choice of enzyme blends and processing conditions [8]. In industry, both the acid / enzyme and enzyme / enzyme routes are still used today [7].

A variety of enzymes is used to produce starch hydrolysates with different sugar compositions (see table 1.2) [8]. Industrially applied liquefying enzymes are thermo-stable endo-acting α-amylases from bacterial origin. These enzymes randomly hydrolyze α-1,4 bonds in the amylose and amylopectin chains. This reduces the polymer chain length efficiently, which leads to a rapid decrease in viscosity and prevents retrogradation [4]. Typically, the DE of a liquefied starch is 8-15 DE (equivalent to an average chain length of 7 to 14 glucose units). For the saccharification reaction, a variety of enzymes is used, depending on the desired sugar profile of the product [4]. Fungal α-amylase is used to produce maltose and high-conversion (high DE) syrups. β–Amylases are exo-hydrolases and cleave α-1,4 linkages from the non-reducing end of the starch polymers to produce β-maltose. High glucose syrups are produced using glucoamylase [9], which is an exo-hydrolase as well and releases glucose from the non-reducing end of the polymers. When adsorbed on a chain, glucoamylase hydrolysis the chain by releasing glucose until the chain is completely hydrolysed or until a 1,6 branch point. Glucoamylase is not able to pass a branch point and desorbs from the chain, although the enzyme is capable of cleaving α-1,6 bonds, albeit at a lower rate than α-1,4 bonds [10]. To speed up the hydrolysis of starch to high glucose syrups, pullulanase can be added to the reaction mixture. Pullulanase cleaves only α-1,6 branches in the amylopectin molecule, however at a much higher rate than glucoamylase.

Table 1.2: Commonly used enzymes for starch hydrolysis

Enzyme	Source	Point of cleavage	Main product
α-Amylase (Liquefying)	Bacterial	α-1,4random	Low DE
α-Amylase	Fungal	α-1,4	α-Maltose
β-Amylase		α-1,4	β-Maltose
Glucoamylase	Bacterial	α-1,4	Glucose
		α-1,6 (slow rate)	
Pullulanase	Bacterial	α-1,6	
Isomerase			Fructose

1.3 Starch hydrolysis processes

The hydrolysis process of starch to hydrolysates consists of two reaction stages, followed by down stream purification and concentration of the product to meet the desired product specifications (see figure 1.4) [7]. The first stage, liquefaction process is best described as a combination of two processes [11]:

- Complete gelatinization of the starch polymers to assure complete accessibility for subsequent hydrolysis.

- Hydrolysis to a degree that prevents retrogradation of the starch polymer during further processing.

Gelatinization is a complex process. Amylose and amylopectin are disclosed from its granular structure and starch crystals are melted to obtain a more or less homogeneous mass. Gelatinization of corn starch occurs at temperatures above 60 °C in excess water [12]. Starch granules swell rapidly under these conditions, resulting in disruption of the granules and melting of the polymer crystals to form a homogeneous starch melt. The viscosity increases rapidly during the gelatinization process. The peak viscosity during gelatinization can be reduced, by simultaneously hydrolyzing the starch. In current industrial processes, the starch slurry is diluted to 30-35% dry matter (D.M.) and thermo-stable α-amylase is added prior to liquefaction. The slurry is heated rapidly to 105 – 110 °C through direct steam injection in a so-called jet-cooker, where the gelatinization takes place. The slurry is maintained at this temperature for several minutes in a retention loop to prevent retrogradation phenomena to occur. Then, the starch slurry is cooled to 95-100 °C to complete the liquefaction during the next 60 - 90 minutes. The resulting intermediate product has a DE in the range of 8-15 [5].

The second reaction stage is the saccharification process, where the liquefied starch is further hydrolyzed. The liquefact is cooled to 60 °C and glucoamylase is added to the system. The reaction time for saccharification is in the order of 24 to 48h, depending on the processing conditions and type and concentration of the enzyme. After the saccharification

reaction, the product stream can be purified by filtration (to remove large solid particles), ion-exchange (to remove salts and proteins including enzymes), carbon column (to remove color) and evaporation to meet the desired product purity and concentration [11].
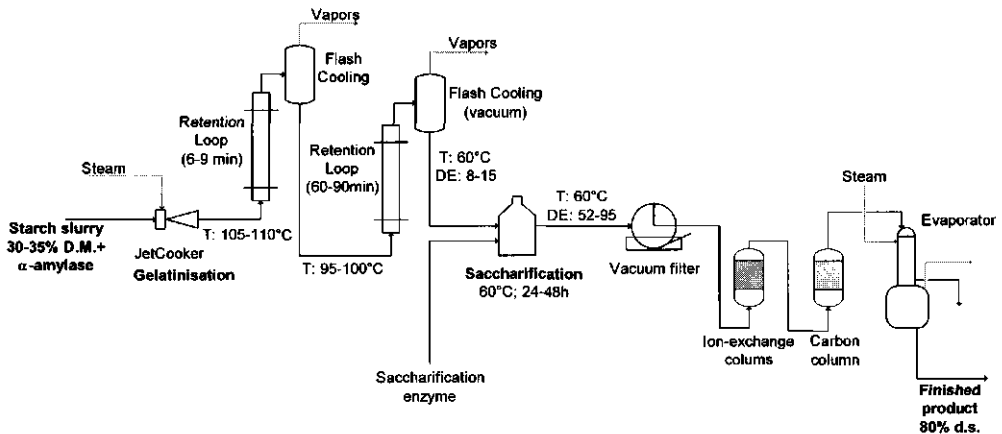

Figure 1.4: Process layout for the production of glucose syrups via the single heating liquefaction process [5]

1.4 Intensification of Starch Hydrolysates processing

From society, there is a drive towards more efficient usage of our natural resources [13]. For chemical industry, this includes reduction of the energy and solvent consumption, better use of the raw materials and subsequent less production of waste streams. Lowering energy and solvent consumption also reduces processing costs, which is an economic driver for industry. In the field of food processing, water is the main solvent. In many cases, streams are dilute in solids or other components to facilitate reactions and down stream processing. However, the dilution also means that the installations have to be proportionally bigger, and that the excess water has to be removed, usually by evaporation. This of course involves a significant amount of energy. Furthermore, the availability of fresh water is the main global concern of the next decades[1] [14], and it is expected that reduction of water consumption will become an important issue in the near future in the food processing industry as well.

As described in the previous section, the initial dry matter content for starch hydrolysis processes is approximately 35%, which means 1.85 ton of water per ton dry starch, excluding further addition of steam during processing. Water is consumed during the hydrolysis reaction

---

[1] *It is expected that in the year 2025 two out of every three people live in water stressed areas. Today 450 million people in 29 countries suffer from water shortage. Source: Letter of Secretary-General of UN to World Water Forum 2000*

(10% of the initial dry matter (= 0.1 ton / ton starch)) and the final product should contain 80% dry matter. This implies that, in theory, only 0.375 ton water / ton dry starch would be necessary to completely hydrolyze starch to a glucose syrup with 80% dry matter. So in current operation, 80% of the initial amount of water is excess. The relative streams of water and dry solids in the current industrial hydrolysis process are represented in figure 1.5. It may be clear that in view of sustainability, the starch hydrolysis processes is an interesting industrial example to explore the possibilities of process intensification.
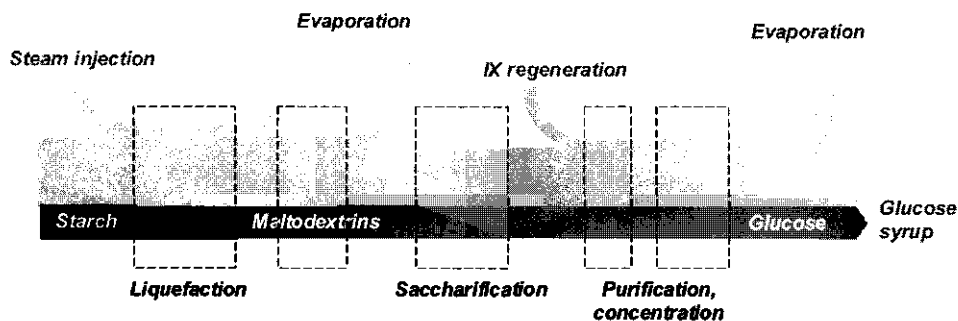

Figure 1.5: Schematic representation of the mass flow of water and starch in the current hydrolysis process (Diagram inspired on the Sankey diagrams for enthalpy flows; the width of the arrows shows the relative size of the stream).

Reducing the water concentration in starch hydrolysis leads to some major processing issues. Firstly, the viscosity will increase, making the starch paste more difficult to handle in traditional equipment [15-17]. Secondly, starch gelatinization becomes more difficult. In current conditions, the starch is gelatinized mainly by means of a thermal treatment. At very low water concentrations, the melting temperature increases to temperatures at which α-amylase is thermally unstable [18,19]. Application of shear is known to enhance the gelatinization at lower moisture conditions and lower temperatures [20]. The liquefying enzyme is usually added to the mixture before gelatinization to reduce the viscosity. However, it is not clear whether the enzyme can resist the shear forces that result from the high viscosity, as enzymes are generally referred to as being shear sensitive [21,22]. Furthermore, many enzymes require some free water to catalyse a reaction. This means that the water concentration may affect the rate of hydrolysis. Besides the water necessary for the chemical activity, reduced mass transfer in the highly viscous pastes may affect the rate of hydrolysis [23]. Another interesting question is the effect of the water concentration (or more precise water activity) on the reaction kinetics. This effect is expected in the saccharification reaction, because the water activity decreases during the reaction as water is being consumed. The water activity is further reduced by reduction of the molar fraction of water, due to the

increase in the number of molecules present, during the reaction. It is possible that the catalytic activity of the enzyme is reduced as well. Besides changes in activity, enzyme inhibition may be affected as well. Finally, it should be noted that the hydrolysis reaction is an equilibrium reaction, with water being one of the reactants [24]. Reducing the water concentration favours the polymerization, which could lead to incomplete hydrolysis [25-27].

Table 1.3 summarizes all issues involved when the water concentration is reduced in the starch hydrolysis process. The main part of the thesis therefore focuses on the issues raised in table 1.3 concerning the production of high glucose syrup (DE 95) from cornstarch, with thermo-stable α-amylase is liquefying enzyme and glucoamylase as saccharification enzyme in low water conditions.

Table 1.3:Effect of using low water conditions on the starch hydrolysis process

	Points of attention compared to conventional conditions
Gelatinisation	- Melting temperature increases rapidly, shear may be required
Enzyme stability	- Temperature inactivation may limit temperatures that can be applied - Shear necessary for gelatinisation; shear sensitivity of applied enzymes yet not sufficiently known - Maillard reactions may limit enzyme activity
Reaction rate	- Might decreases in time (because of water usage) per kg product - Enzyme inhibition might become stronger
Productivity	- May be much higher due to much higher product concentration
Reaction equilibrium	- The product formed may contain more and longer oligomers, because low water favours condensation reaction
Water activity	- Lower water activity will reduce conversion rate (on kg base)

2. Preservation of granular materials

A part of this thesis focuses on the use of microwave heating as means for preservation of granular products such as starch and gluten. Quality demands on food products are continuously increasing. At the same time the microbial safety of the same products has to be ensured. This results in a dilemma for the food processing industry to meet both demands, as generally, preservation processes have a negative impact on product quality [28]. It is therefore important to avoid any form of over-processing. Besides the impact on product quality, over-processing requires more energy than necessary, which influences processing costs negatively. Therefore, there is a trend towards minimal processing: application of conditions that still guarantee microbial safety but that minimise the negative impact on product quality.

Most operational preservation processes are based on thermal treatments. The transfer of heat into the product stream often limits the rate of heating and can result in uneven and suboptimal treatment and subsequent non-optimal product quality. The loss of quality might be reduced through using techniques that avoid transfer limitations; microwave technology possesses ideal properties in this respect [29,30]. With this technique, heat is generated locally inside the product and no conductive or convective heat transfer is necessary [31]. Not all materials are susceptible to microwave heating to the same extend [32-34]. These differences in heating rate can lead to different heating profiles in heterogeneous systems [35]. In a heterogeneous product, bacteria may be concentrated in domains that contain more moisture. Alternatively, it might be that bacteria themselves represent a phase containing more moisture than their environment. Since in general, moisture absorbs the microwave radiation effectively, this might open opportunities to selectively heat those domains that contain bacteria. This has led to the hypothesis that microwaves can be used to selectively heat micro-organisms in a dry environment, thereby reducing the overall thermal load on the product, and yielding less impact on the product quality of the dry product. Chapter 2 in this thesis reports a study on the feasibility of the concept using microwave technology to sterilize granular materials such as starch, vital gluten or milk powder.

3 Outline of the thesis

This thesis discusses the development of design guidelines for processing of starch that allow a substantial reduction of the amount of water that is needed in hydrolysis and in further treatment of the products streams. Since this field is too broad to cover in one thesis, some choices have been made. The largest part of the thesis focuses therefore on low-water

liquefaction and saccharification processes and an assessment is made of the feasibility of microwave-based thermal treatment of materials with low moisture content.

Heating of heterogeneous food media is discussed in chapter 2. The dynamics and the difference in temperature that can be obtained in a dispersed phase that is more susceptible to microwave heating than its surrounding matrix are estimated with an approximate analytical solution. On this basis, an outlook is given on possibilities and limitations for utilizing this technology.

Chapters 3-5 focus on aspects of reducing the use of water during starch hydrolysis. Chapter 3 describes the effect of shear forces on irreversible enzyme inactivation of thermo stable α-amylase in extrusion like conditions. The enzyme inactivation was modelled with first order inactivation kinetics as a function of the temperature, shear stress and treatment time. The effect of water concentration on both the reaction kinetics of glucoamylase and the reaction equilibrium is described in chapter 4. In chapter 5, the opportunities and implications of starch hydrolysis in highly concentrated conditions are discussed and are compiled into a conceptual process design.

Reference List

1   Swinkels, J. J. M (1985) Composition and properties of commercial native starches. *Starch*, 37, 1 - 5.

2   LMC International Ltd. (2002) The structure of the world market. 1 - 13.

3   Zobel, H. F. (1992) Starch: Sources, Production and Properties. 23 - 44.

4   Schenk, F. W. (2002) Starch hydrolysates - An Overview. *International Sugar Journal*, 104, 82 - 89.

5   Schenk, F. W. (1992) Starch hydrolysis products: An introduction and history. 1 - 22.

6   Zherebtsov, N. A., Ruadze, I. D., Yakovlev, A. N. (1995) Mechanism of acid-catalyzed and enzymatic hydrolysis of starch. *Applied Biochemistry and Microbiology*, 31, 511 - 514.

7   Howling, D. (2004) Glucose syrup: Production, Properties and Applications. 277 - 317.

8   Bhat, M. K. (1998) Enzymatic processing of starch: present and potential benefits. *International Sugar Journal*, 100, 372-376 - 426-427.

9   Roels, J. A. and Tilburg, R. van (1979) Kinetics of reactions with amyloglucosidase and their relevance to industrial applications. *Starch*, 31, 338 - 345.

10   Pandey, A (1995) Glucoamylase research: an overview. *Starch*, 47, 439 - 445.

11   Reeve, A. (2004) Starch hydrolysis: Process and Equipment. 79 - 120.

12   Donovan, J. W. (1979) Phase transitions of the starch - water system. *Biopolymers*, 18, 263 - 275.

13   Stankiewicz, A. and Moulijn, J. A. (2002) Process intensification. *Ind.Eng.Chem.Res.*, 41, 1920 - 1924.

14   Annan, K (2000) UN Committed to ensuring World Water Security and 'Blue Revolution'. *World Water Forum 2002*,

15   Zuilichem, D. J., Roekel, G. J., Stolp, W., Riet, K. van't (1990) Modelling of enzymatic conversion of cracked corn by twin-screw extrusion cooking. *Journal of Food Engineering*, 12, 13 - 28.

16   Chouvel, H., Chay, P. B., Cheftel, J. C. (1983) Enzymatic hydrolysis of starch and cereal flours at intermediate moisture contents in a continuous extrusion reactor. *FoodSscience and Technology*, 16, 346 - 353.

17   Roussel, L., Vieille, A., Billet, I., Cheftel, J. C. (1991) Sequential heat gelatinisation and enzymatic hydrolysis of corn starch in an extrusion Reactor. optimisation for a maximum dextrose equivalent. *Food Science and Technology*, 24, 449 - 458.

18   De Cordt, S., Hendrickx, M., Maesmans, G, Tobback, P. (1994) The influence of polyalcohols and carbohydrates on the thermostablity of α-amylase. *Biotechnology and Bioengineering*, 43, 107 - 114.

19   Souza, R. C. R. and Andrade, C. T. (2001) Investigation of the gelatinization and extrusion processes of cron starch. *Advances in Polymer Technology*, 21, 17 - 24.

20   Linko, P and Linko, Y. Y (1983) Extrusion cooking and bioconversions. *Journal of Food Engineering*, 2, 243 - 257.

21   Komolprasert, V and Ofoli, R. Y. (1990) Effect of shear on thermo-stable α-amylase activity. *Food science and Technology*, 23, 412 - 417.

22   Charm, S. E. and Wong, B. L. (1981) Shear effects on enzymes. *Enzyme and Microbial Technology*, 3, 111 - 118.

23   Komolprasert, V. and Ofoli, R. Y. (1991) Starch hydrolysis kinetics of *Bacillus licheniformis* α-amylase. *Journal of Chemical Technology and Biotechnology*, 51, 209 - 223.

24   Marchal, L. M. and Tramper, J. (1999) Hydrolytic gain during hydrolysis reactions: Implications and correction procedures. *Biotechnology Techniques*, 13, 325 - 328.

25   Flory, P. J. (1953) Molecular size and chemical reactivity; Principles of condensation polymerisation. 69 - 105.

26   Ajisaka, K, Nishida, H., Fujimoto, H. (1987) The synthesis of oligosaccharides by the reversed hydrolysis reaction of β-glucosidase at high substrate concentration and at high temperature. *Biotechnology Letters*, 9, 243 - 248.

27   Fujimoto, H, Nishida, H., Ajisaka, K (1988) Enzymatic synthesis of glucobioses by a condensation reaction with α-glucosidase, β-glucosidase and glucoamylase. *Agric.Biol.Chem.*, 52, 1345 - 1351.

28   Knutson, K. M., Marth, E. H., Wagner, M. K. (1987) Microwave heating of food. *Food Science and Technology*, 20, 101 - 110.

29   Villamiel, M., Lopez, Fandino R., Corzo, N., Martinez, Castro I., Olano, A., Fandino, R. L., Castro, I. M. (1996) Effects of continuous flow microwave treatment on chemical and

microbiological characteristics of milk. *Zeitschrift fur Lebensmittel Untersuchung und Forschung*, 202, 15 - 18.

30 Villamiel, M., Lopez, Fandino R., Olano, A., Fandino, R. L. (1997) Microwave pasteurization of milk in a continuous flow unit. Effects on the cheese-making properties of goat's milk. *Milchwissenschaft*, 52, 29 - 32.

31 Metaxas, A. C. and Meredith, R. J. (1993) Industrial microwave heating. 3ed edition,

32 Kozempel, M. F., Scullen, O. J., Cook, R., Whiting, R. (1997) Preliminary investigation using a batch flow process to determine bacteria destruction by microwave energy at low temperature. *Food Science And Technology*, 30, 691 - 696.

33 Pelesko, J. A. and Kriegsmann, G. A. (2001) Microwave heating of ceramic composites. *Journal of applied Mathermatics*, 64, 39 - 50.

34 Thomas, J. R. (1997) Particle size effect in microwave-enhanced catalysis. *Catalysis Letters*, 49, 137 - 141.

35 Sastry, S. K. and Palaniappan, S. (1991) The temperature difference between a microorganism and a liquid medium during microwave heating. *Journal of Food Processing and Preservation*, 15, 225 - 230.

2 On the potential of uneven heating of heterogeneous food media with dielectric heating

Abstract

A dynamic model was developed describing dielectric heating dynamics of a heterogeneous material, in which the dispersed phase heats more quickly than the surrounding phase. The model includes effects of scattering by small particles, absorption and differences in thermal and conduction properties, as well as domain size. The model shows that the smallest domain sizes that can be heated selectively are determined by dielectric and thermal properties of both domains and the applied field strength. In the case of food products, it can be concluded that the minimal size at which significant temperature differences can occur is about 1 mm applying current available microwave technology. However, in the case of pulsed fields, the domains that can be heated selectively can be orders of magnitude smaller than with constant fields, without requiring higher overall energy inputs.

1. Introduction

Dielectric heating processes generate different amounts of heat in different media. In heterogeneous materials, therefore, the rate of heating is unequal over regions having different composition, due to differences in dielectric properties and heat capacities. The use of this phenomenon is the subject of discussion in the field of food science as well as in several other physical and chemical applications [1-3].

In food science, selective heating is especially relevant to preservation processes. Several authors reported the inactivation of micro-organisms in heterogeneous products at sub-lethal temperatures during microwave treatment [4-6]. One of the given explanations for the experimental results describing the inactivation of micro-organisms at sub-lethal temperatures, is selective absorption of microwave energy by micro-organisms resulting in a temperature difference between the micro-organism and its environment. In thawing processes, inhomogeneous heating also occurs, but is generally undesired. To improve control of thawing processes, detailed knowledge of the processes leading to uneven heating is required.

In a theoretical study, Sastry and Palaniappan estimated the power densities necessary to obtain a temperature difference of 1K between a micro-organism in a liquid environment [7]. They concluded that a significant temperature difference is unlikely to occur at the scale of a micro-organism using current microwave technology. Their conclusions are based on the fact that the differences in heat generation in the micro-organism and the water are small compared to the thermal diffusion rates. However, in case of a micro-organism on a dry material, the differences in heat generation could possibly be larger due to the large difference in susceptibility of dry and wet material to microwaves.

The phenomena of selective heating can in principle be studied experimentally and theoretically. Due to the small scale of the dispersed phase, experimental determination of the actual temperature during a microwave treatment is difficult. Although promising new techniques such as temperature sensitive colorants and time-temperature integrators (based on enzyme inactivation) have become available [8], the authors did not succeed to measure the temperature of the dispersed phase experimentally. To our best knowledge, these data are also not available in open literature. Therefore, we have chosen to study the possibility of selective heating using a theoretical approach.

This paper presents a heat transfer model, including scattering effects and relevant material properties. The food system is modelled as a spherical object having a size smaller than 5 mm in an infinite surrounding medium, in which the spherical object dissipates more energy per volume than its surroundings (figure 1). We developed a relation between power dissipation in small conducting spheres and material properties, starting from Maxwell's law (see appendix I). We combined the outcome with a thorough analysis of the thermal phenomena occurring at small scale. The results of the study are used to exploit the possibilities of selective heating in heterogeneous food media.
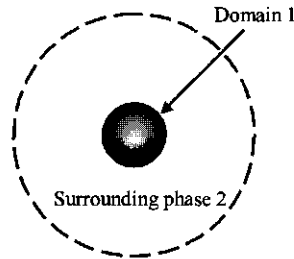

Figure 1: A Schematic overview of the heterogeneous system: a spherical domain 1 with radius R, dispersed in an infinite surrounding medium 2.

2. Theory

Part 1: the relation between microwave energy and heat generation

The treatment of heterogeneous materials with dielectric fields causes differences in heating rates of different materials. The tendency of a material to heat in an alternating electro-magnetic field, e.g. microwaves, is described by the complex dielectric permittivity

$$\varepsilon = \varepsilon' - i\varepsilon'' \qquad (1)$$

The relative dielectric constant ε' is the ability of a material to store electrical energy relative to vacuum. The loss factor ε'' is the tendency of the material to dissipate and convert the electrical energy into heat [9]. Generally, food materials containing moisture tend to convert microwave energy more efficiently compared to dry materials, evidenced by a high value for ε'' [9].

The dissipated power density during dielectric heating can be calculated by:

$$P = \tfrac{1}{2}\omega\varepsilon_0\varepsilon''|E|^2 \qquad (2)$$

in which, ω is the angular frequency, ε_0 the electric permittivity in free space, ε'' the dielectric loss factor and E the electric field strength.

The tendency of a heterogeneous system to heat unevenly is not only due to the differences in susceptibility to electromagnetic radiation of both phases, but also the product structure influences the distribution of heating of both phases. Reflection and refraction of waves occurs as a consequence of the spatial distribution of the phases, as a result of which differences in field strengths in both media will occur. The amount of reflection depends on the relative values of ε' of the object and the surrounding medium. Furthermore, the local field strength is influenced by the absorption of the wave in the surrounding phase. To quantify these effects, the Mie-theory can be used [10]. Simulations, based on the Mie-theorie, revealed for water droplets (r < 3 mm) in vacuum or starch that the electric field strength is constant within the object, implying that no resonance or starvation of waves occurs inside the object. For less absorbing materials, the particle size at which the field is constant increases. This leads to a simplified relation, from which we can calculate the field strength inside the object (as shown in appendix I):

$$|E_1| = |E_2| \frac{|k_2|^2}{|k_1|^2} \qquad (3)$$

where E_2 is the amplitude of the incident wave, k is the complex propagation constant of the dispersed phase or the surrounding medium, which are defined in appendix I.

The potential of uneven heating within a heterogeneous system can be expressed by the ratio of the dissipation of both phases. The ratio of the dissipation of both phases can be calculated by only the dielectric properties of both media, by combining equations 2 and 3:

$$\frac{P_1}{P_2} = \frac{\varepsilon_1''}{\varepsilon_2''} \left(\frac{|k_2|^2}{|k_1|^2} \right)^2 \qquad (4)$$

Part 2: The effect of thermal conduction on temperature differences in heterogeneous media

Apart from differences in heat generation, also thermal conduction effects have to be taken into account. We therefore developed a model comprising a non-moving spherical dispersed phase, having radius R, in an infinite surrounding medium 2. We assume that the dispersed phase heats up faster than medium 2. For the dispersed phase, the equation for the temperature $T_1(r,t)$ reads [11]:

$$\frac{\partial T_1}{\partial t} = \left(\frac{\lambda_1}{\rho_1 C_{p,1}}\right)\frac{1}{r^2}\left(\frac{\partial}{\partial r}(r^2\frac{\partial T_1}{\partial r})\right) + \frac{P_1}{\rho_1 C_{p,1}} \tag{5}$$

where ρ_1, $C_{p,1}$, and λ_1 are density (kg/m^3), heat capacity (kJ/kg·K) and thermal conductivity (W/m·K) and P_1 is the locally dissipated power density (W/m^3). For the surrounding medium, a comparable equation can be derived.

$$\frac{\partial T_2}{\partial t} = \left(\frac{\lambda_2}{\rho_2 C_{p,2}}\right)\frac{1}{r^2}\left(\frac{\partial}{\partial r}(r^2\frac{\partial T_2}{\partial r})\right) + \frac{P_2}{\rho_2 C_{p,2}} \tag{6}$$

From equation 6, the maximum temperature difference between the dispersed phase and the surrounding medium can be calculated (see appendix II):

$$\Delta T_{1,\max} = \frac{\Pi_1 - \Pi_2}{6D_1}\left(R^2 - r^2\right) + \frac{\Pi_1 - \Pi_2}{3D_2}\left(\frac{\rho_1 C_{p,1}}{\rho_2 C_{p,2}}\right)R^2 \tag{7}$$

in which $D = \dfrac{\lambda}{\rho C_p}$. We now have derived an expression, from which we can calculate the maximum temperature difference between the dispersed phase and its surrounding medium.

Figure 2 shows a typical temperature profile of the temperature development in time. It can be seen that the maximum temperature difference is obtained in the first part of the heating process. After some time, a semi-steady state situation is reached, where the temperature difference between both domains becomes constant, even though the temperature of the total systems still increases.

As described in appendix II, we can estimate the time dependency of the temperature differences with the help of a boundary layer model. This yields the following expression:

$$T_{diff} = \overline{T_1} - T_{hom} = \Delta\Pi\,\tau\,(1 - e^{-\frac{t}{\tau}}) \tag{8}$$

with

$$\tau = \frac{1}{3}R^2\rho_1 C_{p,1}\left(\frac{1}{5\lambda_1} + \frac{1}{\lambda_2}\right) = \frac{R\rho_1 C_{p,1}}{3K} \tag{9}$$

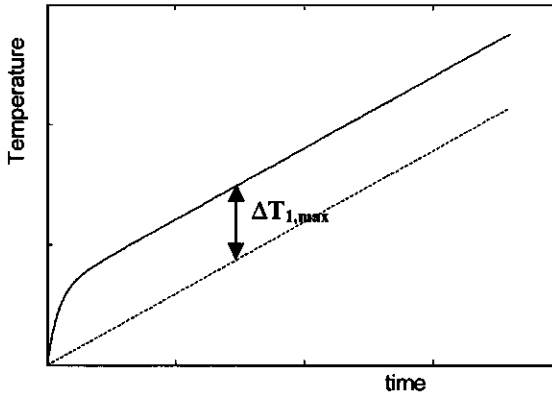in which K is the overall heat transfer coefficient.

Figure 2: Development of the semi steady state temperature difference between domain 1 (solid line) and the surrounding medium (dashed line).

In equation 8, a time constant τ is defined, which indicates the characteristic time involved in the heating process. Even though the model is just an approximation to the total dynamic process, the exact characteristic time involved will be close to the given approximation [12]. It can be seen that the thermal conductivity of phase 2 is more important than the conductivity of phase 1. In other words, the matrix seems to determine to what degree inhomogeneous heating takes place, next to the product morphology (R), and the relative heating density ($\Delta \Pi$). The actual average temperatures of the object and the surrounding medium can now be calculated by:

$$\overline{T_1} = T_{\text{hom}} + T_{\text{diff}} = \Delta \Pi \tau \left(1 - e^{-\frac{t}{\tau}} \right) + \Pi_2 t$$

$$\overline{T_2} = T_{\text{hom}} = \Pi_2 t$$

(10)

3. Results and discussion

In the model, the dispersed phase was modelled as small particles, in which a continuous field was present. In many food applications, the domain size falls within this range, e.g. micro-organisms in dry materials such as starch or liquid materials such as water, but also thawing of food materials can be evaluated. In the first part of the results we focus on power dissipation; in the second part we describe the consequences of differences in power dissipation using the thermal analysis outlined in the theoretical part of the paper.

3.1 The generation of heat in heterogeneous materials

The differences in heat generation rate in a heterogeneous system, $\Delta\Pi$, indicate the possibilities for selective heating, as shown in equation 9. The difference in heat generation rate $\Delta\Pi$ is a function of physical properties of both media and the power dissipation, which is a function of ε_i'' as well as the field strength E_i (equation 2). Figure 3 shows the heat generation rates in case the dispersed phase is water and the dielectric properties of the surrounding medium are varied, while figure 4 shows the effect of varying the dispersed phase and water being the surrounding medium. In both cases, the power input in the surrounding medium was 10^7 Wm^{-3}, which is a realistic value for microwave ovens [13].

The results shown in figure 3 and 4 can be interpreted with the following reasoning. The rate of heat generation is a strong function of the absolute as well as relative values of the ε' and the ε'' of both materials. When ε_1' is of the same order of magnitude as the surrounding materials, hardly any reflection occurs, therefore the difference in power dissipation becomes more or less linear with the ratio of ε''. In case the water droplet is the dispersed phase, the rate of dissipation increases with an increase in ε'_2 or a decrease in ε''_2. When ε'_2 increases while keeping the power input constant in the surrounding phase, the electric field strength in the water droplet increases due to reduced reflection phenomena. As water tends to convert dielectric energy more efficiently, the dissipation rate will increase with constant $\varepsilon''_1/\varepsilon''_2$. Reflection can also lead to values of $\Pi_1 - \Pi_2 < 0$, meaning that the surrounding medium heats up faster than the dispersed phase.
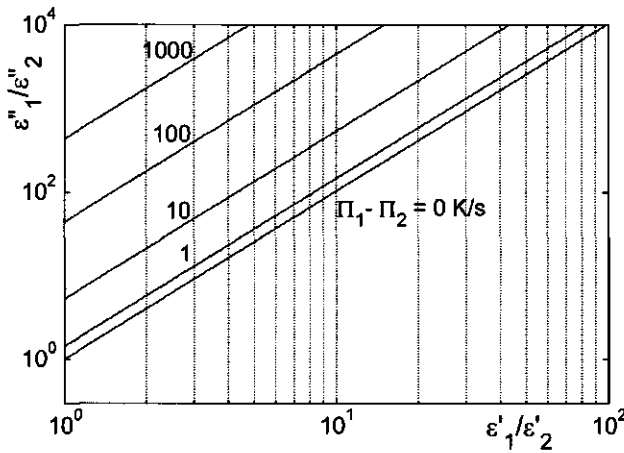
Figure 3: The effect of the dielectric properties of the surrounding medium on the dissipation rate Π_1-Π_2 with water being the dispersed phase (P_2 : 10^7 Wm^{-3}) The graph is a result of simulations, based on equation 4. The density and heat capacity of both domains are considered being water (see table 1)
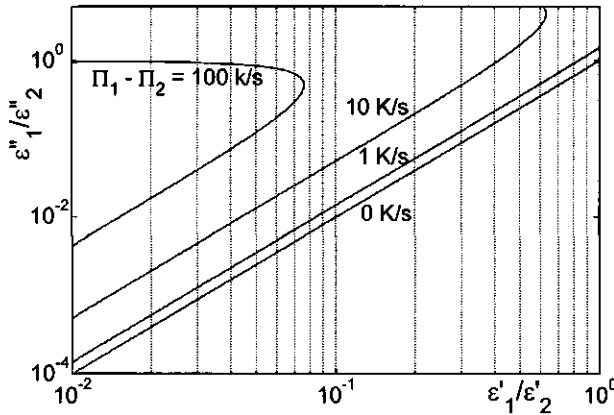
Figure 4: The effect of the dielectric properties of the dispersed phase on the dissipation rate Π_1-Π_2 with water being the surrounding medium (P_2 : 10^7 Wm^{-3}) . The graph is a result of simulations, based on equation 4. The density and heat capacity of both domains are considered being water (see table 1)

In case water is the surrounding medium, we have a somewhat different situation. We see an optimum in the rate of power dissipation (figure 4). By increasing ratio of the loss factors, the amount of reflected energy increases, thereby decreasing the electric field strength inside the dispersed phase. So, from figure 3 and 4, it can be concluded that although

increasing the loss factor generally leads to an increase in energy dissipation, in a heterogeneous system the dissipation rate can decrease and even lead to the opposite effect, despite a favourable loss factor of the dispersed phase.

Table 1: Physical properties of some food products[19]

	ρ [kg m^{-3}]	C_p [J kg^{-1} K^{-1}]	λ [W m^{-1} K^{-1}]	ε' [13]	ε'' [13]
Water	1000	4206	0.568	76.7	12
Salt water	a	a	a	67	41.87
Ice	917	2022	2.27 [b]	3.2	0.003
Milk powder	1500 [c]	1520	0.419	2.29	0.048

[a] approximated by physical properties of water

[b] T: 266 K

[c] *Starch*

3.2 Relevance to food media

In case of food materials, two categories can be distinguished [9]. Dry materials posses low ε' and ε'' and wet materials, including water, have high values for ε' as well as ε''. Table 2 shows the ratio of power dissipation for a number of materials relevant to food industry, using figure 3.

Table 2 outlines that it is possible to generate differences in power generation in the object and the surrounding medium. However, for most heterogeneous food materials the differences in power dissipation will be maximally in the order of a factor 4 for small objects except for thawing processes, in which a power ratio of 7 is possible.

Table 2: Power dissipation ratios of some heterogeneous food systems.

	$\dfrac{P_1}{P_2}$	$\Pi_1 - \Pi_2$ [a] [K / s]
Water / milk powder	0.22	-3.93
Salt water / milk powder	0.73	-2.70
Salt water / water	3.37	5.63
Water / ice	6.79	10.77

[a]: $P_2 = 10^7$ W m^{-3}

3.3 The effect of thermal diffusion on the possibility of selective heating.

Figure 5 outlines the combined effect of both object size and absolute power dissipation on the temperature difference of a saline droplet in water. The input power varies from a normal kitchen microwave (10^6 Wm^{-3}) to industrial microwaves (10^{10} Wm^{-3}) [13].

In a domestic microwave oven, small temperature differences can be obtained only in case of domain sizes larger than millimetres. At smaller domain sizes, thermal diffusion is too fast to establish a significant temperature difference. Significant temperature differences at smaller sizes can be obtained by increasing the input power. With industrial equipment significant temperature differences can be obtained for object sizes even at the size of 100 μm.

In principle, a temperature difference is possible at every scale provided that field strengths can be increased without any limitation. Currently available microwave technology can provide a power density of 10^{10} Wm^{-3}, although progress is being made in pulsed microwave technology enabling higher field strengths [13].

As described in the theoretical part of this paper, the time needed to obtain the maximum temperature differences is dependent on the square root of the object size. It can be calculated that for objects having a typical size of microns, the maximum temperature difference is already obtained after 10^{-5} s, while it takes more than 70 seconds to obtain the maximum temperature difference for object that have a radius of 5 mm. It should be noted that the time to obtain the maximum temperature difference is independent of power input.

3.4 Relevance to preservation processes

For preservation processes, it is desirable to selectively heat the micro-organisms, because thermal treatment of most food materials negatively influences the quality. As moist materials (i.e. bacteria) are more susceptible to microwaves than dry materials, the suggestion of the possibility of selective heating has been made. If a bacterium is approximated by a saline solution, and the surrounding medium has properties of milk powder, calculations show that milk powder heats up faster than the saline solution. Therefore, inactivation of micro-organisms is very unlikely to occur.

In case of micro-organisms in water, approximated by the saline water droplet in water, it is probable that the power dissipation favours selective heating. However, when current microwave powers are used, thermal diffusion is too fast to establish a significant temperature difference. Only when power densities 1000 times larger than current microwave technology are available, selective heating becomes a feasible option. Due to the development of pulsed

microwave fields, these higher power densities may indeed be realised. In the next section, we will discuss the possibilities of pulsed microwave ovens.
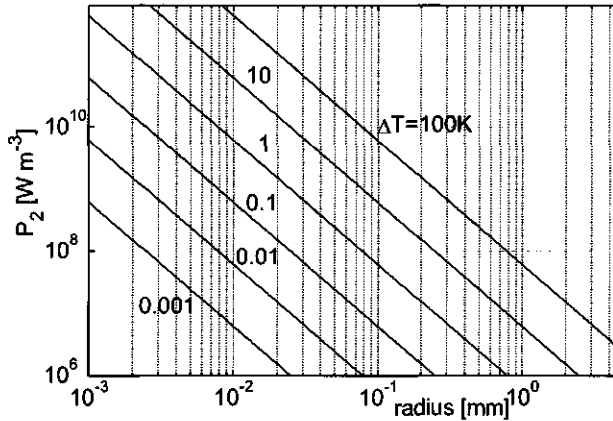

Figure 5: The power densities needed for obtaining certain temperature difference as function of the radius of the domain with power inputs from a domestic microwave ((P₂ : 10⁶ Wm⁻³) to industrial available microwaves (P₂ : 10¹⁰ Wm⁻³). (The simulations are based on equation II.15)

3.5 The use of pulsed microwaves

Pulsed microwave offers the possibility to apply higher fields. The overall energy input can remain constant if the increase in power input equals the reduction in heating time. In that case, the temperature difference obtained during a pulse equals:

$$T_{diff} = \overline{T_1} - T_{hom} = \phi\,\tau\,(\Pi_1 - \Pi_2)\left(1 - e^{-\frac{t}{\phi\tau}}\right) = \tau\left(\Pi_{1,pulse} - \Pi_{2,pulse}\right)\left(1 - e^{-\frac{t_{pulse}}{\tau}}\right) \qquad (11)$$

with τ given by equation 9 and ϕ indicates the increase in relative power density:

$$\phi = \frac{\Pi_{n,pulse}}{\Pi_n} = \frac{t}{t_{pulse}}\,,\ \text{where n refers to the domain type.}$$

In case of short t_{pulse}, $\phi \rightarrow \infty$, the temperature difference becomes:

$$T_{diff} = \left(\Pi_{1,pulse} - \Pi_{2,pulse}\right)t_{pulse} = \left(\Pi_1 - \Pi_2\right)t \qquad (12)$$

which equals the temperature difference in case of no heat transfer from the object to the surrounding medium.

In most food applications, we would like to heat the spherical domain to a certain temperature T_1, (e.g the temperature needed to inactivate the micro-organism) thereby keeping the temperature of the surrounding medium T_2 as low as possible. The use of pulsed electromagnetic fields can indeed be beneficial as can be seen in figure 6. A short pulse (a

high value of ϕ) with higher power density leads to a lower temperature of the surrounding medium, implying that the thermal load is reduced. However, a certain increase cannot be avoided, mainly due to the fact that at high values of ϕ only part of the maximum attainable temperature difference is obtained.

Because it is expected that shortening of pulse duration leads to higher equipment costs, the pulse duration should be optimised, e.g. by defining a maximum acceptable surrounding temperature increase. In case the duration of the pulse is shorter than 0.2τ, the additional increase of the medium temperature T_2 becomes:

$$\Delta T_{2,additional} < 0.1\, \Pi_2\, t \tag{13}$$

A further shortening of the pulse, and thereby increased power density, does not result in significant additional thermal advantages. Typically, the time constant for the size of bacteria is approximately 10^{-5} s to 10^{0} s for objects within the millimetre range (see figure 7). Therefore, development of microwave technology providing pulses in the range of microseconds seems to be interesting in case of preservation processes.
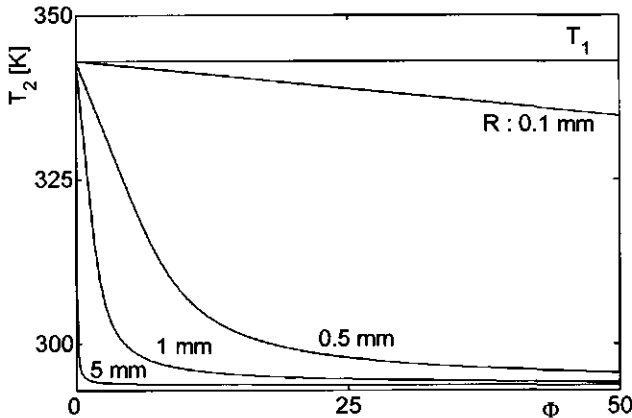

Figure 6: Temperature of the medium (2) as function of the reduction factor in pulse time for saline droplet in a water environment, using equation 12. The initial temperature was 273 K, while the final temperature of the saline droplet is 343 K. The radius of the dispersed phase was 0.1, 0.5 1.0 and 5.0 mm with a power input in medium 2 of $P_2 : 10^7$ Wm^{-3}.

4. Concluding remarks

A comprehensive model was derived that gives estimates of the dynamic temperature difference in and around a specific domain embedded in another material.

For small particles, a relation was derived to calculate the local power dissipation, based on the dielectric properties. It was shown that in case of an aqueous domain, e.g. a bacterium, in dry material, the water droplet will not heat faster despite its favourable loss factor. A bacterium in an aqueous environment will dissipate at most 4 times more energy.

The heat transfer model shows two regimes during the heating process: a transient period, in which the temperature difference develops and a semi steady state, in which the temperature difference becomes constant. The transient period varies from 10^{-5} s for a micro-organism size domain to minutes for domain sizes around centimetres.

The heat transfer model reveals that current microwave technology is not able to establish a significant temperature difference between a micro-organism and its surrounding medium. For larger objects, temperature differences can easily be obtained provided that sufficient microwave power can penetrate into both media. It could be shown that by applying very short pulses of microwave radiation in the microsecond range, selective heating of bacteria under the previously described conditions may become feasible.

Acknowledgment

Appendix I
Approximation of the electric field within a small sphere.

Based on Maxwell's laws and the so-called Mie-theory[14], it is possible to calculate the electric field components within a sphere, irradiated from one side [15,16]. For very small spheres the first terms in the expansion of the field components are dominant. They read:

$$E_r^{(1)} = E_2 \frac{3}{k_1 r} \sqrt{\frac{\pi}{2k_1 r}} b J_{3/2}(k_1 r) \cos\varphi \sin\theta \qquad (I.1)$$

$$E_\theta^{(1)} = E_2 \frac{3i}{2} \sqrt{\frac{\pi}{2k_1 r}} \left[a J_{3/2}(k_1 r) - ib \left\{ \frac{2}{k_1 r} J_{3/2}(k_1 r) - J_{5/2}(k_1 r) \right\} \cos\theta \right] \cos\varphi \qquad (I.2)$$

$$E_\varphi^{(1)} = E_2 \frac{3i}{2} \sqrt{\frac{\pi}{2k_1 r}} \left[-a J_{3/2}(k_1 r) \cos\theta + ib \left\{ \frac{2}{k_1 r} J_{3/2}(k_1 r) - J_{5/2}(k_1 r) \right\} \right] \sin\varphi \qquad (I.3)$$

where r (m), ω (rad) and φ (rad) are polar coordinates. The symbol k_1 (m^{-1}) is the complex propagation constant of the dispersed phase, E_2 is the amplitude of the incident wave and J refers to Bessel functions. The complex propagation constant of the dispersed phase or the surrounding medium 2, defined as:

$$k_j = \alpha + i\beta \qquad (I.4)$$

in which α is the phase constant and β the attenuation constant:

$$\alpha = \frac{\omega}{c} \sqrt{\frac{\varepsilon'(\sqrt{1 + \tan^2 \delta} + 1)}{2}} \qquad (I.5)$$

$$\beta = \frac{\omega}{c} \sqrt{\frac{\varepsilon'(\sqrt{1 + \tan^2 \delta} - 1)}{2}} \qquad (I.6)$$

with $\tan\delta = \dfrac{\varepsilon''}{\varepsilon'}$.

We have[17]:

$$J_{3/2}(x) = \sqrt{\frac{2}{\pi x}} (\frac{\sin x}{x} - \cos x) \qquad J_{5/2}(x) = \sqrt{\frac{2}{\pi x}} \left\{ (\frac{3}{x^2} - 1)\sin x - \frac{3}{x}\cos x \right\} \qquad (I.7)$$

Applying Taylor expansions to sinus and cosines for small x in these Bessel functions, results in:

$$J_{3/2}(x) \approx \frac{x^2}{12} \sqrt{\frac{2}{\pi x}} \qquad\qquad J_{5/2}(x) \approx \frac{x^3}{15} \sqrt{\frac{2}{\pi x}} \qquad (I.8)$$

The a and b in the equations of the field components are size dependent factors. They read:

$$a = \frac{-2i\sqrt{k_1 k_2} / \pi R}{\dfrac{2(k_1 - k_2)}{R} J_{3/2}(k_1 R) H_{3/2}(k_2 R) - k_1^2 J_{5/2}(k_1 R) H_{3/2}(k_2 R) + k_2^2 J_{3/2}(k_1 R) H_{5/2}(k_2 R)} \qquad (I.9)$$

$$b = \frac{-2i\sqrt{k_1 k_2} / \pi R}{-k_1 k_2 J_{5/2}(k_1 R) H_{3/2}(k_2 R) + k_1 k_2 J_{3/2}(k_1 R) H_{5/2}(k_2 R)} \qquad (I.10)$$

where R (m) is the radius of the sphere; k_2 (m^{-1}) is the propagation constant of the medium outside the sphere.

Besides the Bessel functions we have Hankel functions H present. It is possible to write these as:

$$H_{3/2}(x) = J_{3/2}(x) + iJ_{-3/2}(x) \qquad H_{5/2}(x) = J_{5/2}(x) - iJ_{-5/2}(x) \qquad (I.11)$$

where,

$$J_{-3/2}(x) = \sqrt{\frac{2}{\pi x}}(\frac{\cos x}{x} + \sin x) \qquad (I.12)$$

$$J_{-5/2}(x) = \sqrt{\frac{2}{\pi x}}\left\{\frac{3}{x}\sin x + (\frac{3}{x^2} - 1)\cos x\right\} \qquad (I.13)$$

So the 3/2- Hankel function will be:

$$H_{3/2}(x) = \sqrt{\frac{2}{\pi x}}\left\{\frac{\sin x + i\cos x}{x} + (-\cos x + i\sin x)\right\} = \sqrt{\frac{2}{\pi x}}\left\{\frac{ie^{-ix}}{x} - e^{-ix}\right\} = \sqrt{\frac{2}{\pi x}}e^{-ix}(\frac{i}{x} - 1) \quad (I.14)$$

For small x (small sphere radius) this will be approximately

$$H_{3/2}(x) \approx \frac{i}{x}\sqrt{\frac{2}{\pi x}} \qquad (I.15)$$

In the same way it can be demonstrated that the 5/2- Hankel function equals:

$$H_{5/2}(x) = \sqrt{\frac{2}{\pi x}}(e^{ix})\left\{-i(\frac{3}{x^2} - 1) - \frac{3}{x}\right\} \approx \frac{-3i}{x^2}\sqrt{\frac{2}{\pi x}} \qquad (I.16)$$

Substituting these approximations in a and b yields:

$$a \approx \frac{-k_1 k_2}{k_1^2\left(\dfrac{-(k_1 - k_2)}{6k_1} + \dfrac{k_1^3 R^2}{15k_1} - \dfrac{1}{4}\right)} \qquad b \approx \frac{-k_2}{k_1^2 R^2\left(\dfrac{-k_1}{15} - \dfrac{1}{4k_2 R^2}\right)} \qquad (I.17)$$

The components of the electric field are approximately:

$$E_r^{(1)} = E_2 \frac{1}{4}b\cos\varphi\sin\theta \qquad (I.18)$$

$$E_\theta^{(1)} = E_2 \frac{3i}{2}k_1 r\left[\frac{a}{12} - ib\left\{\frac{1}{6k_1 r} - \frac{k_2 r}{15}\right\}\cos\theta\right]\cos\varphi \qquad (I.19)$$

$$E_\varphi^{(1)} = E_2 \frac{3}{2}k_2 r\left[-\frac{a\cos\theta}{12} + ib(\frac{1}{6k_1 r} - \frac{k_2 r}{15})\right]\sin\varphi \qquad (I.20)$$

We see that the E_r component is radius independent.

Let us assume that the field in a small sphere is constant and equals the field in the centre ($r = 0$). This leads to three simple equations for the field in a small sphere, irradiated from one side.

$$E_r^{(1)} = \frac{b}{4} E_2 \cos\varphi \sin\theta \tag{I.21}$$

$$E_\theta^{(1)} = \frac{b}{4} E_2 \cos\theta \cos\varphi \tag{I.22}$$

$$E_\varphi^{(1)} = -\frac{b}{4} E_2 \sin\varphi \tag{I.23}$$

The square of the total field strength within the dissipative sphere is:

$$\left|E_{sum}^{(1)}\right|^2 = \left|E_r^{(1)}\right|^2 + \left|E_\varphi^{(1)}\right|^2 + \left|E_\theta^{(1)}\right|^2 = \frac{E_2^2 |b|^2}{16} \tag{I.24}$$

$$|b|^2 = \frac{|k_2|^2}{\frac{|k_1|^4}{16|k_2|^2}\left|\frac{4k_1 k_2 R^2}{15} + 1\right|^2} \approx \frac{16|k_2|^4}{|k_1|^4} \tag{I.25}$$

because R is small. The final result is:

$$\left|E_{sum}^{(1)}\right| = E_2 \frac{|k_2|^2}{|k_1|^2} \tag{I.26}$$

where E_2 is the amplitude of the incident wave, and k_n is the complex propagation constant.

Appendix II
Approximation of temperature differences in heterogeneous media

A non-moving spherical dispersed phase 1, having radius R, is considered in a non-moving infinite surrounding medium 2. We assume that the dispersed phase heats up faster than the surrounding medium 2. The equation for the temperature $T_1(r,t)$ reads [11]:

$$\frac{\partial T_1}{\partial t} = \left(\frac{\lambda_1}{\rho_1 C_{p,1}}\right)\frac{1}{r^2}\left(\frac{\partial}{\partial r}(r^2 \frac{\partial T_1}{\partial r})\right) + \frac{P_1}{\rho_1 C_{p,1}} \tag{II.1}$$

where ρ_1, $C_{p,1}$, and λ_1 are density (kg/m^3), heat capacity (kJ/kg·K) and thermal conductivity (W/m·K) and P_1 is the locally dissipated power density (W/m^3) of the dispersed phase. For the surrounding medium, a comparable equation can be derived:

$$\frac{\partial T_2}{\partial t} = \left(\frac{\lambda_2}{\rho_2 C_{p,2}}\right)\frac{1}{r^2}\left(\frac{\partial}{\partial r}(r^2\frac{\partial T_2}{\partial r})\right) + \frac{P_2}{\rho_2 C_{p,2}} \tag{II.2}$$

In case of an equal temperature increase in the domain and the surrounding medium $\left(\frac{P_1}{\rho_1 C_{p,1}} = \frac{P_2}{\rho_2 C_{p,2}}\right)$, the temperature increase equals:

$$\frac{\partial T_1}{\partial t} = \frac{\partial T_2}{\partial t} = \frac{P_2}{\rho_2 C_{p,2}} \equiv \frac{\partial T_{\text{hom}}}{\partial t} \tag{II.3}$$

This temperature increase is depicted as the homogeneous temperature increase. The difference in temperature between homogeneous and non-homogeneous heating ΔT_1 can now be described by:

$$\frac{\partial \Delta T_1}{\partial t} = \frac{\partial T_1}{\partial t} - \left(\frac{\partial T}{\partial t}\right)_{\text{hom}} = \left(\frac{\lambda_1}{\rho_1 C_{p,1}}\right)\frac{1}{r^2}\left(\frac{\partial}{\partial r}(r^2\frac{\partial T_1}{\partial r})\right) + (\Pi_1 - \Pi_2) \tag{II.4}$$

in which $\Pi_n = \frac{P_n}{\rho_n C_{P,n}}$, where n refers to domain 1 or continuous phase 2.

The value of $\Pi_1 - \Pi_2$ can be calculated by:

$$\Pi_1 - \Pi_2 = P_2\left\{\left(\frac{P_1}{P_2}\right)\frac{1}{\rho_1 C_{p,1}} - \frac{1}{\rho_2 C_{p,2}}\right\} \tag{II.5}$$

in which P_2 can be calculated from equation 2 and the ratio of the dissipated power can be calculated from equation 4.

The maximum temperature difference is obtained when the rate of heat transfer from 1 to 2 equals to the difference in heat generation between 1 and 2:

$$\frac{\partial \Delta T_1}{\partial t} = 0 = \left(\frac{\lambda_1}{\rho_1 C_{p,1}}\right)\frac{1}{r^2}\left(\frac{\partial}{\partial r}(r^2\frac{\partial T_1}{\partial r})\right) + (\Pi_1 - \Pi_2) \tag{II.6}$$

From equation II.6, the maximum temperature difference can be calculated:

$$\Delta T_{1,\text{max}} = \frac{\Pi_1 - \Pi_2}{6D_1}(R^2 - r^2) + \frac{\Pi_1 - \Pi_2}{3D_2}\left(\frac{\rho_1 C_{p,1}}{\rho_2 C_{p,2}}\right)R^2 \tag{II.7}$$

in which $D = \frac{\lambda}{\rho C_p}$. The boundary conditions are for $r = R$, $T_1 = T_2$ and for $r = 0$,

$\frac{\partial T_1}{\partial r} = 0$ [18]. We now have derived an expression for the maximum attainable temperature difference in a heterogeneous system between. The temperature in the dispersed phase and the homogeneous temperature increase.

To obtain an impression of typical times involved, we approximate the situation with a film model, which is in principle valid for larger Biot number [12]. The heat transfer resistances are located in two hypothetical boundary layers: one in the object and one in the surrounding medium (figure 7). The energy balances for both the dispersed phase and the surrounding medium read:

$$V_1 \rho_1 C_{p,1} \frac{\partial \overline{T_1}}{\partial t} = K A_1 \left(\overline{T_2} - \overline{T_1} \right) + P_1 V_1 \tag{II.8}$$

$$V_2 \rho_2 C_{p,2} \frac{\partial \overline{T_2}}{\partial t} = K A_1 \left(\overline{T_1} - \overline{T_2} \right) + P_2 V_2 \tag{II.9}$$

Domain 1   **Surrounding Medium 2**
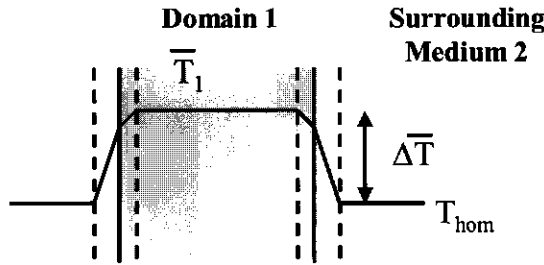
$\overline{T}_1$

$\Delta \overline{T}$

T_{hom}

Figure 7: Schematic representation of the film-model

If we assume that the dispersed phase is small compared to the surrounding medium, we can neglect the first term of the right hand side of equation II.9. The temperature in the surrounding medium can be approximated with:

$$\frac{\partial \overline{T_2}}{\partial t} = \Pi_2 \tag{II.10}$$

Now, the temperature difference T_{diff} in the heterogeneous system can be described by:

$$\frac{\partial T_{diff}}{dt} = \frac{3K}{R \rho_1 C_{p_1}} (\overline{T_1} - T_{hom}) + \Delta \Pi \tag{II.11}$$

in which R is the radius of the dispersed phase, K is the overall heat transfer coefficient, $\frac{\partial T_{diff}}{\partial t} = \frac{\partial T_1}{\partial t} - \frac{\partial T_{hom}}{\partial t}$ and $\overline{T_1}$ and T_{hom} are the average temperature in both phases. Integration of equation II.11 yields the average temperature difference as a function of time:

$$T_{diff} = \overline{T_1} - T_{hom} = \Delta \Pi \, \tau \, (1 - e^{-\frac{t}{\tau}}) \tag{II.12}$$

with

$$\tau = \frac{R\rho_1 C_{p,1}}{3K} \tag{II.13}$$

In equation II.12, a characteristic time τ is defined, which indicates the typical times involved in the heating process. For $t \rightarrow \infty$, the average maximum temperature difference can be calculated by the integration of equation II.7 with respect to the volume of the inner domain:

$$T_{diff,max} = \frac{1}{V} \int_0^V \Delta T_{1,max} dV \tag{II.14}$$

Integration of equation yields the average maximum temperature difference:

$$T_{diff,max} = \frac{\Delta \Pi}{3} R^2 \rho_1 C_{p,1} \left(\frac{1}{5\lambda_1} + \frac{1}{\lambda_2} \right) \tag{II.15}$$

For t is infinite, and substituting equation II.15 in equation II.12, we can derive an expression for the overall heat transfer coefficient K:

$$K = \frac{1}{R} \left(\frac{1}{5\lambda_1} + \frac{1}{\lambda_2} \right)^{-1} \tag{II.16}$$

If we substitute the overall heat transfer coefficient K in equation II.13, the characteristic time constant τ is defined as

$$\tau = \frac{1}{3} R^2 \left(\rho_1 C_{p,1} \right) \left(\frac{1}{5\lambda_1} + \frac{1}{\lambda_2} \right) = \frac{R\left(\rho_1 C_{p,1} \right)}{3K} \tag{II.17}$$

The absolute temperatures of the object and the surrounding medium can now be calculated by:

$$\overline{T_1} = T_{hom} + T_{diff} = \Delta \Pi \tau \left(1 - e^{-\frac{t}{\tau}} \right) + \Pi_2 t \tag{II.18}$$

$$\overline{T_2} = T_{hom} = \Pi_2 t$$

Equations II.12 and II.18 show that after some time the temperature *difference* becomes constant, although the absolute temperature of the dispersed phase and the surrounding medium still increase.

List of symbols

Symbol

a	coefficient in the sum of the electric field components within the sphere	
b	coefficient in the sum of the electric field components within the sphere	
C_p	heat capacity	J/(kg K)

D	thermal diffusion coefficient	m^2/s
E	electric field strength	V/m
E_2	amplitude of the incoming wave	-
$E_r^{(1)}, E_\theta^{(1)}, E_\varphi^{(1)}$	Spherical components of the electric field	-
J_n	Bessel function of the first kind of order n	-
H_n	Hankel function of the first kind of order n	-
K	overall semi steady state heat transfer coefficient	W/m^2K
k	complex propagation constant	-
P	volumetric power dissipation	$J/(s\ m^3)$
R	radius of the dispersed phase	m
T_1	temperature of dispersed phase	K
$\overline{T}_1$	average temperature of the dispersed phase	K
ΔT_1	temperature difference in the dispersed phase	K
$\Delta T_{1,max}$	maximum temperature difference in the dispersed phase	K
T_2	temperature of surrounding medium	K
$\overline{T}_2$	average temperature of the surrounding medium	K
T_{hom}	homogeneous temperature	K
T_{diff}	temperature difference between dispersed phase and surrounding medium	K
t	time	s
t	pulse duration	s
V	volume	m^3

Coordinates

$r,\ \theta,\ \varphi$	Polar coordinates	m, rad, rad

Greek symbols

ε	dielectric constant	–
ε_0	electric permittivity in free space	$F\ m^{-1}$
ε'	relative dielectric constant	-
ε''	dielectric loss factor	-
λ	thermal conductivity	W/m^3
Π	heat generation rate $\left(\dfrac{P}{\rho C_p}\right)$	K/s
ρ	density	kg/m^3
τ	time constant	s
Φ	pulse constant	-
ω	angular frequency	Hz

Subscript

1	referring to domain 1
2	referring to surrounding medium
hom	homogeneous (i.e. is the absence of dispersed phase)
diff	difference between dispersed phase and surrounding medium

Reference List

1   Chemat, F., Esveld, D. C., Poux, M., DiMartino, J. L. (1998) The role of selective heating in the microwave activation of heterogeneous catalysis reactions using a continuous microwave reactor. *Journal Of Microwave Power And Electromagnetic Energy*, 33, 88 - 94.

2   Pelesko, J. A. and Kriegsmann, G. A. (2001) Microwave heating of ceramic composites. *Journal of applied Mathermatics*, 64, 39 - 50.

3   Thomas, J. R. (1997) Particle size effect in microwave-enhanced catalysis. *Catalysis Letters*, 49, 137 - 141.

4   Fung, D. Y. and Cunningham, F. E. (1980) Effect of microwaves in microorganisms in food. *Journal of Food Protection*, 43, 641 - 650.

5   Kozempel, M. F., Scullen, O. J., Cook, R., Whiting, R. (1997) Preliminary investigation using a batch flow process to determine bacteria destruction by microwave energy at low temperature. *Food Science And Technology Lebensmittel Wissenschaft And Technologie*, 30, 691 - 696.

6   Kozempel, M. F., Annous, B. A., Cook, R. D., Scullen, O. J., Whiting, R. C. (1998) Inactivation of microorganisms with microwaves at reduced temperatures. *Journal of Food Protection*, 61, 582 - 585.

7   Sastry, S. K. and Palaniappan, S. (1991) The temperature difference between a microorganism and a liquid medium during microwave heating. *Journal of Food Processing and Preservation*, 15, 225 - 230.

8   Deng, Y, Singh, R. K., Lee, J. H. (2003) Estimation of temperature profiles of microwaved particulates using enzyme and vision system. *Journal of Food Science and Technology*, 331 - 338.

9   Datta, A and Anantheswaran, R. C. (2001) Handbook of microwave technology for food applications.

10   Jackson, H. W. and Barmatz, M (1991) Microwave absoption by a lossy sphere in a rectangular cavity. *Journal of Applied Physics*, 70, 5193 - 5204.

11   Crank, J. (1975) The mathematics of diffusion. 2nd, 89 - 98.

12   Incropera, F. D. and DeWitt, D. P. (1996) Fundamentals of heat and mass transfer. 4th,

13   Metaxas, A. C. and Meredith, R. J. (1993) Industrial microwave heating. 3ed edition,

14   Mie, G (1908) Beiträge zur Optik Trüber Medien, Speziell Kolloidaler Metallösungen. *Annalen der Physik*, 25, 377 - 445.

15   Stratton, J. A. (1941) Electromagnetic theory.

16   Vriezinga, C. A. (1997) Thermal runaway in microwave heated isothermal slabs, cylinders and spheres. *Journal of Applied Physics*, 83, 438 - 442.

17   Spiegel, M. R. (1968) Mathematical handbook of formulas and tables.

18   Carslaw, H. S. and Jeager, J. C. (1959) Conduction of heat in solids. 2nd Ed., 351 - 352.

19   Singh, R. K. and Heldman, D. R. (1993) Introduction to food engineering. 2nd,

3 Shear induced inactivation of α-amylase in a plain shear field

Abstract

A newly developed shearing device was used to study shear-induced inactivation of thermo-stable α-amylase in a plain shear field, under conditions comparable to extrusion. The results show that the inactivation can be described well with a first order process, in which the inactivation energy largely depends on the shear stress, instead of specific mechanical energy or strain history. The resulting dependency of the rate of inactivation on the shear stress is very strong and non-linear, which leads to the conclusion that in many cases the maximally applied shear stress determines the inactivation. Quantification of the inactivation rates gives design criteria for the application of enzymes in more viscous systems than conventionally done, provided that the reactor is designed such that no peak shear stresses occur.

1. Introduction

Hydrolysis of starch is usually performed in aqueous conditions with solids concentrations up to 35% w/w. Process intensification by increasing starch concentration up to 70% dry solids could lead to significant savings in equipment volume, solvent and energy usage. In case of starch or more general in case of biopolymers, process intensification generally leads to highly viscous media, due to increased polymer concentration. Extruders may be used to handle those highly viscous biopolymer melts. Characteristic for these types of processes is the occurrence of high shear forces, which may induce inactivation of enzymes [1].

The functionality of enzymes is usually dependent on their tertiary structure. Deforming or destroying the tertiary structure to a certain extent, e.g. by means of a thermal or a shearing treatment, can lead to enzyme inactivation. Although shear induced inactivation of enzymes is reported, a quantitative description is still lacking. In recent literature, a number of studies are presented, in which the effect of shear forces on proteins and enzymes is described [2-5] and which can roughly be divided into 2 categories. In the first category, pilot scale equipment, such as extruders is used [6-11]. Partial deactivation of enzymes in concentrated polymer solutions is reported, which is thought to be a result of the shear forces [12]. However, quantification of the effects of shear forces on the inactivation of enzymes is difficult due to the complex shear fields in an extruder. The second category comprises studies using well-defined shear fields through applying rheometer type equipment. Low viscous solutions are used and partial inactivation is reported [13,14]. Typically, enzyme inactivation in diluted systems was reported to be dependent on strain histories ($\dot{\gamma} t$). Strain histories higher than 10^5 resulted in significantly reduced enzyme activity, although its effect differed per enzyme. Unfortunately, the relevance of those studies to inactivation in concentrated solutions is not clear. Komolprasert and Ofoli studied the inactivation of thermo-stable α-amylase in both low viscous and high viscous media [1]. The experiments in low viscous media were carried out in a well-defined flow cell, which was most probably operated in turbulent flow conditions. The viscous system was studied using an extruder. Their study revealed a clear correlation between the strain history and the inactivation in case of inactivation measured in a low viscous system. However, the shear inactivation in the extruder could not be explained by either the strain history nor by the specific energy consumption. These results may indicate that shear induced inactivation in concentrated systems is more complex than can be explained only by the strain history.

The objective of this study is to investigate the effect of shear forces in a well-defined shear field on the irreversible inactivation α-amylase in concentrated starch solutions. A

newly developed shearing device was used, which enables the application of a homogeneous plain shear field of the same order of intensity typically present in extruder-like equipment at constant temperature. A kinetic model to describe the experimental data is discussed. Furthermore, consequences for process design of the phenomena observed are briefly discussed.

2. Theoretical Basis

Charm and Wong proposed that shear induced inactivation of enzymes follows a first order reaction that is typical for the inactivation reactions caused by random bond breaking during thermal inactivation [13]:

$$\frac{dA}{dt} = -k_0 A \tag{1}$$

where A is the enzyme activity and k_0 is a first order reaction rate constant, defined as:

$$k_0 = k_\infty e^{-\left(\frac{E_a}{RT}\right)} \tag{2}$$

where k_∞ is an pre-exponential factor and E_a is the activation energy of the inactivation reaction.

Shear forces have been reported to accelerate bond breakage in a polymer chain. The proposed mechanism for shear induced breaking of bonds is that shear forces lead to a reduction in the energy needed for bond breakage [15,16]. The Gibbs energy of molecular bonds is increased when a molecule is subjected to a shear field. This reduces the energy needed to overcome the activation energy. Therefore the activation energy under shear conditions E_a can be described by:

$$E_a = E_{a,0} - E_{a,s} \tag{3}$$

where $E_{a,0}$ is the activation energy of the inactivation reaction in case no shear is applied, e.g. in case of thermal inactivation. $E_{a,s}$ is the decrease of the activation energy due to the shear forces. The value of $E_{a,s}$ is given by:

$$E_{a,s} = \int_{r_b}^{r_s} F_s \, dr \tag{4}$$

in which r_b is the equilibrium bond length, r_s the bond length under shear and F_s the force applied on the bond. It is clear that there will be a relation between the forces on these bonds and the externally applied shear stress τ. Such a relation is derived for amylopectin, describing the molecule as a rigid sphere [17]. For enzymes in a concentrated starch solution, the situation is more complex, among others due to the flexibility of the enzyme and the non-uniformity of the molecular bonds and their distribution. This explains why an exact relation

between F_s and τ, not its effect on stretching bonds inside the enzyme is not described in literature yet. However, it is likely that a positive relation between the shear stress and the force of the bond or the bond energy exists. We therefore propose a simple power law to describe the reduction of the activation energy due to the shear forces:

$$E_{a,s} = \zeta\tau^n \tag{5}$$

Shear induced enzyme inactivation can now be described by:

$$\frac{dA}{dt} = -Ak_\infty e^{\left(\frac{-E_{a,0}+\zeta\tau^n}{RT}\right)} = -Ak_\infty' e^{\left(\frac{\zeta\tau^n}{RT}\right)} \tag{6}$$

where $k_\infty' = k_\infty e^{-\frac{E_a}{RT}}$. The shear stress during our experiments was not constant in time, due to changing viscosity. Therefore, the variation in shear stress was taken into account completely. Equation 6 was adjusted to account for the dynamic shear stress profiles by numerical integration of the dynamic shear stress profiles. This leads to the following relation:

$$-\ln\frac{A}{A_0} = \int_0^t k_\infty' e^{\left(\frac{\zeta\tau(t)^n}{RT}\right)} dt \tag{7}$$

3. Materials and methods

3.1 Materials

The enzyme used was Termamyl 120 LC from Novozyme and was a gift from Cargill b.v., the Netherlands. The enzyme was a thermo-stable α-amylase, produced by *Bacillus Licheniformis*. The starch was commercially available corn starch (C2000, food grade), and was also provided by Cargill b.v., the Netherlands. The dry matter content of the corn starch was 89% w/w. The buffer solution was a 50 mM sodium acetate buffer with pH 5.8 and 5 ppm calcium chloride. The buffer solution was used in both the experiments and the enzyme activity test. The glycerol used was 99% pure.

3.2 Methods

3.2.1 Raw material preparation

Just prior to a shearing experiment, the moisture content of the starch was adjusted to the desired moisture content with a mixture of 50 mM sodium acetate buffer (pH 5.8) with 5 ppm calcium added and, in some experiments, glycerol. The glycerol (if used), the buffer solution and the enzyme-solution were premixed. The resulting mixture was then added to the dry starch in a lab scale mixer, while mixing continuously. The sample compositions are summarized in table 1, in which the sample mass is defined as the total mass of wet sample

used in the shearing experiment. The fraction glycerol of the total moisture added to the starch varied from 0 to 0.75. The ratio enzyme on dry starch was kept constant during all experiments at 4.5 ml enzyme (commercial solution) per kg dry starch.

3.2.2 Shearing treatment

The shear treatment was performed in a newly developed shearing device (figure 1) [18]. The shear device was based on the cone and plate geometry, which gives a homogeneous shear field throughout the sample at constant temperature. The maximum shear stress that can be applied is 70 kPa, which is comparable to extrusion conditions, typically a factor 1000 higher than conventional rheometers. After filling the shearing zone with the starch-buffer/glycerol-enzyme mixture, the cell was closed and heated to the desired temperature, by electrical heating elements. When the temperature set point was reached, the sample was sheared between the none-rotating cone and rotating plate. The shear rate was set to 24 s^{-1}, to avoid slip. After 120 s, the shear rate was increased gradually to 120 s^{-1} (50 rpm) and maintained at this shear rate during the experiment. The typical treatment time was in the order of 480 seconds at the highest shear rate. The shear stress during the treatment was determined by continuously measuring the torque. The dry starch content in the shear cell was varied from 100 g to 125 g, except in experiment 6, where the shear cell was filled with 156 g dry starch. The overall weight of the sample was dependent on the moisture content. Directly after a shear cell run, the treated material was frozen in liquid nitrogen en stored at −18 °C. Prior to analysis, the samples were dried at 35 °C under vacuum for 48h.
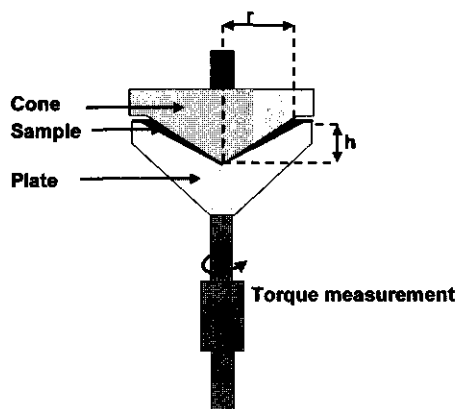

Figure 1: A schematic picture of the shearing device to apply a well defined shear field. Design parameters: Cone angle: 100 °; shear zone angle θ: 2.5 °; r: 0.1 m; h: 0.082m

3.2.3 α-amylase activity test

The activity of α-amylase was determined with a modified DNS-test of Bernfeld [19]. 100 μg dried sample was dispersed in a 5 ml buffer solution. 100 μl of the sample solution was added to a dispersion of 2 ml 5% cornstarch in a 50 mM sodium acetate buffer pH 5.8 with 5 ppm calcium. The mixture was then incubated at 95 °C for 10 minutes. The hydrolysis reaction was stopped by the addition of 2 ml DNS-solution and incubated at 95 °C for 5 minutes and subsequently cooled in an ice-bath to room temperature. 1 ml of the cooled dispersion was diluted with 5 ml de-mineralized water and centrifuged at 13000 rpm in an Eppendorf centrifuge for 15 minutes. The clear supernatant was measured with a spectrophotometer (Spectronic 20 genesis) at 540 nm. The absorption was measured against a blank, which was treated as described above, without the incubation of 10 minutes at 95 °C. The enzyme activity before the treatment, A_0, was measured using the native starch mixture, which was treated in the same way as the other samples just prior to shearing. Experiments confirmed that the subsequent freezing and drying steps did not influence the outcome of the enzyme activity.

4. Results and Discussion

4.1 Shearing treatment

Figure 2 shows a typical shear stress profile of a starch-water mixture with 70% w/w dry matter. As explained in the experimental section, the initial shear rate was set to 24 s^{-1}, after 120 s, the shear rate was increased to 120 s^{-1} for the rest of the experiment. The shear stress then increased, probably due to gelatinisation of the starch [20]. The maximum shear stress was reached 30 s later. After 2 minutes, the shear stress decreased, among others due to degradation of starch [18]. The reduction in molecular weight resulted in reduced viscosity, and therefore a reduction in shear stress. When α-amylase was added to the mixture, a similar shear stress profile could be observed. However, the maximum torque and the final torque value were significantly lower. This is thought to be a result of the hydrolysis of starch by the α-amylase. Under these conditions, hardly any inactivation of α-amylase was measured as a result of the hydrolytic activity of the enzyme, which made it difficult to obtain sufficiently high torque values. To expand the experimental window towards higher torque values, part of the buffer was replaced by glycerol, which decreased the rate of starch hydrolysis. The addition of glycerol therefore resulted in increased torque values, and subsequently in higher shear stresses onto the mixture. The thermal stability of α-amylase is reported not to be affected by the addition of glycerol, because glycerol was reported to stabilize the enzyme to a comparable extent as starch [21]. This finding was confirmed in an experiment in which

97% of the initial activity was measured after a heating shearing treatment in the presence of glycerol (table 1; experiment 9).
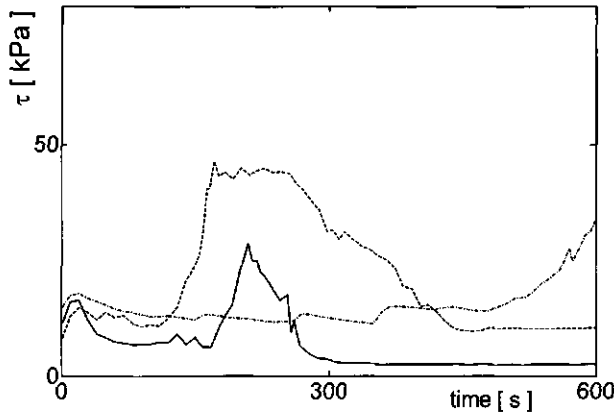

Figure 2: Shear stress profiles (smoothened) of typical shearing treatments, where the shear stress is plotted as a function of time. A starch - water mixture (---), a mixture of starch with buffer and α-amylase (—) and a mixture of starch with buffer – glycerol – α-amylase (----) were treated at 90°C.

4.2 Enzyme inactivation

The experimental set-up, processing conditions and the measured irreversible inactivation are summarized in table 1. The results show that hardly any inactivation occurred at low shear stresses. Increasing the shear stress led to significant irreversible inactivation of α-amylase. The residual enzyme activity varied from 100% to 47% with maximum shear stresses varying from 4.3 kPa to 68.5 kPa respectively, while the shear rate was kept constant in all experiments. The processing times varied within a range from 180 s to 627 s, which are typical for extrusion conditions [22].

The irreversible inactivation of enzymes as a function of the maximum shear stress, τ_{max}, is plotted in figure 3. As expected, we observe a good correlation. Hardly any enzyme inactivation occurred when a shear stress lower than about 25 kPa was applied. Increasing the maximum shear stress above this threshold value resulted in increased inactivation, approximately following a linear relation. However, the experiments resulting in the highest inactivation show some deviation. Experiment 2 was treated for 458 s with τ_{max} of 68.5 kPa and experiment 6 was treated for 600 s with τ_{max} of 49.0 kPa. Both experiments resulted in a residual activity of 48%. This indicates that the maximum shear stress is not the only parameter involved. As indicated in the theoretical section, time also can influence the

51

inactivation. To fully understand the combined effects of time and shear stress, we have to take a closer look at the shear profiles. The shear profiles of experiments 2, 6 and 7 are plotted in figure 4. The shear stress profiles of experiment 2 and 7 are comparable; the shear stress was rather constant until 270 s after which the shear stress increased gradually to a maximum shear stress of 68.5 kPa respectively 65.1 kPa. The initial shear stress in experiment 6 was higher than in experiment 2 and was rather constant until 250 s. From that moment on, the viscosity of the paste started to decrease, probably due to thermo-mechanical degradation of starch, which resulted in reduced shear stresses. Although the shear history of the three samples was different, the resulting inactivation is of the same order. These results indicate that both time and shear stress are involved in the shear-induced inactivation of α-amylase. However, a time effect will only be relevant if the material is under stress conditions, as it is known from literature that the enzyme is quite thermo-stable at the temperatures and process times applied [21]. Also, our experimental results show that 100% of the enzyme activity remained after a shearing treatment at 383 K (table 1, experiment 4), which demonstrated the thermo-stability of the enzyme within the temperature range and treatment time of this research.

Table 1: experimental conditions and results

| Experiment	Temperature [K]	Sample mass [kg]	Dry matter content [% w/w]	Glycerol / total moisture	Treatment time [s]	$\dot{\gamma}$ [s^{-1}]	τ_{max} [kPa]	Strain history [10^3]	A_{res} [%]
1	363	0.159	63	0	490	120	31.1	58.8	83
2	363	0.150	69	0.72	458	120	68.5	55.0	47
3	363	0.190	70	0	600	120	33.4	72.0	73
4	383	0.22	58	0	180	120	4.3	21.6	100
5	383	0.196	63	0.5	600	120	31.8	72.0	93
6	383	0.249	63	0.75	600	120	49.0	72.0	49
7	383	0.155	69	0.72	510	120	65.1	61.2	48
8	383	0.165	70	0.25	600	120	21.1	72.0	94
9	383	0.205	70	0.5	337	120	19.7	40.4	97
10	383	0.165	70	0.5	627	120	43.5	75.2	66
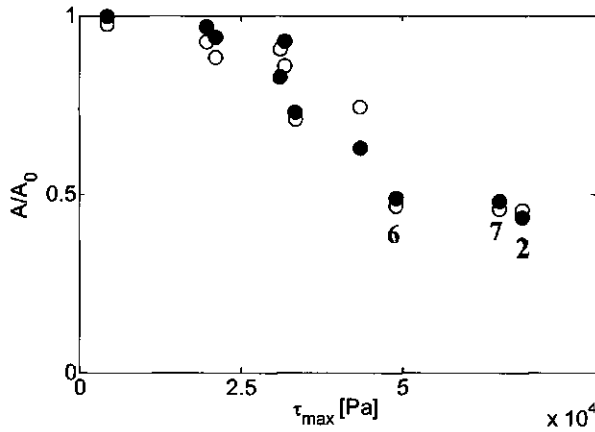
Figure 3: The residual α-amylase activity as a function of the maximum shear stress during a shearing treatment (●) and according to the model fit (○), using equation 7.
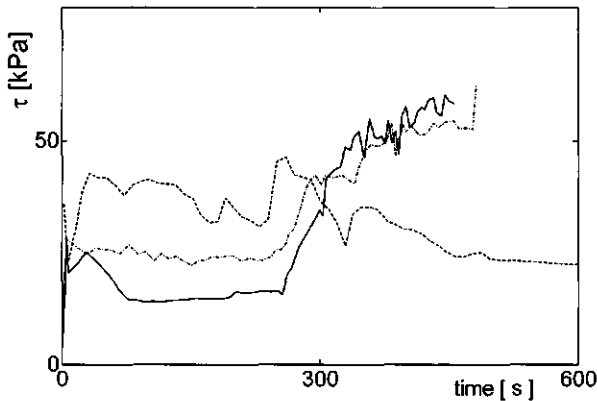

Figure 4: Typical shear stress profiles (smoothened) measured during a sharing treatment of experiments 2, 6 and 7 (table 1).

Equation 7 was used to fit all data at once, using ζ, k'_∞ and n as adjustable parameters and was numerically integrated over the complete experimental τ t profile. The estimated parameters are:

k'_∞ : $6.05 \cdot 10^{-5}$

ζ : 25.1 $[m^3 mol^{-1} Pa^{1-n}]$

n : 0.57

The experimental values (●) and model estimations (○) are plotted in figure 3 and in a parity plot in figure 5. The figures show that shear inactivation could be well described with first order kinetics using shear stress and time. The average deviation of the predicted values and the measured values is 6%. The time dependency implies that the inactivation of the enzyme is not an instantaneous process as found for the shear induced primary degradation of biopolymers, which involves the breakage of covalent bonds in e.g. starch [18]. In our case, the reduction of the activation energy was less than linear with increasing shear stress (n > 1). A possible explanation could be that the enzyme is somewhat flexible and allows a certain alignment to the shear field. Alignment to the shear field reduces the hydrodynamic diameter of the enzyme and as a result of which the enzyme becomes less sensitive to the shear forces. However, it may well be that significant modification of the tertiary enzyme structure, and thus the inactivation, involves the rupture of several bonds (which may be covalent as well as hydrogen bonds). This could also explain a non-linear dependency of E_a on τ.
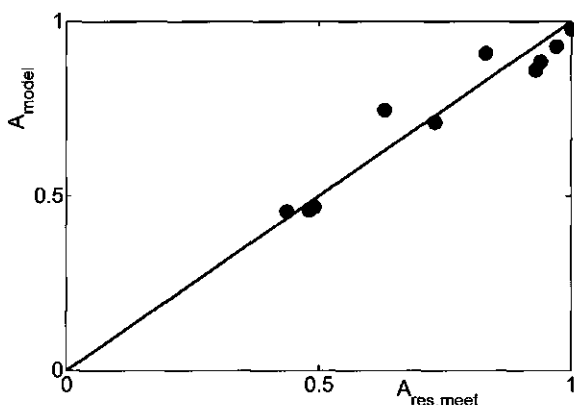

Figure 5: Parity plot of the experimental data and the estimated data, using equation 7.

The activation energy for thermal inactivation is in the order of 240 kJmol^{-1}[21]. If we assume that inactivation by shear is comparable to inactivation by heat, we may assume that the activation energy $E_{a,0}$ for shear induced inactivation is of the same order as the activation energy for thermal inactivation. The shear stress then reduces the activation energy with maximally 8% in the experimental range investigated. Although the reduction in activation energy seems only limited, the (thermo)-stability of the enzyme is drastically reduced. This may also explain why we find time-dependent behavior, while thermo-mechanical degradation seems to occur (almost) instantaneously. Probably, the reduction in E_a is so large in that case, that the time scales become small compared to those of the experiment.

4.3 The effect of time and shear stress

The model, proposed in equation 7, to describe shear-induced inactivation of α-amylase can be used to illustrate the effect of time shear equivalence (τ t) on the inactivation of α-amylase. Three different theoretical shear stress profiles were simulated (see figure 6a), comprising a constant shear profile and 2 peak shaped shear profiles, with a maximum shear stress of 50 kPa and 175 kPa respectively. The product of τ and t is equal for all three profiles, implying an equal energy input, suggested in literature to determine enzyme inactivation. The inactivation of the enzyme predicted by the model is depicted in figure 6b. The constant shear stress results in a slow, linear decrease in residual activity in time. The application of a maximum shear stress of 50 kPa resulted in a residual activity of approximately 0.7, where the maximum rate of inactivation can be seen at the maximum shear stress. When the same amount of energy is applied in a short time with a maximum shear stress of 175 kPa, the simulation shows that the enzyme is irreversibly inactivated almost instantaneously and completely. The simulations emphasize the importance of the maximum shear stress, and illustrate what can be done with different process designs.

Our model indicates that application of shear stresses reduces the thermo-stability of the enzyme to a large extent, but it was also shown that the precise form in which the shear forces are applied is very important for the final inactivation achieved. It should be noted that without shear applied, the enzyme is stable at temperatures used. At higher temperatures, the influence of shear with equal shear stresses is much larger and the apparent thermo-stability is reduced. However, since the paste viscosity is generally reduced at higher temperatures, the shear stresses will be reduced at equal shear rates. Thus, we have two opposing effects and therefore the stability of the enzyme as a function of temperature will be complex. It is clear, however, that at higher temperatures, the effects of even lower shear stresses should not be ignored.
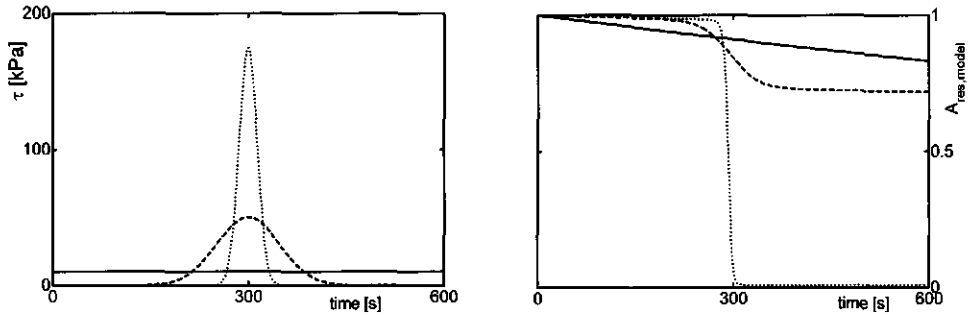
Figure 6a: Simulated shear stress profiles; the integral (τ t) is equal for all three profiles. b: The simulated residual enzyme activity as a result of the shear stress profile of figure 6a, using equation 7.

4.4 Consequences for the design of enzymatic processes

The results presented in this paper show a quantitative relation between shear stresses and enzyme inactivation, indicating that peak stresses are responsible for most of the inactivation. Our finding is therefore in agreement with a study of Komolprasert and Ofoli, who reported that inactivation of enzymes in an extruder could not be explained by the strain history or the specific energy consumption, based on the average shear rate [1]. Averaging of shear rates underestimated the actual inactivation. The consequence of the foregoing is that shear stress should be regarded as design parameter for new processing equipment, to optimally use the beneficial effects of enzymatic action in starch hydrolysis.

The activity and stability of α-amylase could open opportunities for the hydrolysis of starch in highly concentrated conditions, provided that exact equipment design enable the application of shear to enhance mass transfer phenomena without inactivation of the enzyme. The use of shear stress as design parameter might also open opportunities for wider application biopolymer processing, e.g. structure formation processes. A typical example is structure formation of proteins by enzymatic cross-linking [23,24]. The increasing viscosity during the reaction can easily result in high shear forces, thereby inactivating the enzyme and destroying protein structure. Exact design of equipment can reduce the inactivation of enzymes by controlling the shear forces applied.

It should be mentioned that we have only considered plain shear. It is probable that extensional flow may be even more effective in inactivating the enzyme. However, one may expect the dependency of the inactivation on time and shear has the same relation for both types of flow (albeit with different values).

5. Conclusion

A newly developed shear device was used to study the effect of plain shear forces on the inactivation of thermo-stable α-amylase. The study reveals that a first order inactivation model can describe the inactivation process. The activation energy involved was found to be reduced by the application of shear forces. The resulting dependency of the rate of inactivation on the shear stress is very strong and non-linear. This strong dependency leads to the conclusion that in many cases the maximally applied shear stress mainly determines the inactivation. Thermo-stable α-amylase appears to have a shear resistance to approximately 25 kPa in a plain shear field. When the critical shear stress is exceeded, the enzyme is rapidly deactivated.

It can therefore be concluded that no fundamental limitations have been encountered for the application of α-amylase in highly concentrated biopolymers solutions, provided appropriate design of equipment to avoid peak shear stresses.

List of symbols

A	Enzyme activity	[KNU g^{-1}]
A_0	Initial enzyme activity	[KNU g^{-1}]
E_a	Activation energy of the inactivation reaction	[kJ mol^{-1}]
$E_{a,0}$	Activation energy of the inactivation reaction in case no shear is applied	[kJ mol^{-1}]
$E_{a,s}$	Decrease of activation energy due to shear forces	[kJ mol^{-1}]
F_s	Force applied on a bond	[N]
k_0	Reaction rate constant	[s^{-1}]
k_∞	Pre-exponential factor	[s^{-1}]
k'_∞	Reaction rate constant in case no shear is applied	[s^{-1}]
R	Gas constant	[Jmol^{-1}K^{-1}]
r_b	Equilibrium bond length	[m]
r_s	Bond length under shear	[m]
T	Temperature	[K]
t	Process time	[s]

Greek symbols

η	viscosity	[Pa s]
$\dot{\gamma}$	shear rate	[s^{-1}]
τ	Shear stress	[Pa]
τ_{max}	maximum shear stress	[Pa]
ζ	constant (equation 5)	[m^{3}mol^{-1}Pa^{1-n}]

Reference List

1   Komolprasert, V and Ofoli, R. Y. (1990) Effect of shear on thermo-stable α-amylase activity. *Food science and Technology*, 23, 412 - 417.

2   Ganesh, K., Joshi, J. B., Sawant, S. B. (2000) Cellulase deactivation in a stirred reactor. *Biochemical Engineering Journal*, 4, 137 - 141.

3   Gunjikar, T. p., Sawant, S. B., Joshi, J. B. (2001) Shear deactivation of cellulase, exoglucanase, endo-glucanase and β-glucosidase in a mechanically agitated reactor. *Biotechnology Progress*, 17, 1166 - 1168.

4   Kaya, F., Heitmann Jr., J. A., Joyce, T. W. (1996) Deactivation of cellulase and hemicellulase in high shear fields. *Cellulose Chemistry and Technology*, 30, 49 - 56.

5   Maa, Y. F. and Hsu, C. C. (1996) Effects of high shear on proteins. *Biotechnology and Bioengineering*, 51, 458 - 465.

6   Chouvel, H., Chay, P. B., Cheftel, J. C. (1983) Enzymatic hydrolysis of starch and cereal flours at intermediate moisture contents in a continuous extrusion reactor. *Food Science and Technology* , 16, 346 - 353.

7   Govindasamy, S., Campanella, O. H., Oates, C. G. (1996) High moisture twin screw extrusion of sago starch II : saccharification as influenced by thermo-mechanical history. *Carbohydrate Polymers*, 32, 267 - 274.

8   Govindasamy, S., Campanella, O. H., Oates, C. G. (1997) Enzymatic hydrolysis of sago starch in a twin-screw extruder. *Journal of Food Engineering*, 32, 403 - 426.

9   Hakulin, S., Linko, Y. Y., Linko, P., Seiler, K., Seibel, W. (1983) Enzymatic conversion of starch in twin-screw HTST-extruder. *Starch*, 12, 411 - 414.

10   Hout, R. van den, Jonkers, J., Vliet, T. van, Zuilichem, D. J. van, Riet, K. van 't (1998) Influence of extrusion shear forces on the inactivation of trypsin inhibitors in soy flour. *Trans.Ichem*, 76, 155 - 161.

11   Ilo, S and Berghofer, E. (1998) Kinetics of thermo-mechanical destruction of thiamin during extrusion cooking. *Journal of Food Science*, 63, 312 - 316.

12   Linko, P, Mercier, C., Colonna, P. (1981) High-temperature short-time extrusion cooking. *Advances in Cereal Science and Technology*, 4, 145 - 235.

13   Charm, S. E. and Wong, B. L. (1981) Shear effects on enzymes. *Enzyme and Microbial Technology*, 3, 111 - 118.

14   Thomas, R. C. and Dunhill, P. (1979) Action of shear on enzymes: studies with catalase and urease. *Biotechnology and Bioengineering*, 21, 2279 - 2302.

15   Bueche, F. (1960) Mechanical degradation of high polymers. *Journal of Applied Polymer Science*, 4, 101 - 106.

16   Cai, W. and Diosady, L. L. (1993) Model for gelatinization of wheat starch in a twin screw extruder. *Journal of Food Science*, 58, 872 - 887.

17   Einde, R. M. van den, Linden, E. van der, Goot, A. J. van der, Boom, R. M. (2004) A mechanistic model on the relation between molecular structure of amylopectin and macromolecular degradation during heating-shearing treatment. *Polymer degradation and Stability*, accepted for publication -

18   Einde, R. M. van den, Bolsius, A., Soest, J. J. G. van, Janssen, L. P. B. M., Goot, A. J. van der, Boom, R. M. (2004) The effect of thermomechanical treatment on starch breakdown and the consequences for process design. *Carbohydrate Polymers*, 55, 57 - 63.

19   Bernfeld, P. (1955) Amylases, α and β. *Methods Enzymol.*, 1, 149 - 158.

20   Vergnes, B. and Villemaire, J. P. (1987) Rheological behavior of low moisture molten maize starch. *Rheological acta*, 26, 570 - 576.

21   De Cordt, S., Hendrickx, M., Maesmans, G, Tobback, P. (1994) The influence of polyalcohols and carbohydrates on the thermostablity of α–amylase. *Biotechnology and Bioengineering*, 43, 107 - 114.

22   Komolprasert, V. and Ofoli, R. Y. (1991) Starch hydrolysis kinetics of *Bacillus licheniformis* α-amylase. *Journal of Chemical Technology and Biotechnology*, 51, 209 - 223.

23   Flanagan, J, Gunning, Y, FitzGerald, R. J. (2003) Effect of cross-linking with transglutaminase on the heat stability and some functional characteristics of sodium casinate. *Food Research International*, 36, 267 - 274.

24   Zhu, Y, Rinzema, A, Tramper, J. (1995) Microbial transglutaminase- a review of its production and application in food processing. *Applied Microbial Biotechnology*, 44, 277 - 282.

4 Production of glucose syrups in highly concentrated systems

Abstract

We have investigated the hydrolysis of maltodextrins in a high concentration (up to 70%), by means of enzymatic and acid catalysis. The study revealed that the equilibrium compositions of the catalysed reactions were kinetically determined by the selectivity of the catalyst, the substrate concentration and the reaction time. A model comprising of a set of 2 kinetic equations was used to describe the hydrolysis and condensation reactions of glucoamylase-catalysed reactions, even to highly concentrated systems. Increased substrate concentration resulted in the formation of more condensation products. The enzyme inhibition was low and was found to be independent on the substrate concentration.

1. Introduction

In the industrial process of starch hydrolysis to glucose syrup, water is used extensively as solvent. A large amount of water is added during the process and subsequently removed through evaporation, requiring a significant amount of energy. It is desired to reduce water and energy consumption during processing to develop a more sustainable process, which can be achieved by increasing the dry matter content.

The hydrolysis process can be divided into several steps, among which liquefaction and saccharification are the most important. In literature, much focus is laid upon liquefaction of starch to maltodextrins in highly concentrated systems [1-5]. This step can be performed successfully at high dry matter conditions, but the liquefact is generally diluted prior to saccharification to 35% dry matter to avoid possible limitations such as by-product formation and enzyme inhibition.

Liquefied starch is hydrolyzed to glucose by means of an enzymatic or acid catalyzed reaction. The main difference between both catalysts is the selectivity. In case of acid catalysed reactions, the glycosidic bonds are attacked by protons in random fashion [6]. Besides a hydrolysis reaction, also decomposition reactions can take place in acidic conditions, at high temperatures. Enzymatic liquefied starch is often hydrolyzed by glucoamylase to glucose syrups [7]. Glucoamylase hydrolyses α-1,4 bonds very efficiently from the non-reducing end of the maltodextrin and, at a much lower rate, α-1,6 bonds [8]. Besides hydrolysis reactions, glucoamylase also catalyses condensation reactions to a certain extend [9].

In this paper, we present our studied on the hydrolysis and condensation of saccharides in highly concentrated systems, with substrate concentrations varying from 1.7 to 3.9 mole/kg (30% – 70% dry matter). We studied the effects of type of catalyst, concentration and type of substrate on the rate of hydrolysis and condensation reactions. The experimental results for enzymatic hydrolysis are compared to kinetic models developed for enzymatic hydrolysis and condensation reactions in more diluted conditions, presented in literature [10,11]. The kinetics of acid catalysed reactions are not included because of reasons of complexity of the reaction.

2. Theoretical considerations

Glucoamylase catalyzes the hydrolysis of maltodextrins and the formation of 8 different di-and trisaccharides from glucose, with isomaltose being the main condensation product [12]. Isomaltotriose and maltose are also formed, however at a lower rate. In high dry solids

conditions, the formation of even higher oligomers occurs [13]. Therefore, we considered the hydrolysis of maltodextrins to glucose and the subsequent condensation of isomaltose and isomaltotriose starting from glucose using two kinetic models presented in literature to describe the experimental data. The kinetic scheme is presented in figure 1.
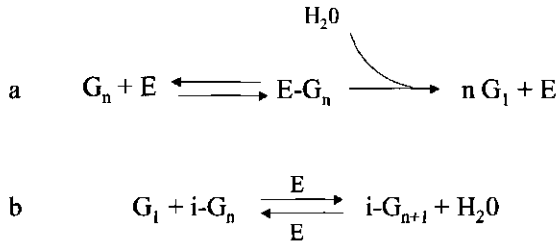

$$\text{a} \qquad G_n + E \; \rightleftharpoons \; E\text{-}G_n \; \xrightarrow{\; H_2O \;} \; n\,G_1 + E$$

$$\text{b} \qquad G_1 + i\text{-}G_n \; \underset{E}{\overset{E}{\rightleftharpoons}} \; i\text{-}G_{n+1} + H_2O$$

Figure 1: The hydrolysis (a) and condensation (b) reaction scheme's used for kinetic modeling.

Maltodextrins are a mixture of α-1,4 oligomers with various chain lengths. Modelling the full hydrolysis reaction of maltodextrins with a mechanistic model would require the inclusion of molecular weight distributions, which becomes complex [14,15]. Cepeda and co-workers modelled maltodextrins as a single reacting component, instead of a complex mixture [11]. In this paper, maltodextrins are also described as a single reaction component, which is being hydrolysed to glucose. Cepeda *et al.* compared several kinetic models and concluded that the hydrolysis reaction could be well described by Michaelis-Menten kinetics, including competitive inhibition. The rate of hydrolysis is then described by:

$$r_h = \frac{k_{cat,hyd} E C_S}{K_m \left(1 + \dfrac{(C_{S0} - C_S)}{K_i} \right) + C_S} \qquad (1)$$

where $k_{cat,hyd}$ (mole kg^{-1}s^{-1}) is a rate constant, E (g kg^{-1}) is the enzyme concentration, K_m (mole kg^{-1}) is a Michaelis-Menten constant, K_i (mole kg^{-1}) is the inhibition constant, C_S (mole kg^{-1}) the substrate concentration and C_{S0} (mole kg^{-1}) is the initial substrate concentration. The temperature dependency of the kinetic constants $k_{cat,hyd}$, K_m and K_i were included by Arrhenius relations. Cepeda *et al.* validated the model with substrate concentrations varying from 1.05 mole/kg to 1.85 mole/kg, at a temperature range from 50 to 75 °C. The model of Cepeda *et al.* was based on units of mass and was therefore corrected for the chemical gain. This correction factor becomes redundant when the concentrations are expressed in moles, as in this paper.

The condensation reactions can be described with rate equations describing reversible reactions, as presented by Beschkov [10]. The model of Beschkov was modified by the

introduction of the enzyme concentration to account for enzyme activity. The rate equation for the condensation reaction can be described by:

$$r_{c,n} = k_{cat,iso} E\left(C_{G1} C_{iGn-1} - \frac{C_{iGn}}{K_{eq,iso}} \right)$$ (2)

where $k_{cat,iso}$ (kg mole^{-1}s^{-1}), E (g kg^{-1}) is the enzyme concentration, $K_{eq,iso}$ (kg mole^{-1}) is a constant, G_1 (mole kg^{-1}) the glucose concentration and iG_n (mole kg^{-1}) the concentration iso-oligomer with length n. The rate constant $k_{cat,iso}$ was used as adjustable parameter to correct for the difference in temperature between the study of Beschkov *et al.* and this study and to account for the difference in enzyme concentration between both studies.

As already stated, formation of components larger than penta-mers can often be neglected. In the reaction scheme, we have taken this into account by stating that isomaltopentaose cannot polymerise further. Nikolov and co-workers showed that the formation of maltose was small compared to the formation of isomaltose and isomaltotriose and was therefore not included in the kinetic scheme, depicted in figure 1 [12]. The rate equations for the individual components then become:

$$\frac{dC_{G1}}{dt} = r_h - 2r_c$$

$$\frac{dC_{iG2}}{dt} = 0.5r_{c,2} - r_{c,3}$$

$$\frac{dC_{iG3}}{dt} = r_{c,3} - r_{c,4}$$ (3)

$$\frac{dC_{iG4}}{dt} = r_{c,4} - r_{c,5}$$

$$\frac{dS}{dt} = -r_h$$

Where G_1 is the glucose concentration, iG_2 is isomaltose, iG_3 is isomaltotriose and iG_4 is isomaltotetraose, S is the maltodextrin concentration and r_h and r_c the rate equations for respectively the hydrolysis and condensation reaction, defined above.

The adjustable parameters were fitted to the experimental data in Aspen Custom Modeller version 12.1.6, using a least square method.

3. Materials and methods

3.1 Materials

The D-glucose and crystalline maltose were obtained from Merck. The maltodextrins (DE 16.5 – 19.5) were obtained from Sigma-Aldrich (419699). The average degree of polymerisation of the maltodextrins was found to be 5.66, analysed with HPLC method (see 2.2.2). Maltodextrins were considered to be straight α-1,4 glucose chains. The degree of branching (α-1,6) was assumed to be low (<5%) and therefore was assumed to hardly influence the reaction kinetics [11]. Glucoamylase from *Aspergillus niger* (Fluka 10113; activity 120 U/mg) was used. The enzyme (8.3 mg/ml buffer solution) was dissolved in a 20 mM Sodium Acetate buffer solution at pH 5.5, just prior to the experiment.

3.2 Methods

3.2.1. Experimental methods

Two experimental methods were applied to study the hydrolysis and condensation reactions. The concentrations glucose, maltose and maltodextrins are expressed as glucose-units per unit of mass (i.e. 0.5 mole kg^{-1} maltose = 1 mole kg^{-1} glucose units). The concentrations equivalent to glucose used are 1.65 mole kg^{-1}, 2.75 mole kg^{-1} and 3.9 mole kg^{-1}, equivalent to 30% w/w, 50% w/w and 70% w/w dry matter respectively.

Method A comprises the following steps:

We prepared solutions of a specific glucose and maltose composition in 1.5 ml reaction tubes, with 1 g reaction mixture. The substrate was mixed with demineralised water (in case the acid catalysed experiments) or buffer solution (in case the glucoamylase experiments) and was heated to 100 °C to dissolve the substrate. Subsequently, the reaction mixtures were cooled a thermo-stated block heater (Grant) to the reaction temperature. Adding the catalyst, being either HCl (leading to 1M HCl in the reaction mixture) or glucoamylase solution (100 µl), started the reaction. The enzyme reactions were carried out at 60 °C, the acid catalysed reactions 75 °C. The reaction time was 2 h in most experiments. The reaction was stopped by diluting 0.5 g reaction mixture in 0.1 M NaOH. The diluted enzyme reaction mixtures were filtered using Microcon YM 10 filters with a molecular weight cut-off of 10 kDa to remove the enzyme. After the centrifuge step, the samples were analysed using HPLC (see 2.2.2). The composition after the reaction was compared to the initial composition. If the relative concentrations of the relevant components were not changed, it indicated that the system was in equilibrium (or steady-state) for that reaction. The method was used to study both the dynamics of reactions and the equilibrium composition

Method B:

The hydrolysis and condensation reactions were carried out starting with glucose of maltodextrins and analysed as described in the in the previous section. Samples were taken at various time intervals during the reaction.

3.2.2 HPLC Analysis

The composition of the reaction mixture was quantified on the fraction of oligomers per DP with an RSO-oligosaccharide column (Phenomenex, Amstelveen, the Netherlands) and analysed using refractive index. The column was operated at 80 °C and was eluted with Millipore water at a flow rate of 0.3 ml/min. The oligomers range that can be distinguished with this column is from DP1 to DP 11.

The presence of α-1,4 and α-1,6 bonds in some final samples was analysed with a Carbopac PA1 column (Dionex), in combination with electrochemical detection. The system was eluted with a gradient of 0.1 M sodium hydroxide, 1 M sodium acetate in 0.1 M sodium hydroxide and Millipore water, at a flow rate of 1 ml/min. The retention times of specific mono- and oligosaccharides were validated with standard solutions of the specific components.

4. Results

4.1 Enzyme catalysed reactions

Figure 2 shows the results of experiments with mixtures of glucose and maltose (method A), where the degree of polymerisation (d.p.) at t_0 (i.e. before the reaction) is plotted versus the d.p. at t_1 (i.e. after the reaction) at 60 °C at various times. When going from 1 to 2 h, more maltose was hydrolysed. However, after 24 h, an increased d.p. was observed indicating that a slow condensation reaction occurred. HPLC (Dionex) analysis revealed the formation of 1,6 bonds, which is in agreement with results by Nikolov *et al.* [12], who reported that glucoamylase mainly catalyses the condensation reactions to isomaltose and isomaltotriose.
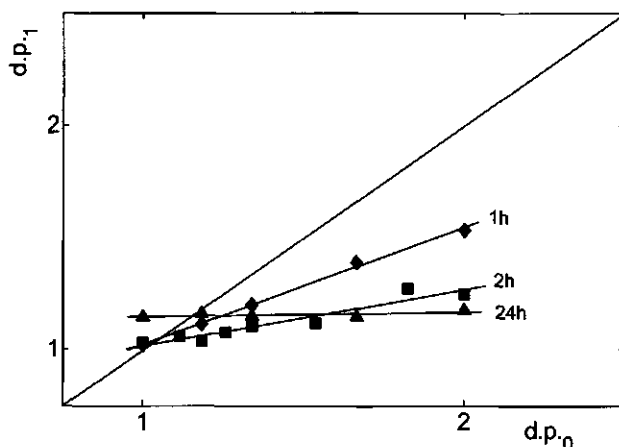
Figure 2: Effect of substrate concentration on the development of the equilibrium, measured with experimental method A. The d.p. is plotted at t_0 and after 1h ($\blacklozenge$), 2h ($\blacksquare$) and 24h ($\blacktriangle$). The substrate concentrations was 3.9 mole kg^{-1},

Method B was used to gain insight in the dynamics of the reaction. Glucose and maltodextrins were incubated for 24h at three different substrate concentrations. After 24 h reaction time, hardly any colour formation was observed, suggesting limited Maillard reactions. The enzymatic reaction of glucose and maltodextrins at high dry solids conditions are compared in figure 3. The lines are simulations of the reaction kinetics, using two kinetic models describing the hydrolysis of maltodextrins and the condensation of glucose and will be discussed in section 5.2. The figure shows a rapid hydrolysis of maltodextrins to glucose, followed by a consecutive reaction. The figure also shows that the extent of the condensation reaction is almost independent of the starting material, after a certain reaction time. The experimental results were confirmed by measuring the product composition after a reaction of 24 h using HPLC (see table 1). The compositions of the final products were rather independent of the starting material, being either glucose or maltodextrins. HPLC analysis (Dionex) showed that the DP2 and DP3 fractions mainly comprised α-1,6 bonds and that hardly any α-1,4 bonds were present after a reaction of 24 h. This means that the DP2 fraction is mainly isomaltose and the DP3 fraction is mainly isomaltotriose.

Furthermore, it was found that increased dry matter content resulted in increased formation of condensation products, both in quantity as well as the length of the polymer increased. The maximum length of the polymer chain comprised 5 monomer units.
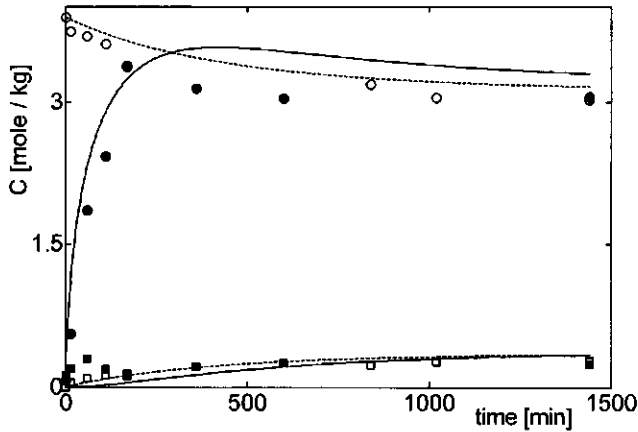
Figure 3: The concentration glucose (●) and disaccharide (■) are plotted in time during enzymatic hydrolysis of maltodextrins and the condensation of isomaltose time, starting with glucose (open symbols) or maltodextrins (closed symbols) in conditions with 60% dry matter. Also the predicted concentrations are plotted for the same conditions starting from glucose (dashed line) or maltodextrins (solid line).

Table 1: Product composition in mass fractions after 24 h, starting with 3.9 mole kg^{-1} dry matter of glucose, maltose or maltodextrins.

Substrate	x_{Dp1}	x_{Dp2}	x_{Dp3}	x_{Dp4}	x_{Dp5}
Glucose	0.79	0.14	0.05	0.02	-
Maltose	0.77	0.13	0.06	0.03	0.01
Maltodextrins	0.81	0.12	0.04	0.02	-

4.2 Acid catalysed reaction

The effects of substrate concentration and temperature on the condensation of glucose and the hydrolysis of maltodextrins with acid catalysis (HCl) were studied. The substrate concentration and composition were both varied at a reaction temperature of maximally 75 °C. As in section 1, short time experiments (method A) were carried out to get an initial estimate of the equilibrium concentration. Figure 4 shows formation of glucose at high maltose concentrations, while dp2 oligomers were formed at high glucose concentrations. This effect was enhanced by increased substrate concentration. HPLC analysis revealed that during the reaction, also tri- and tetramers were formed. Therefore, the reaction was followed for 24h to study the dynamics of the reaction system, starting with either glucose or maltodextrins (method B). These results showed that increased substrate concentration led to a higher degree of polymerisation, which trend corresponds to the glucoamylase catalysed

reactions (figure 5). HPLC analysis revealed that the lengths of the polymers chains found were up to 7 monomer units, which is longer than found with glucoamylase-catalysed reactions, at comparable substrate concentrations.
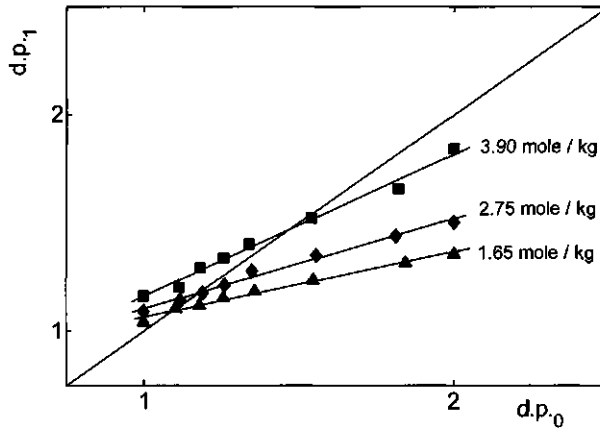

Figure 4: Effect of substrate concentration on the equilibrium with acid catalysis, measured with method A. The d.p. is plotted at t_0 and after 2 h. The initial substrate concentration was 1.6 mole kg^{-1} (30% D.M.; ▲), 2.7 mole kg^{-1} (50% D.M.; ◆) and 3.9 mole kg^{-1} (70% D.M.; ■) expressed in glucose units.
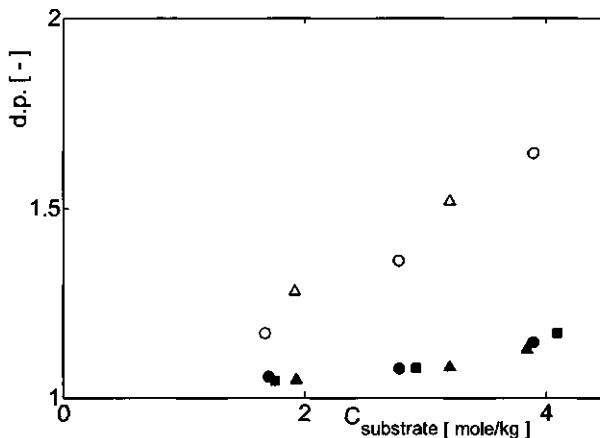

Figure 5: The degree of polymerisation is plotted as a function of the initial substrate concentration for both acid catalysed (open symbols; T = 75 °C) and glucoamylase (filled symbols; T = 60 °C) catalysed reactions after a reaction time of 24 h. The initial substrates were glucose (●), maltose, (▲) or maltodextrins (■).

5. Discussion

5.1 The effect of the type of catalyst

The final product composition strongly depended on the catalyst used. The acid catalysed system resulted in a number average degree of polymerization of 1.7 at the highest dry matter content, where the final d.p. for the enzyme system was only 1.15 (figure 5) at comparable conditions. The differences in behaviour of the catalyst can be explained by the selectivity of the catalyst. The enzyme is very selective for α-1,4 glycoside bonds and α-1,6 bonds [12], with the latter reaction being slower than the former one. Condensation products were only formed from glucose. In case of a reaction in acid conditions, many other reactions are possible due to the random nature of proton catalysis [6]. The occurrence of other reactions makes complete, selective hydrolysis to glucose unlikely. In other words, the final composition of the product is kinetically controlled.

5.2 Kinetic modelling of the glucoamylase reactions

The adjusted kinetic models by Cepeda *et al.* [11] and Beschkov *et al.* [10}, described in section 2, were used to describe the hydrolysis and condensation reactions respectively. The kinetic constants used in this study are plotted in table 2. The enzyme concentration (mg kg^{-1}) was incorporated in the condensation model. The inhibition constant of the hydrolysis reaction was increased with a factor 3. This implies that the level of inhibition is lower than that reported by Cepeda and co-workers, even at high substrate concentrations. This is remarkable, because the use of very high substrate concentrations could lead to stronger substrate inhibition compared to conventional conditions. The reversible reaction of glucose and maltose was not included in the reaction scheme, which justified by HPLC (Dionex) results showing hardly any maltose after 24h reaction time. The condensation model was applied for the condensation of isomaltotriose and isomaltotetraose. The models describe the dynamics of the reactions well, starting from both glucose and maltodextrins, even for the highly concentrated conditions. This confirms the consecutive nature of the reaction as outlined in figure 1.

Table 2: The kinetic parameters of the kinetic models, describing the hydrolysis and condensation reaction

Constant	A	E_a (kJ mol^{-1})
$k_{cat,hyd}{}^a$	1.61^e-2 mole kg^{-1} s^{-1}	4.51
$K_m{}^a$	0.339 mole kg^{-1}	2.20
$K_i{}^a$	8.9^{e}3 mole kg^{-1}	35.20
$k_{cat,iso}$	3^e-6 kg mole^{-1} s^{-1}	-
$K_{eq,iso}$	0.037 kg mole^{-1}	-

^{a}: $k = Ae^{\left(-\frac{Ea}{RT}\right)}$

Based on the results described above, it can be concluded that the formation of side products is a function of the substrate concentration, reaction time and selectivity of the catalyst.

6. Concluding remarks

The possibilities for the hydrolysis of maltodextrins in highly concentrated systems were studied. We can conclude that the use of very high concentrations for hydrolysis of starch or maltodextrins is certainly possible, where exact reaction conditions to be used depends on the importance of product composition. The hydrolysis of maltodextrins leads to a product composition that is kinetically controlled. This conclusion can also be drawn from other kinetic experiments that showed that the yield of glucose decreased at higher substrate concentrations and showed an optimum in time. The reaction kinetics could be well described even in highly concentrated conditions, by using a model comprising two kinetic equations presented in literature, after slight modifications. Since higher substrate concentrations leads to higher formation of by-products, it is beneficial to develop enzymes having improved selectivity to improved product yields.

Kinetic studies in which the substrate composition was varied (method A) proved to be a fast and useful tool to study equilibrium reactions. Short reaction times have the advantage that slow side reactions can be virtually excluded. By comparing short and longer reaction times, information about the nature of the equilibrium could be obtained after sufficient reaction time.

Reference List

1   Govindasamy, S., Campanella, O. H., Oates, C. G. (1997) Enzymatic hydrolysis of sago starch in a twin-screw extruder. *Journal of Food Engineering*, 32, 403 - 426.

2   Hakulin, S., Linko, Y. Y., Linko, P., Seiler, K., Seibel, W. (1983) Enzymatic conversion of starch in twin-screw HTST-extruder. *Starch*, 12, 411 - 414.

3   Linko, P, Mercier, C., Colonna, P. (1981) High-temperature short-time extrusion cooking. *Advances in Cereal science and technology*, 4, 145 - 235.

4   Reinikainen, P., Suortti, T., Olkku, J., Malkki, R, Linko, P (1986) Extrusion cooking in enzymatic liquefaction of wheat starch. *Starch*, 38, 20 - 26.

5   Roussel, L., Vieille, A., Billet, I., Cheftel, J. C. (1991) Sequential heat gelatinisation and enzymatic hydrolysis of corn starch in an extrusion Reactor. optimisation for a maximum dextrose equivalent. *Food science and Technology*, 24, 449 - 458.

6   Zherebtsov, N. A., Ruadze, I. D., Yakovlev, A. N. (1995) Mechanism of acid-catalyzed and enzymatic hydrolysis of starch. *Applied Biochemistry and Microbiology*, 31, 511 - 514.

7   Pandey, A (1995) Glucoamylase research: an overview. *Starch*, 47, 439 - 445.

8   Chiba, S (1997) Molecular mechanism in α-glucosidase and glucoamylase. *Biosci.Biotech.Biochem*, 61, 1233 - 1239.

9   Roels, J. A. and Tilburg, R. van (1979) Kinetics of reactions with amyloglucosidase and their relevance to industrial applications. *Starch*, 31, 338 - 345.

10   Beschkov, V., Marc, A, Engasser, J. M. (1984) A kinetic model for the hydrolysis and synthesis of maltose, isomaltose and maltotriose by glucoamylase. *Biotechnology and Bioengineering*, 26, 22 - 26.

11   Cepeda, E., Hermosa, M., Ballosteros, A. (2001) Optimization of maltodextrins hydrolysis by glucoamylase in a batch reactor. *Biotechnology and Bioengineering*, 76, 70 - 76.

12   Nikolov, Z. L., Meagher, M. M., Reilly, P. J. (1989) Kinetics, equilibrium and modeling of the formation of oligosaccharides from d-Glucose with *Aspergillus niger* Glucoamylase I and II. *Biotechnology and Bioengineering*, 34, 694 - 704.

13   Fujimoto, H, Nishida, H., Ajisaka, K (1988) Enzymatic synthesis of glucobioses by a condensation reaction with α-glucosidase, β-glucosidase and glucoamylase. *Agric.Biol.Chem.*, 52, 1345 - 1351.

14   Akerberg, C., Zacchi, G., Torto, N., Gorton, L. (2000) A kinetic model for enzymatic wheat starch saccharification. *Journal of Chemical Technology and Biotechnology*, 75, 306 - 314.

15   Dean III, S. W. and Rollings, J. E. (1991) Analysis and quantification of a mixed exo-acting and endo-acting polysaccharide depolymerisation system. *Biotechnology and Bioengineering*, 39, 968 - 976.

5 Starch hydrolysis under low water conditions: a conceptual process design

Abstract

A process concept is presented for the hydrolysis of starch to glucose in highly concentrated systems. Depending on the moisture content, the process consists of two or three stages. The two-stage process comprises combined thermal and enzymatic liquefaction, followed by enzymatic saccharification. The three-stage process starts with shear induced melting of starch, followed by enzymatic liquefaction and saccharification. At low moisture content, the shear stress needed to completely melt corn starch is so high that significant enzyme inactivation cannot be avoided, which leads to a need for separating starch melting and liquefaction in two separate processing steps. Assuming the use of currently available enzymes, the final product composition was estimated to contain 69% to 93% glucose, starting with respectively 65% and 35% dry starch. These results showed that the formation of side-products, mainly isomaltose and isomaltotriose, increased with increasing dry matter content. Increasing the dry matter content from 35% to 65% resulted in increasing reactor productivity of 17%, while the amount of water that should be removed from the system was reduced by 87%.

Key words: Corn starch hydrolysis, liquefaction, saccharification, enzymes, low water conditions

1. Introduction

Currently, industrial processes producing glucose syrups from starch use excess water. Starch is hydrolyzed using a dry matter content of about 35% initially. During the hydrolysis reaction, a certain amount of water is consumed. The theoretical amount of water that is required for complete hydrolysis of starch to glucose is defined to as chemical gain [1]. In case of a solution containing 35% starch initially, approximately 5% of the initial water concentration is used for this chemical gain. Considering that the final product contains about 80% w/w dry matter, it can be calculated that 10 to 15% of the water will still be present in the final product (80% dry matter). In this view, the excess of water in the current industrial processes is approximately 5 times the minimal required amount, leaving space for process intensification by reducing the water content during the hydrolysis process. Design of a starch hydrolysis process at ultra-low water content is interesting for a number of reasons. Reduction of the initial water content will reduce the amount of water that needs to be evaporated from the final product, thus reducing processing costs and simplifying the process layout. Secondly, a reduction in water content leads to an improved utilisation of assets, either by a higher throughput through existing equipment or the same throughput through smaller equipment.

Most industrial processes use enzymes to hydrolyze starch to high DE glucose syrups, usually in a two-step process: liquefaction and saccharification [2]. In the first step, starch is gelatinised by a thermal treatment in excess water at temperatures higher than 110 °C. During the thermal treatment, starch is also hydrolysed by a thermo-stable α-amylase, which is added to the starch slurry just prior to the thermal treatment. Due to the differences in time-scale of the gelatinisation and enzymatic liquefaction process, the starch paste is flash-cooled to 95 °C and maintained at this temperature for 60 to 90 minutes to complete the enzymatic liquefaction. After this step, a product resembling maltodextrins (DE 9-14) is obtained. In the second step, the mixture is cooled to approximately 60 °C and the maltodextrins are hydrolyzed completely to glucose by a glucoamylase [3]. Excess water is used to facilitate gelatinization and ensure sufficient mixing during the reaction.

A reduction of the water content is expected to complicate processing. A reduction of the water content will lead to an increasing viscosity of the reaction mixture and an increasing melting temperature of starch [4]. The melting temperature increases from 72 °C at 60% moisture to 109 °C at 40% moisture and 120 °C at 30% moisture [5]. Barron et al. studied the effect of a heating and shearing treatment on the disruption and melting of starch and reported that starch could be melted completely by a combined heating shearing treatment [6]. Since an extruder is able to continuously create high shear, it is often studied to perform the first step in the hydrolysis process with dry matter conditions from 50% up to 80% w/w, combining

melting and initial enzymatic hydrolysis [7-10]. Despite of some positive initial results, several reasons make it unlikely that the extruder is the best means for the enzymatic liquefaction process. Firstly, an important effect is the large changes in viscosity of the reaction mixture while the reaction proceeds. The drop in viscosity makes operation of the extruder unstable [11]. Furthermore, shear induced inactivation of enzymes is expected to occur, due to peak shear stresses [12]. Several researchers experimentally observed this effect [13-16]. To overcome these problems, Grafelman and Meagher combined shear-induced disclosure of starch using a single screw extruder, followed by a post extrusion reaction in a static mixer reactor [11]. The α-amylase was injected just prior to the die of the extruder, thereby avoiding most shear induced inactivation of the enzyme.

Another processing issue might be that enzyme activity during liquefaction and saccharification could be influenced negatively, for example by various inhibition reactions. However, enzymatic liquefaction under highly concentrated conditions can be successful with 45 to 65% starch at temperatures of 100 - 125 °C [17,18]. The rate of hydrolysis of α-amylase was reported to reduce only slightly when increasing the dry matter content from 45% to 65% [19]. Unfortunately, no kinetic model has been presented, that describes the enzymatic hydrolysis of starch to oligomers in low water conditions in quantitative terms.

The saccharification step is often carried out with glucoamylase from *Aspergillus niger* [20,21]. The enzyme hydrolyses α−1,4 bonds efficiently to glucose and catalyses a condensation reaction of primarily 1-6 bonds [22,23]. Prior to saccharification, the mixture is often diluted to 30 − 35% dry matter, thereby losing the potential benefits of high dry matter conditions [10]. Some of the reasons to do this are the avoidance of possible enzyme inhibition and Maillard reactions [24]. Also, consecutive reactions can be suppressed by dilution [25]. Recently, Van der Veen and co-workers presented a quantitative description combining the kinetics of hydrolysis of maltodextrins and the condensation of isomaltose and isomaltotriose [26]. It was also shown that product inhibition of the enzyme was rather limited, even at high dry matter contents. They concluded that maltodextrins could be hydrolysed to glucose, although some formation of isomaltose and higher oligomers could not be avoided at high starch concentrations.

In perspective of the available literature, there seems potential for the hydrolysis of starch in ultra low water conditions. For an optimal process design, a quantitative correlation between process parameters and product properties should be investigated. In this paper, we will investigate starch hydrolysis in low water conditions (< 43% water) and the implications of the design of the process on product properties. For this purpose, we used a shearing

device, in which the processing conditions occurring in high shear devices such as extruders can be studied in detail [27]. The shearing device was based on the cone and plate concept. The shear rate can be controlled, while the shear stress can be accurately measured. The shearing device was applied to study melting and initial enzymatic liquefaction of corn starch in low water conditions. After that, we investigated whether the liquefied corn starch can be enzymatically hydrolysed to high DE-products by means of glucoamylase. Finally, these results were concluded in a conceptual process design, indicating configuration and conditions in all processing steps.

2. Materials and methods

2.1 Materials

The starch used was commercially available corn starch (C2000, food grade) and was kindly provided by Cargill R & D Europe. The dry matter content of the starch was 89%. The liquefying enzyme used was thermo-stable α-amylase from *Bacillus licheniformis* from Novozyme (Termamyl 120 LC) and kindly provided by Cargill R & D Europe. The saccharification enzyme was glucoamylase from *Aspergillus niger*, obtained from Fluka (10113). Just prior to the experiment, the enzyme (8.3 mg / ml buffer solution) was dissolved in 1 ml 20 mM sodium acetate buffer solution with pH 5.5. The moisture content of starch was adjusted to the desired moisture content with a 50 mM sodium acetate buffer solution, pH 5.8, with 5 ppm calcium chloride.

2.2 Experimental methods

Shearing treatments were carried out in a shearing device, previously used to study the effect of shear stress on the inactivation of α-amylase by Van Der Veen and co-workers [12]. Just prior to a shearing experiment, a buffer solution, with or without α-amylase, was added to the starch, while mixing continuously to assure homogeneous distribution of the buffer solution over the dry starch. In case of enzyme addition, 4.5 ml enzyme per kg dry starch was added. The shearing device was then filled with the starch / buffer / enzyme mixture after which the system was closed and heated to 90 or 110 °C. When the temperature set point was reached, the initial rotational speed was set at 10 rpm, which corresponds to a shear rate of 24 s^{-1}. After 120 s, the rotational speed was increased to 50 rpm ($\dot{\gamma}$ =120 s^{-1}) and was kept constant during the remaining of the experiment. Directly after the shearing treatment, part of the sample was diluted in 90% DMSO, as preparation for Gel Permeation Chromatography (GPC) analysis. A small amount of the liquefied material was transferred from the shear cell

into reaction tubes of 1.5 ml and diluted to a moisture content varying from 35 to 70% w/w. After the dilution step, glucoamylase was added to the mixture and was incubated for 24 h at 60 °C in a thermo stated heater block (Grant). The samples were mixed at regular intervals. After the incubation, the reaction was stopped by diluting 0.5 g of the reaction mixture in 0.1 M sodium hydroxide solution. The insoluble parts were removed by centrifugation (Eppendorf centrifuge, 15 min, 13000 rpm). The clear supernatant was filtered using Microcon YM-10 filters, followed by a centrifugation step (Eppendorf, 15 min. 13000 rpm) and subsequently diluted and analysed using HPLC.

2.3 Analysis

2.3.1 X-ray analysis:
X-ray analyses were carried out according to the method, described by Van Den Einde and co-workers [27].

2.3.2 Gel Permeation Chromatography
The samples obtained after the shearing treatment were dissolved in a mixture containing 90% DMSO and 10% water and analysed with Gel Permeation Chromatography (GPC). The columns used were Shodex KS-806, KS-804 and KS-802 and were operated at 75 °C. The columns were eluted with 50 mM NaOH with a flow rate of 1 ml / min. The samples were analysed with refractive index measurement. The system was calibrated with pullulans of various molecular weights. The calibration curve is plotted in figure 3. The number average and weight average molecular weight were calculated, based on the calibration with pullulans.

2.3.3 HPLC
The soluble part of the products after saccharification was analyzed by a HPLC with a RSO Oligosaccharide column (Phenomenex) at 80 °C, eluted with Milli-Q water (flow rate 0.3 ml / min). The samples were analysed using refractive index measurement (RI).

2.4 Degree of Polymerisation
The number average degree of polymerisation (d.p.) of the reaction mixture was calculated using [28]:

$$DP = \frac{\sum_n n C_n}{\sum_n C_n} \tag{1}$$

where n is the number of monomer units in the oligomer and C_n the concentration of the oligomer with length n.

2.5 Dextrose equivalent

The degree of polymerisation is often expressed as Dextrose equivalent [29]. For a single oligomer with length n, the DE can be calculated with [29]:

$$DE = \frac{Mw_{Glucose}}{Mw_{Gn}} 100 \tag{2}$$

where $Mw_{glucose}$ is the molecular weight of glucose and Mw_{Gn} the molecular weight of an oligomer with length n. For mixtures of oligomers with various chain lengths, the DE can be calculated with:

$$DE = \frac{Mw_{Glucose}}{\sum_{n} x_x Mw_{Gn}} 100 \tag{3}$$

where x_n is the mole fraction of oligomer with length n.

3. Results and discussion

Starch - water mixtures, with α-amylase added in some cases, were sheared at 90 °C or 110 °C. In some experiments, some inhomogeneity of the starch paste was observed after shearing. The colour of the starch paste was yellowish in all cases. In some experiments, the use of α-amylase resulted in a low viscous liquid instead of a paste, indicating significant hydrolysis of starch. The colour of the viscous liquid was slightly darker than the colour of the starch paste.

3.1 Liquefaction in low moisture conditions

Complete disclosure and melting of starch is a prerequisite for complete hydrolysis of starch. We used the shearing device to study the effect of shear forces on the melting behaviour of corn-starch and the starch hydrolysis reaction by means of α-amylase. Table 1 summarizes the experimental conditions, the maximum shear stress obtained and the number average and weight average molecular weight of the liquefied starch.

Two typical shearing profiles are plotted in figure 1. The moisture content of the starch was 30% and the temperature during the shearing treatment was 90 °C (1). The shear stress started to increase after 120 s, probably due to gelatinisation of the starch. After 280 s, the shear stress decreased again, which is probably caused by thermo-mechanical breakdown of the corn starch [27]. When α-amylase was present in the mixture (2), a comparable shear stress profile was observed, although the maximum shear stress was only half compared to the experiment without the enzyme. Furthermore, the shear stress decreased more rapidly than without α-amylase. These results indicate that α-amylase was active in conditions with 30%

moisture, which is in agreement with results presented by Curic *et al.* [19]. When the starch granules were disrupted, they were susceptible to enzymatic hydrolysis immediately [30]. The random hydrolysis resulted in a large rapid decrease of the paste viscosity, which is monitored as a fast reduction in torque value.
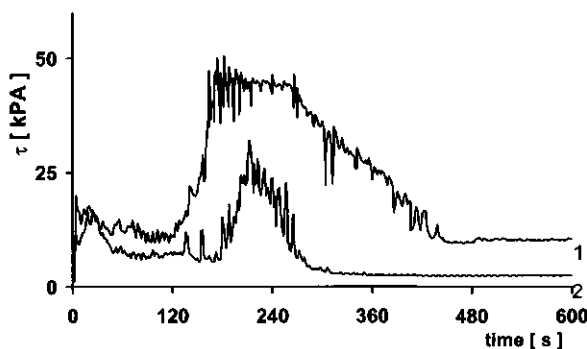

Figure 1: The effect of α-amylase on the shear stress profile of cornstarch during a shearing treatment at 90 °C with 30% w/w moisture initially (2), in comparison with starch treated in similar conditions without α-amylase (1).

To evaluate the remaining crystallinity, some samples were analysed with X-ray diffraction. Figure 2 shows X-ray diffraction patterns of starch after a shearing treatment, in comparison with native corn starch (n). Starch with 30% moisture was almost completely melted, by means of a shearing treatment at 90 °C (2). When a comparable mixture was sheared in the presence of α-amylase, almost all native crystals were still present, indicating that hardly any melting occurred (1). The main difference between both experiments was the maximum shear stress, which decreased from 50.5 kPa (2) to 24.3 kPa, in case □-amylase was added to the system (1). When a comparable mixture, with 30% moisture and α-amylase, was sheared at 110 °C (4), the shear stress was increased to 38 kPa. The extent of melting was significantly larger, although still a large fraction of native starch granules was observed. The increased shear stress can probably be explained by enhanced melting. Shearing starch with 37% moisture at 110 °C resulted in almost complete melting of the sample and a maximum shear stress of 31 kPa (3). It seems therefore possible to melt starch below the melting temperature, provided that a shear stress higher than 30 kPa is applied in case of reaction temperatures of 110°C.
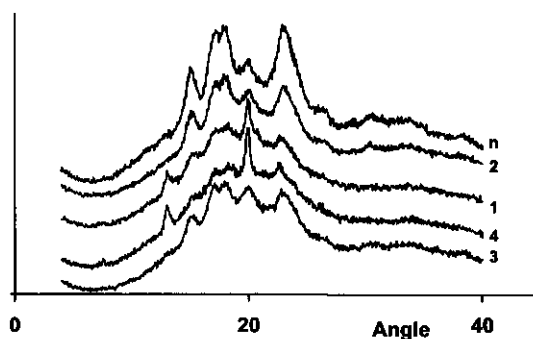
Figure 2: X-ray diffraction patterns of native corn starch (n); 30% moisture at 90 °C (1); 30% moisture at 90 °C + α-amylase (2); 30% moisture at 110 °C + α-amylase (3); 37% moisture at 110 °C (4).

The molecular weight distributions of several samples were analysed with GPC-analysis. Three typical chromatograms are depicted in figure 3. The weight-averaged molecular weight of native cornstarch was found to be around 23 MDa. Two distinct peaks can be seen in the chromatogram for native cornstarch (1), the first peak after 15 minutes, the second after 19 minutes. The first peak disappeared (2) after a shearing treatment with 30% moisture at 90 °C, which can probably be explained by thermo-mechanical breakdown of starch [27]. When α-amylase was present, the weight-averaged molecular weight was reduced to 56 kDa after a shearing treatment of almost 1800 s (3), as shown in table 1, experiment 2. Increasing the temperature to 110 °C resulted in even a lower molecular weight, just as an increase in the moisture content from 30% to 43%.

3.2 Saccharification

Enzymatically liquefied starch, obtained after a shearing treatment (table 1: experiment 5, 6 and 7), was incubated with glucoamylase at 60 °C for 24 h, with dry matter contents varying from 65% w/w to 30% w/w. The experimental conditions and results are summarised in table 2. The substrate concentrations given in table 2 are estimates of the concentration at the start of the saccharification reaction, since some evaporation of water during the opening of the shear cell and sample handling could not be avoided. After the saccharification reaction, some native starch granules were observed in the insoluble part of the sample, indicating that the starch was not completely gelatinised, thereby confirming the results of the X-ray measurements described in the previous section. The composition of the soluble sample was determined using HPLC-analysis.
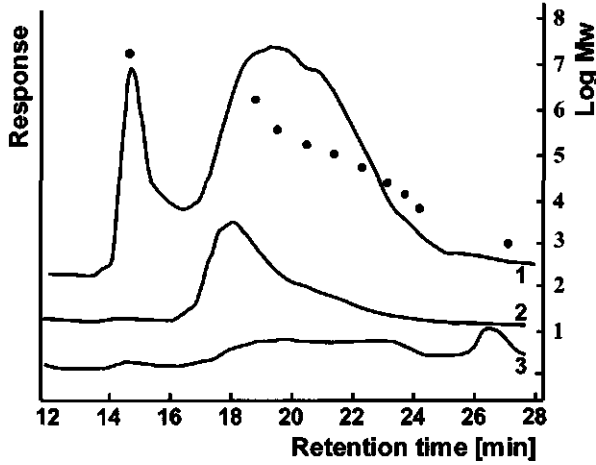
Figure 3: GPC analysis of native cornstarch (1) and after a shearing treatment at 90 °C without (2) and with (3) the presence of α-amylase with 30% moisture initially. The calibration curve of the GPC-system (●) is plotted on the second y-ax

The degree of polymerisation of the soluble part after saccharification varied from 1.04 in case of approximately 30% D.M. to 1.26 in case of 65% dry matter (table 2). The lower glucose concentration and higher degree op polymerization at higher dry matter concentration were in agreement with results earlier reported using maltodextrins as staring material [26].

Table 1: overview of shear cell experiments and results

Sample code	D.M. initial [% w/w]	T [°C]	α-amylase added	τ_{max} [kPa]	Processing time [s]	M_w [kDa]
Corn starch (native)	89	-	-	-	-	2286
1	70	90	NO	50.4	984	971
2	70	90	YES	32.0	1762	501
3	70	110	YES	38.1	480	441
4	63	110	NO	31.4	720	684
5	70	110	YES	-	1790	56.4
6	60	110	YES	-	480	3.4
7	57	110	YES	-	1790	7.5

Table 2: Experimental conditions during the saccharification reaction of liquefied starch after a shearing treatment

Sample code	Shearing sample	Dry matter content [% w/w] [a]	Degree of polymerisation
S 1	5	65	1.17
S 2	5	60	1.14
S 3	5	50	1.07
S 4	5	30	1.04
S 5	6	55	1.10
S 6	6	50	1.14
S 7	6	40	1.09
S 8	6	30	1.04
S 9	7	55	1.26
S 10	7	50	1.11
S 11	7	40	1.09
S 12	7	30	1.05

[a] estimated moisture content at the start of the saccharification reaction

The results presented in this paper showed that glucose syrups with high DE values (or low DP values) could be produced under low water conditions, provided that starch is completely melted. In case of low moisture content (<35% w/w), shear forces were successfully applied to enhance melting of corn starch at temperatures below the melting temperature by applying high shear stresses, although complete melting could not be obtained in presence of enzymes.

4. Process design

The consequences of reducing the water content on process design and product composition are discussed in this section. Based on the experimental results described above, a conceptual process design is postulated and the opportunities and drawbacks of the process are discussed.

4.1 the effect of moisture content on process design

The main effect of the moisture content is its effect on the liquefaction step. At conditions with maximally 60% dry matter, corn starch can be gelatinised thermally at 110 °C [5]. Because α-amylase is thermally stable at this temperature at relevant time-scales [31], it should be possible to carry out the gelatinisation of starch in a single heating treatment in the presence of α-amylase, after which the reaction mixture could be cooled to 90 – 95 °C in a

holding tank to complete the liquefaction (figure 4a). This process is analogous to current practise, except for the large initial difference in the viscosity of the reaction mixture.

At conditions with dry matter content larger than 60% w/w, a thermo-mechanical treatment has to be applied to achieve complete gelatinisation (figure 4b). The shear stress required for complete melting depends on the moisture content and temperature, but should be at least 30 kPa, as shown in section 3.1. However, under those conditions α-amylase is inactivated because of high shear stresses exceeding 25 kPa [12]. Therefore, the liquefaction step should be carried out in a 2-step process, where the starch is melted completely by means of a thermo-mechanical treatment in the first step, followed by an enzymatic hydrolysis step with α-amylase (figure 4b). Based on the reasoning mentioned above, it seems logical that Grafelman and Meagher obtained good results by combining an extruder and static mixer for the liquefaction process at high dry matter content [11]. In this set-up, the enzyme is added to the starch paste just prior to the die of the extruder and is then homogeneously distributed in the starch matrix by means of the static mixer. The proposed 2-stage liquefaction process has not been experimentally revealed due to the fact that for an accurate measurement of the shear stress, complete filling of the shear cell was essential and therefore addition of substances during processing was not possible.

Prior to saccharification, the liquefied starch should be cooled to 60 °C before adding glucoamylase, to prevent significant thermal inactivation of the enzyme. The experimental results reported in section 3.2 show that starch can be hydrolyzed to glucose in highly concentrated systems.

.

4.2 effect of moisture content on product composition

The use of glucoamylase resulted not only in fast hydrolysis of maltodextrins but also to a consecutive condensation reaction, with isomaltose being the main product [23]. The hydrolysis reaction of maltodextrins could be well described by Michealis-Menten kinetics including competitive inhibition [24], while the condensation reactions can described as an equilibrium reaction [32]. Van der Veen et al. extrapolated these findings to high dry matter conditions and showed that the equations could be used to predict the product composition well [26]. The obtained DE value is plotted as a function of the substrate concentration and the reaction time (figure 5). The figure shows that starting with a maltodextrin concentration of 2.5 mole / kg (45% w/w D.M.), still a product with a DE of 95 can be produced. However, a clear optimum in the reaction time exists at approximately 400 minutes. At this stage, conversion is high while the extent of consecutive reactions is still limited. Increasing the

substrate concentration to 4 mole / kg (72% w/w D.M.) can still lead to a product with a DE value larger than 90. It should be noted that these results are specific for this type of glucoamylase used. A more selective enzyme will result in higher DE values, even at high substrate concentration, as our previous study showed that the final product composition is kinetically controlled in those process conditions[26].
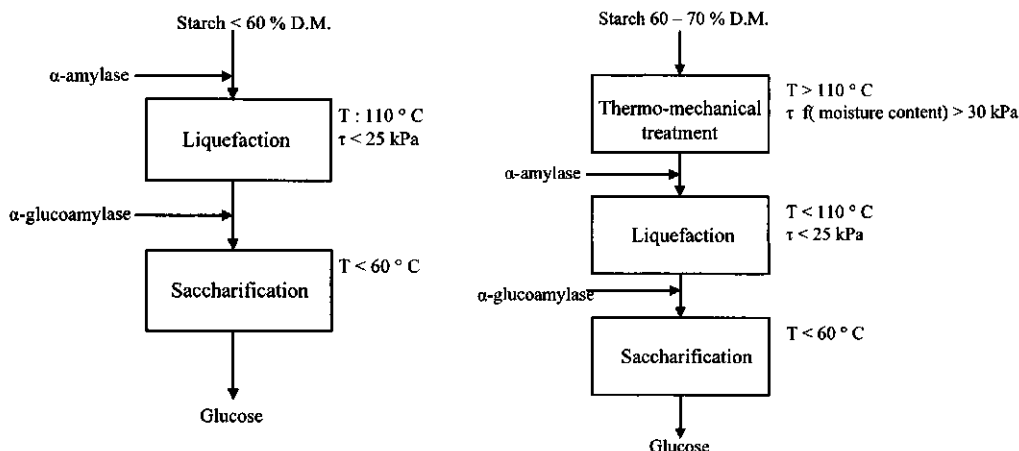

Figure 4: The hydrolysis of starch with maximally 60% dry matter can be carried out in a 2-step process (a), where starch is melted by means of a thermal treatment and hydrolysed by α-amylase in the first stage and in the second stage hydrolysed to glucose by glucoamylase. Starch with lower moisture contents can be hydrolysed in a 3-step process (b) where starch is melted by a thermo-mechanical treatment and subsequently hydrolysed by α-amylase and glucoamylase
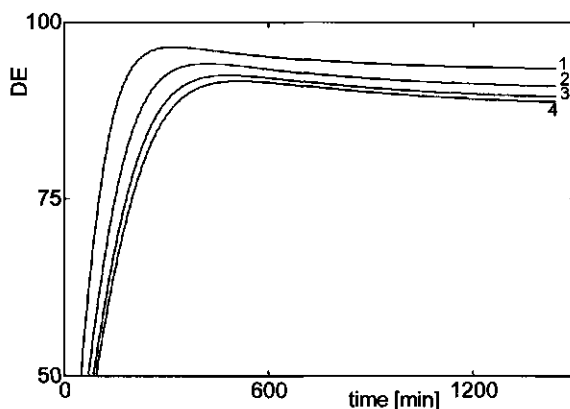

Figure 5: The DE values are plotted as a function of reaction time for initial dry matter concentrations of 35% (1), 50% (2), 60% (3) and 65% (4). The plot is a result of simulations of the hydrolysis of maltodextrins using kinetic models described by van der Veen and co-workers (2005)

4.3 Overall process design for starch hydrolysis in highly concentrated systems.

Three processes for the production of 10 ton/h glucose are compared. The results of the design calculations are summarised in table 3. Process A is comparable to the traditional process, in which the initial dry matter content is around 35% w/w. In process B, the initial dry matter content is 60% w/w, which enables complete melting of starch by a thermal treatment in conditions at which α-amylase is thermally stable, according to results presented by Donovan [4]. Process C starts with 65% dry weight, implying that shear combined with a high temperature is needed to obtain complete gelatinisation. The saccharification of liquefied starch is considered as a consecutive reaction, with glucose being the intermediate, which can subsequently be converted into isomaltose. Therefore, a continuous stirred reactor is unsuitable, because this reactor is operated at maximum glucose concentration, which influences the yield negatively. A batch reactor or a plug flow reactor seems more appropriate.

Table 3: The volumetric reactor volume, the required reactor volumes for liquefaction and saccharification and the maximal DE as a function of the initial dry matter content.

Process	Dry matter content [% w/w]	DE_{max}	Reactor volume liquefaction [m^3]	Saccharification reactor productivity [kg / m^3 min]	Reactor volume saccharification [m^3]
A	35	96	33	1.07	119
B	60	92	17	1.22	94
C	65	91	16	1.25	90

Based on the results described in the previous sections, the following processes are proposed, assuming a production rate of 10 ton glucose per hour. It should be noted that the production of 10 ton / h glucose syrup requires the hydrolysis of 9 ton starch only, as a result of the chemical gain. In process A, with a dry matter content of 35%, the flow of the reaction mixture was calculated to be 6 l/s. The density of the reaction mixture was calculated using a linear mixing rule, based on the starch and water fractions. Starch is gelatinised and enzymatic hydrolysed simultaneously in a thermal treatment at 105 – 110 °C. After the gelatinisation, the starch paste is cooled and maintained at 95 °C for 90 minutes in a holding tank to complete liquefaction [3], which yields a volume for the holding tank of almost 33 m^3 at a flow rate of 6 l/s. The kinetic equations shown in appendix I were used to estimate the reaction time for obtaining the highest DE for the saccharification step, which was found to be 327 min for these specific conditions. The calculated reactor volume was 120 m^3 for the saccharification reaction. Also for process B, a thermal treatment with a short residence time could be applied to gelatinise the starch completely. Because less water is transported in process B, the

volumetric flow rate of the reaction mixture is reduced to 3.2 l/s in this process, resulting in a required volume of the holding tank of 17 m^3, assuming that the reaction rate during liquefaction was not influenced by the starch concentration. The reactor size for the subsequent saccharification was estimated to be 95 m^3, taking a reaction time of 488 min. for the saccharification reaction. This reaction time was calculated using the kinetic equation described in appendix I. In process C, a combination of an extruder and static mixer can be used to completely liquefy starch. The melting process requires a residence time in the order of seconds in the shearing section of the extruder. The total volume of the static mixer to liquefy starch completely is estimated to be 16 m^3 at a flow rate of 2.9 l/s. The reactor volume for saccharification was calculated to be 90 m^3 given a reaction time of 519 min.

The calculations show that the required reaction volume decreased with increased dry matter contents for a given production rate. The volumetric reactor productivity, which is defined as the average conversion rate per reactor volume, increased with 17% when the dry matter content was increased from 30 to 65% (table 3). The effect of the increased dry matter content was partly counterbalanced by an increased reaction time. In total, increasing the dry matter content from 35% to 65% leads to an increased utilisation of current assets of 17%.

Besides the improved volumetric productivity, the driver towards high dry matter contents is the reduced consumption of energy. In the current industrial processes, excess water is removed by evaporation. We assume that the final glucose syrup contains 80% glucose and 20% water. Then it can be calculated that the excess water is reduced with 78% and 87% respectively, starting with 60% and 65% dry matter compared to 35%. So, the water consumption is reduced and more importantly the energy consumption can be decreased drastically. Increasing the dry matter content from 60% to 65% results in even higher savings, although also more practical difficulties are involved leading to some additional investments and larger process modifications.

5. Conclusions

It was experimentally demonstrated that the hydrolysis of starch to glucose can be carried out in new operating conditions, with substrate concentrations up to 65%. Temperature ranges and processing time are comparable to current industrial starch hydrolysis processes.

The increase in substrate concentration in this process leads to a number of advantages: reduced energy consumption, reduced water consumption and the improved utilisation of

current assets of 17%. The main drawback of starch hydrolysis in high dry matter conditions is the increased formation of isomaltose, which can lead to 8% of the dry matter content. At very high substrate concentrations, gelatinisation by heating alone is not sufficient; a shearing treatment becomes necessary to obtain complete gelatinisation. It was shown that can be done efficiently and with high throughput.

Acknowledgement

Reference List

1   Marchal, L. M. and Tramper, J. (1999) Hydrolytic gain during hydrolysis reactions: Implications and correction procedures. *Biotechnology Techniques*, 13, 325 - 328.

2   Reeve, A. (2004) Starch hydrolysis: Process and Equipment. 79 - 120.

3   Fullbrook, P. D. (1984) The enzymatic production of glucose syrups. 65 - 115.

4   Donovan, J. W. (1979) Phase transitions of the starch - water system. *biopolymers*, 18, 263-275.

5   Souza, R. C. R. and Andrade, C. T. (2001) Investigation of the gelatinization and extrusion processes of cron starch. *Advances in Polymer Technology*, 21, 17 - 24.

6   Barron, C., Bouchet, B., Valle, G. della, Gallant, D. J., Planchot, V. (2001) Microscopical study of the destructuring of waxy maize and smooth pea starches by shear and heat at low hydration. *Journal of Cereal Science*, 33, 289 - 300.

7   Govindasamy, S., Campanella, O. H., Oates, C. G. (1997) Enzymatic hydrolysis of sago starch in a twin-screw extruder. *Journal of Food Engineering*, 32, 403 - 426.

8   Linko, P and Linko, Y. Y (1983) Extrusion cooking and bioconversions. *Journal of Food Engineering*, 2, 243 - 257.

9   Roussel, L., Vieille, A., Billet, I., Cheftel, J. C. (1991) Sequential heat gelatinisation and enzymatic hydrolysis of corn starch in an extrusion Reactor. optimisation for a maximum dextrose equivalent. *Food science and Technology*, 24, 449 - 458.

10   Zuilichem, D. J., Roekel, G. J., Stolp, W., Riet, K. van't (1990) Modelling of enzymatic conversion of cracked corn by twin-screw extrusion cooking. *Journal of Food Engineering*, 12, 13-28.

11   Grafelman, D. D. and Meagher, M. M. (1995) Liquefaction of starch by single screw and post extrusion static mixer reactor. *Journal of Food Engineering*, 24, 529 - 542.

12   Veen, M. E. van der, Iersel, D. I., Goot, A. J. van der, Boom, R. M. (2005) Shear induced inactivation of α-amylase in a plain shear field. *Biotechnology Progress*, 20 (4), 1140-1145

13   Komolprasert, V and Ofoli, R. Y. (1990) Effect of shear on thermo-stable α-amylase activity. *Food science and Technology*, 23, 412 - 417.

14   Linko, P, Mercier, C., Colonna, P. (1981) High-temperature short-time extrusion cooking. *Advances in Cereal science and technology*, 4, 145 - 235.

15   Linko, P, Hakulin, S., Linko, Y. Y (1983) Extrusion cooking of barley starch for the production of glucose syrup and ethanol. *Journal of Cereal Science*, 1, 275 - 284.

16   Reinikainen, P., Suortti, T., Olkku, J., Malkki, R, Linko, P (1986) Extrusion cooking in enzymatic liquefaction of wheat starch. *Starch*, 38, 20 - 26.

17   Chouvel, H., Chay, P. B., Cheftel, J. C. (1983) Enzymatic hydrolysis of starch and cereal flours at intermediate moisture contents in a continuous extrusion reactor. *Food science and Technology*, 16, 346 - 353.

18   Likimani, T. A., Sofos, J. N., MAga, J. A., Harper, J. M. (1991) Extrusion cooking of corn/soybean mix in presence of thermo stable α-amylase. *Journal of Food Science*, 56, 99-105.

19   Curic, D, Karlovic, D, Tripalo, B, Jezek, D (1998) Enzymatic conversion of corn starch in twin screw extruder. *Chem.Biochem.Eng.*, 12, 63 - 71.

20   Pandey, A (1995) Glucoamylase research: an overview. *Starch*, 47, 439 - 445.

21   Roels, J. A. and Tilburg, R. van (1979) Kinetics of reactions with amyloglucosidase and their relevance to industrial applications. *Starch*, 31, 338 - 345.

22   Meagher, M. M. and Reilly, P. J. (1989) Kinetics of the hydrolysis of di- and trisaccharides with *Aspergillus Niger* glucoamylase I and II. *Biotechnology and Bioengineering*, 43, 689 - 693.

23   Nikolov, Z. L., Meagher, M. M., Reilly, P. J. (1989) Kinetics, equilibrium and modeling of the formation of oligosaccharides from d-Glucose with *Aspergillus niger* Glucoamylase I and II. *Biotechnology and Bioengineering*, 34, 694 - 704.

24   Cepeda, E., Hermosa, M., Ballosteros, A. (2001) Optimization of maltodextrins hydrolysis by glucoamylase in a batch reactor. *Biotechnology and Bioengineering*, 76, 70 - 76.

25   Bruins, M. E., Hellemond, E. W. van, Janssen, A. E. M., Boom, R. M. (2003) Maillard reactions and increased enzyme inactivation during oligosaccharide synthesis by a hyperthermophillic glucosidase. *Biotechnology and Bioengineering*, 81, 546 - 552.

26   Veen, M. E. van der, Goot, A. J. van der, Boom, R. M. (2005) Glucose production in highly concentrated systems. *Accepted for Publication in Biotechnology Progress*,

27   Einde, R. M. van den, Bolsius, A., Soest, J. J. G. van, Janssen, L. P. B. M., Goot, A. J. van der, Boom, R. M. (2004) The effect of thermomechanical treatment on starch breakdown and the consequences for process design. *Carbohydrate Polymers*, 55, 57 - 63.

28   Flory, P. J. (1953) Molecular size and chemical reactivity; Principles of condensation polymerisation. 69 - 105.

29   Schenk, F. W. (2002) Starch hydrolysates – An Overview *International Sugar Journal*, 82-89.

30   Tester, R. F. and Sommerville, M. D. (2001) Swelling and enzymatic hydrolysis of starch in low water systems. *Journal of Cereal Science*, 33, 193 - 203.

31   De Cordt, S., Hendrickx, M., Maesmans, G, Tobback, P. (1994) The influence of polyalcohols and carbohydrates on the thermo-stablity of α-amylase. *Biotechnology and Bioengineering*, 43, 107 - 114.

32   Beschkov, V., Marc, A, Engasser, J. M. (1984) A kinetic model for the hydrolysis and synthesis of maltose, isomaltose and maltotriose by glucoamylase. *Biotechnology and Bioengineering*, 26, 22 - 26.

Summary

Introduction and aims

This thesis covers two topics, both aimed at improving process efficiency and product quality in starch processing. The first topic covers the potential use of microwaves as means for mild preservation for granular materials (chapter 2). The second topic focuses on intensification of the starch hydrolysis process (chapter 3, 4 and 5).

Preservation of granular materials

Different materials show different susceptibilities to microwave radiation. A heterogeneous material consisting of more than one phase may therefore show different rates of heating in domains with different composition. It might be expected that when a heterogeneous matrix contains domains containing more moisture than the surrounding matrix, bacteria will preferentially be present in those domains. It has been hypothesized further, that bacteria themselves can be regarded as very small domains that have more moisture than their surroundings. One of the proposed routes for preservation has been to heat such a material quickly by microwave radiation. In this way the domains or bacteria containing more moisture are heated more quickly than the product matrix. When the temperature in the domain achieves a value needed for inactivation, the field is removed (the product removed from the reactor). If the heating is sufficiently quick, the product matrix has not yet been heated to the same extend and the total thermal load on the product remains lower than with uniform heating. We studied this concept of selective heating in a microwave field in heterogeneous food media through analysis of dissipation of microwave energy and heat transfer phenomena in heterogeneous systems.

We derived an approximate analytical solution to describe the absorption of microwave energy in heterogeneous systems. Calculations based on Mie-scattering showed that for spherical food particles of 5 mm and smaller, the electric field inside the object was constant (i.e. not attenuated). For this condition, we derived an analytical solution from which the energy dissipation could be calculated for a spherical particle surrounded by an infinite continuous medium, using the dielectric properties of both materials and the electric field strength in the continuum. Calculations showed that the difference in energy dissipation depended strongly on the absolute and relative properties of both media. A remarkable situation occurred when a water droplet was supposed to be dispersed in a dry starch environment. The calculations showed, contrary to what is generally believed, that the dry starch heated faster than the water droplet. This was explained by reflection and diffraction phenomena. In other situations, e.g. saline water droplet in water, a maximum difference in

heating rate of a factor 4 could be obtained. Subsequently, we evaluated whether this factor 4 difference in heating rates was sufficient to obtain selective heating in case of a spherical particle that heats faster than its environment. Using an average particle temperature, we derived an approximate analytical solution describing the dynamics of the heating process. It was shown that during the microwave treatment, the temperature difference between both phases increased, until a semi steady state is reached where the heat transfer from the dispersed phase equals the difference in rate of heating of both phases. From that moment, the temperature difference remains constant, while the temperature of the total system still increases. The maximum temperature difference that can be achieved depends strongly on the radius of the dispersed phase. In case of spheres having a radius in the order of micrometers, only small temperature differences could be obtained ($<$ 1K) with current microwave intensities. For spheres having a radius in the order of millimetres, the possible temperature difference could increase to 10 or 100 K; also the time necessary to reach the semi-steady state increases from seconds in the micrometer range to minutes at the scale of a centimetre.

Relations were derived that give the typical power densities needed to selectively heat a domain, as function of the domain size. From these relations, it is clear that preservation of granular materials by means of selective heating of individual bacteria is not likely to occur since a moist droplet in a dry environment will not heat faster and secondly the size of a micro-organism is too small to maintain a significant temperature difference due to fast heat transfer. It was finally shown that use of pulsed microwave fields might help to significantly reduce the typical domain size that can be selectively heated.

Towards process intensification of starch hydrolysis

The second topic covered in this thesis concerns reduction of water usage during enzymatic hydrolysis of corn starch to glucose syrups. The starch hydrolysis process comprises several stages, from which 2 reaction stages are most relevant for the final product properties: liquefaction and saccharification. In the first stage, starch is gelatinised in excess water by a thermal treatment and simultaneously hydrolysed to maltodextrins by a thermo-stable α-amylase. In the second step, the liquefact is hydrolysed further to glucose by glucoamylase. In current industrial starch hydrolysis processes, 80% of the water added is excess water; the rest is consumed during the reaction or is part of the final product, which generally contains 80% dry matter. Reducing the water concentration introduces some implications, such as achieving a significant degree of gelatinisation, handling and mixing of highly viscous pastes, maintaining enzyme activity and stability and control of product

composition. In this thesis a study of these aspects of processing concentrated streams are reported.

Liquefaction

The first step of the liquefaction process is gelatinisation of starch, in which starch is disclosed from its granular structure, melted completely and thus becomes available for hydrolytic action and accessible for catalysts, either acid or enzymes. According to literature, starch can be gelatinised completely by means of a thermal treatment only in conditions with at least 40% moisture. The melting temperature was reported to increase at lower moisture content towards temperatures at which α-amylase is rapidly inactivated. However, shear forces are reported to enhance gelatinisation at temperatures below the melting temperature. In this project, a newly developed pilot-scale shearing device was used to study the effect of plain shear forces on gelatinisation of starch in low moisture conditions. The shear stresses achieved were up to almost 70 kPa, which is comparable to stresses applied during extrusion. The crystallinity of several samples that were exposed to a shearing treatment, were analysed by X-ray diffraction. It was found that the minimal shear stress necessary to completely melt the starch, indeed is a function of the moisture content en temperature. Increasing the moisture content or temperature resulted in lower shear forces necessary to completely melt starch. In experimental conditions with maximally 37% moisture and 110 °C, a shear stress of around exceeding 30 kPa resulted in complete gelatinisation.

In current industrial starch hydrolysis processes, thermo-stable α-amylase is added to the starch slurry before gelatinisation. As mentioned above, shear forces have to be applied in low water conditions to achieve complete melting of the starch, which might also lead to enzyme inactivation. Therefore, shear induced inactivation of thermo-stable α-amylase was studied in pilot scale shearing device. It was found that shear-induced inactivation of α-amylase was a function of the shear stress applied onto the enzyme, the temperature and, to a lesser extent, the exposure time. Remarkably, hardly any irreversible inactivation occurred at shear stresses of 25 kPa and lower. However, when exceeding this threshold value, the enzyme is rapidly deactivated. It was further found that α-amylase can be active in conditions up to 70% dry matter. It was observed that the enzyme started to hydrolyse the starch as soon as starch was disclosed from its granular structure. The hydrolytic activity resulted in a lower shear stress, leading to incomplete gelatinisation of starch in presence of α-amylase.

The results described above led to the conclusion that two distinct regions for starch liquefaction can be identified. At a moisture level higher than 40%, starch can be melted completely by a thermal treatment in conditions, where α-amylase is still thermo-stable at

reasonable timescales. The liquefaction can thus be carried out in a single step. At moisture contents below 40%, the starch melting temperature increases rapidly. To achieve complete gelatinisation, shear has to be applied. Experiments showed that the shear forces necessary to gelatinise the starch exceed the shear stability of the enzyme, which leads to significant enzyme inactivation. To circumvent this problem, a 2-stage liquefaction process at conditions with less than 40% moisture was proposed. In the first step, the starch is melted completely by a thermo-mechanical treatment that can be fast. Then α-amylase can be added to complete the liquefaction at conditions where the enzyme is both thermally and shear stable. In this way, fast liquefaction can be achieved under very low water conditions.

Saccharification

The second reaction stage in the production of glucose syrups is the hydrolysis of the liquefied starch to glucose. In this study, the effect of concentration and composition of the substrate as well as the effect of type of the catalyst on some final product properties was investigated, using a newly developed fast differential method.

The experimental results show that maltose is completely hydrolysed to glucose, by glucoamylase. The hydrolysis reactions is followed by a slow condensation reaction, leading to the formation of side-products. The product composition obtained with acid catalysis was much more complex due to many reactions possible under these conditions. Increased substrate concentrations leads to an increased formation of condensation products, both in quantity as the length of the polymer. The maximum average degree of polymerisation (d.p.) of acid catalysed reactions was 1.7, while only an average d.p. of 1.15 was found in case of enzyme catalysed reactions (both starting with 65% dry matter). The difference between both catalysts can be explained by the difference in their selectivity. Glucoamylase is a more selective catalyst, which results in the formation of less by-products. The large difference in reaction rate of the side-reactions of both catalysts shows that the reactions are kinetically controlled. In case of the enzymatic catalysed system, the composition of the product after reaction was found to be independent of the starting material, being either glucose, maltose of maltodextrins. This leads to the conclusion that the glucose yield of glucoamylase-catalysed reactions is only affected by reaction time and substrate concentration. Furthermore it was found that the rate of the hydrolysis reaction is higher than the rate of the condensation reaction, which leads to an optimum in the glucose concentration in time. At the maximum glucoe concentration, still a significant can concentration of unreacted maltodextrins is present, which leads to a lower glucose yield.

Kinetic models from literature could be used to describe the hydrolysis and condensation reactions for glucoamylase catalyzed reactions. The hydrolysis model was based on Michaelis Menten kinetics with competitive inhibitions. The model could be used to describe the hydrolysis kinetics very well from a range of 30 to 70% dry matter, after adjusting the inhibition constant to 8.9 kmole kg^{-1}. The kinetics of the consecutive condensation reactions were described assuming the reaction being an equilibrium reaction. In addition to the model described in literature, we added the enzyme concentration to correct for differences in enzyme activity. The condensation model was used to describe the condensation reaction up to DP4. The combination of all kinetic equations satisfactorily described the dynamics of the hydrolysis of maltodextrins in highly concentrated conditions.

Based on all results presented in chapter 3, 4 and 5 we concluded that it is possible to hydrolyse starch to glucose in conditions up to at least 65% initial dry matter. Increasing the dry matter content from 35% to 65% already results in a decrease of water consumption of 87%, for a given glucose production. This lower water consumption results in lower energy costs because of less water removal and less fresh water consumption. Furthermore, existing equipment could be used more efficiently, which is a cost benefit as well. The reactor productivity was calculated to increase with 17%, starting with a dry matter content of 65% instead of 35%. This can be explained by the reduction in volume, as water is being replaced by starch, which has a higher density then water. Though a part of the volume saving is necessary to correct for the higher reaction times at higher dry matter. These findings were used in conceptual designs of a two stage (< 60% DS) and a three-stage process (>60% DS), which shows the feasibility of low water conditions. Figure 1 represents the mass flow through the process in case of 65% dry matter initially. It can be seen that the amount of water that needs to be removed in the final concentration step is very small compared to that in the current process. (The representation of the current process can be found in Chapter 1, of this thesis, figure 4).
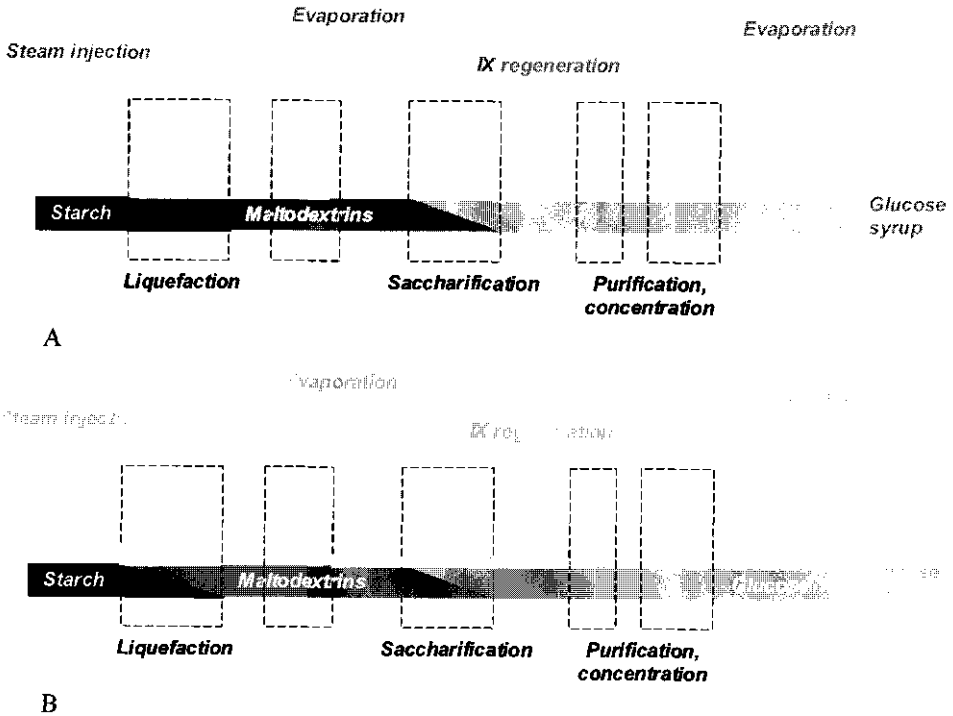
Figure 1: Schematic representation of the mass flow of water and starch in the current process (A) and for conditions of 65% D.M. starch initially (B) (representation inspired on Sankey-diagrams for enthalpy flows).

Concluding remarks

The aim of this thesis was to explore the possibilities of reducing the amount of water in the glucose production process. The results outlined in this thesis show that it is possible to increase the dry matter content up to 70% dry matter. However, before successful introduction, a number of additional issues have to be addressed. Most important is complete gelatinisation at low moisture content. Since the formation of side-products is more pronounced at high dry matter conditions, the development of a more selective enzyme could be useful in case product quality becomes an issue. Furthermore, an assessment should be made of the consequences of using low moisture content during purification. It is clear however that there is potential for making the production processes discussed more efficient in terms of energy and water usage.

Samenvatting

Introductie en doelstelling:

Dit proefschrift omvat 2 onderwerpen, welke beide gericht zijn op verbetering van efficiëntie van zetmeelconversieprocessen en productkwaliteit. Het eerste onderwerp gaat over de mogelijkheid om magnetrontechnologie toe te passen als middel voor milde conservering voor heterogene (disperse) materialen (Hoofdstuk 2). Het tweede onderwerp is het intensiveren van het zetmeelhydrolyseproces (Hoofdstuk 3, 4 en 5).

Conservering van heterogene (disperse) materialen

Het doel van het eerste onderwerp was het onderzoeken van de mogelijkheid om magnetronstraling toe te passen om op een milde manier heterogene levensmiddelen te conserveren. Verschillende materialen hebben een verschillende gevoeligheid voor magnetronstraling en zullen daarom met verschillende snelheid opwarmen. Het is daarom waarschijnlijk dat een heterogeen materiaal verschillende opwarmingssnelheden in verschillende gebieden kan hebben. Het wordt verondersteld dat in een product waarbij het water niet homogeen verdeeld is over het product, de bacteriën zich voornamelijk in de vochtigere gebieden zullen bevinden. Een veronderstelde route voor milde conservering is om het product snel op te warmen met magnetronstraling. Als de opwarming snel en selectief genoeg is, zal de temperatuur van de vochtigere gebieden hoger zijn dan van de rest van het product, wat zal leiden tot minder kwaliteitsverlies dan in conventionele thermische conservering. Dit concept van selectieve verwarming is bestudeerd door analyse van de opname van magnetronenergie en de warmteoverdrachtsverschijnselen in heterogene voedselcomponenten (Hoofdstuk 2).

Dit is gedaan door een combinatie van de Mie-theorie voor verstrooiingsverschijnselen en een benadering voor de tijdsafhankelijke warmteoverdracht van de disperse fase naar de omringende matrix via geleiding Berekeningen laten zien dat het verschil in energiedissipatie strek afhankelijk is van de relatieve en absolute eigenschappen van beide media om magnetronenergie om te zetten in warmte. Een opmerkelijke situatie ontstaat in het geval een waterdruppel in een droge zetmeel omgeving is gedispergeerd. In dit geval zal het zetmeel, door reflectie- en refractieverschijnselen, sneller opwarmen dan de waterdruppel, in tegenstelling tot wat algemeen wordt aangenomen. In andere situaties, bijvoorbeeld van een zout water druppeltje in water, kan een verschil in opwarmingssnelheid van maximaal een factor vier worden bereikt. Onderzocht is of deze factor vier voldoende is om een significant temperatuursverschil te krijgen tussen het gedispergeerde deeltje en het product. Hiervoor hebben we een analytische oplossing afgeleid om het temperatuursverschil tussen beide fasen

te kunnen beschrijven. Het kon worden aangetoond dat het temperatuursverschil tussen beide fasen groter werd gedurende de magnetron behandeling, tot een situatie is bereikt waarna beide fasen even snel opwarmen. Vanaf dat moment zal het temperatuursverschil constant blijven, maar de temperatuur van het totale systeem zal blijven toenemen.

De resultaten van dit onderzoek leidden tot de conclusie dat milde conservering van granulaire materialen door middel van selectieve verwarming onwaarschijnlijk is op de schaal van individuele micro-organismen, omdat een natte druppel in een droge omgeving niet sneller zal opwarmen. Bovendien zal er geen groot temperatuursverschil kunnen ontstaan door de snelle warmte overdracht van de bacterie naar het product.

Intensivering van zetmeel hydrolyse

Het tweede onderwerp dat in dit proefschrift beschreven is, is het reduceren van de waterstromen, die gebruikt worden in de productie van glucosestroop uit zetmeel. Glucose is een belangrijke grondstof voor de levensmiddelenindustrie en wordt onder andere gebruikt voor de productie van frisdranken, bakkerijproducten en snoepgoed. Daarnaast worden glucose en andere kleine suikers gebruikt als grondstof bij fermentatieprocessen, voor de productie van alcohol en andere producten. Zetmeel is opgebouwd uit glucosemonomeren en kan door middel van een hydrolysereactie, die gekatalyseerd wordt door een zuur of een enzym worden afgebroken tot glucose. Deze hydrolyse wordt op grote schaal in de levensmiddelenindustrie toegepast.

Het zetmeelhydrolyse proces bestaat uit verschillende processtappen, waarvan de twee reactieve processtappen het meest belangrijk zijn: vervloeiing en versuikering. In de eerste stap wordt zetmeel verstijfseld in een grote hoeveelheid water door middel van een gelijktijdige thermische behandeling en een enzymatisch hydrolyse met een thermo-stabiel enzym: α-amylase. In de tweede stap wordt het vervloeide zetmeel door het enzym glucoamylase verder gehydrolyseerd tot glucose. Tijdens de hydrolysereactie wordt een klein deel van het water in het hydrolyseproduct ingebouwd en wordt deel van het eindproduct. Daarnaast is een klein deel van het water aanwezig in het eindproduct (glucosestroop dat gemiddeld 20% water bevat). Dit is samen slechts twintig procent van de totale hoeveelheid water die aan het begin van het proces aanwezig is. Tachtig procent van het water is in overmaat aanwezig en moet dus aan het einde van het proces worden verwijderd. Het verwijderen van water gaat door middel van verdamping en kost veel energie. Het toevoegen van minder water aan het begin van het proces leidt tot hogere concentraties gedurende het proces en dat heeft grote invloed op het verloop van het proces. Het zetmeel kan niet volledig verstijfselen, de oplossingen zullen hoogvisceus zijn en het mengen en transporteren van de

stomen wordt gecompliceerder. De stabiliteit van enzymen kan onder die omstandigheden niet voldoende zijn, hetgeen kan leiden tot een lagere activiteit van de enzymen. Daarnaast kan de samenstelling van de producten ook worden beïnvloed door ongewone omstandigheden. In dit proefschrift wordt een studie van deze aspecten van het processen van geconcentreerde stromen beschreven.

Vervloeiing

De eerste stap van het vervloeiingsproces is verstijfseling van zetmeel, waarbij het zetmeel wordt ontsloten uit zijn granulair structuur en geheel wordt gesmolten waardoor het beschikbaar komt voor de hydrolysereactie met zuren of enzymen. Volgens literatuurgegevens kan zetmeel geheel verstijfseld worden door een thermische behandeling met minimaal 40% vocht, bij temperaturen waarbij α-amylase nog stabiel is. Bij lagere vochtgehaltes stijgt de verstijfselingstemperatuur tot temperaturen waarbij α-amylase snel wordt geactiveerd. In de literatuur is beschreven dat door afschuifkrachten op het zetmeel uit te oefenen, de effectieve temperatuur waarbij het zetmeel verstijfseld kan worden verlaagd. In dit project is een nieuw ontwikkelde apparatuur gebruikt om deze effecten van afschuifspanningen op het verstijfselen van zetmeel bij lage vochtgehaltes te bestuderen en te kwantificeren. De resultaten zijn beschreven in hoofdstuk 5. Het bleek dat de minimale afschuifspanning die noodzakelijk is om het zetmeel geheel te verstijfselen, een functie is van het vochtgehalte en de temperatuur. Verhogen van de temperatuur en het vochtgehalte resulteert in een lagere minimale afschuifspanning, die noodzakelijk is om het zetmeel geheel te verstijfselen.

In huidige industriële zetmeel hydrolyse processen wordt thermo-stabiel α-amylase toegevoegd aan de zetmeelslurry voordat het verstijfselingsproces aanvangt. Als de slurry een hoge concentratie zetmeel bevat, zal de viscositeit hoog zijn en zullen forse afschuifkrachten worden uitgeoefend tijdens het proces. In de literatuur is beschreven dat een hoge afschuifspanning kan leiden tot inactivatie van het enzym. Hoofdstuk 3 beschrijft de effecten van afschuiving op de inactivatie van het enzym bestudeerd in dezelfde apparatuur als eerder beschreven. Het bleek dat de inactivering van α-amylase als gevolg van uitgeoefende afschuifspanning beschreven kon worden als een eerste-orde proces, waarvan de effectieve activeringsenergie sterk verminderde als functie van de afschuifspanning. Er is vrijwel geen irreversibele inactivatie gevonden bij afschuifspanningen lager dan 25 kPa. Echter, zodra de spanning groter wordt dan 25 kPa, wordt het enzym snel geactiveerd. Verder bleek dat α-amylase actief kan zijn onder condities met 70% droge stof. Als het α-amylase wordt toegevoegd voordat de verstijfseling (en de afschuifbehandeling wordt gestart, wordt het zetmeel direct gehydrolyseerd, zodra het uit zijn granulaire structuur ontsloten wordt. Deze

97

snelle hydrolyse leidt tot lagere afschuifspanningen. Aan de ene kant zorgt dat ervoor dat het enzym ruimschoots actief kan blijven; aan de andere kant betekenen lagere afschuifspanningen dat de verstijfseling bij dezelfde temperatuur niet volledig is.

Hieruit kon de conclusie getrokken worden dat er 2 gebieden zijn voor zetmeelverstijfseling. Bij vochtgehaltes groter dan veertig procent kan zetmeel geheel worden verstijfseld door een thermische behandeling waarbij α-amylase stabiel is gedurende een behandeltijd van enkele minuten. De vervloeiing kan dan dus in 1 stap worden uitgevoerd. Bij vochtgehaltes lager dan veertig procent stijgt de verstijfselingstemperatuur snel en moet afschuiving toegepast worden om het zetmeel bij redelijke temperatuur geheel te verstijfselen. De spanningen die noodzakelijk zijn om het zetmeel geheel te verstijfselen zijn groter dan het enzym kan weerstaan, wat zal leiden tot snelle inactivering van het enzym. Dit dilemma kan omzeild worden door de vervloeiing in twee stappen uit te voeren. In de eerste stap kan zetmeel geheel worden verstijfseld door een thermo-mechanische behandeling (toepassen van afschuifspanning bij hoge temperatuur). Dit is een snel proces. Na het verstijfselen kan α-amylase worden toegevoegd om het zetmeel te hydrolyseren. Op deze manier kan een snelle vervloeiing bij ultralage vochtgehaltes worden bereikt.

Versuikering

De tweede reactieve fase van de glucosestroop-productie is de verdere hydrolyse van het vervloeide zetmeel tot glucose. In hoofdstuk 4 is het effect onderzocht van de concentratie en de samenstelling van het substraat en van het type katalysator (zuur of enzym) op de samenstelling van het eindproduct. Daarbij is gebruik gemaakt van een nieuwe snelle differentiële.

Tijdens de enzymatische hydrolyse reactie wordt maltose (2 glucosemoleculen) geheel gehydrolyseerd tot glucose. Deze omzetting wordt gevolgd door een veel tragere vorming van bijproducten via condensatie. Het product van een zuur gekatalyseerde reactie is veel complexer dan wanneer een enzym wordt gebruikt. Gebruik van hogere substraat concentraties (en dus lagere waterconcentraties) leidt tot de vorming van meer condensatieproducten, zowel in de hoeveelheid als in de lengte van de polymeren. De maximale gemiddelde graad van polymerisatie die gemeten is voor de zuurgekatalyseerde experimenten is 1.7, bij de enzymatische experimenten is deze slechts 1.15. Het verschil tussen beide katalysatoren kan worden verklaard door het verschil in selectiviteit van beide katalysatoren. Glucoamylase is een veel selectievere katalysator dan zuur, wat resulteert in de vorming van minder bijproducten. Het grote verschil tussen de snelheid van de zijreacties tussen beide katalysatoren laat zien dat de reacties kinetisch gecontroleerd zijn. Bij de

enzymatische gekatalyseerde reacties bleek de samenstelling van het product onafhankelijk te zijn van de substraatsamenstelling (glucose, maltose of maltodextrines). Dat betekent dat de glucoseopbrengst voor glucoamylase gekatalyseerde reacties alleen beïnvloed wordt door de reactietijd en de substraatconcentratie. Verder blijkt dat de hydrolysereactie sneller is dat de condensatiereactie. Dit resulteert in een optimum van de glucose concentratie in de tijd. Op dit glucose-maximum is echter nog wel een significante hoeveelheid maltodextrines aanwezig. Dit wat resulteert in een lagere opbrengst van glucose.

Een aantal modellen uit de literatuur is toegepast om de hydrolyse en condensatie-reacties in het glucoamylase-gekatalyseerde systeem te beschrijven (hoofdstuk 4). Het hydrolyse-model is gebaseerd op Michaelis-Menten kinetiek met competitieve inhibitie en is gebruikt om de hydrolyse kinetiek van 30 – 70% droge stof te beschrijven. De kinetiek van de vervolgreacties (condensatie) wordt beschreven met de aanname dat de reactie een evenwichtsreactie is. Het model uit de is literatuur aangepast door er een term voor de enzymconcentratie aan toe te voegen. Dit model is gebruikt om de condensatie te beschrijven tot een polymerisatie graad van 4. De combinatie van alle kinetische vergelijkingen blijkt de dynamiek van de hydrolyse reactie van maltodextrines in hoog geconcentreerde systeem goed te kunnen beschrijven.

De resultaten in hoofdstukken 3 en 4 leiden tot de algemene conclusie dat het mogelijk is om zetmeel geheel te hydrolyseren in systemen met minimaal 65% droge stof. Het verhogen van het drogestofgehalte van 35% naar 65% levert een waterbesparing van 87% op voor een gegeven hoeveelheid geproduceerd glucose. Deze lagere waterconsumptie resulteert in een energiebesparing, doordat minder water hoeft worden te verwijderd en minder vers water gebruikt hoeft te worden. Verder kan bestaande procesapparatuur efficiënter worden gebruikt. De reactorproductiviteit (doorzet pet m^3 reactorvolume) neemt met 17% toe bij een initiële droge stof concentratie van 65% in plaats van 35%. Deze bevindingen zijn gebruikt voor het conceptuele ontwerp van twee processen: een twee- stapsproces (<60% droge stof) en een drie-stapsproces (60-70% droge stof) Deze ontwerpen zijn beschreven in hoofdstuk 5 en illustreren de haalbaarheid van het gebruik van laag water condities. Figuur 1 laat zien dat de massastroom water door het nieuwe proces veel kleiner is in vergelijking met die in het huidige proces (Hoofdstuk 1, figuur 4)
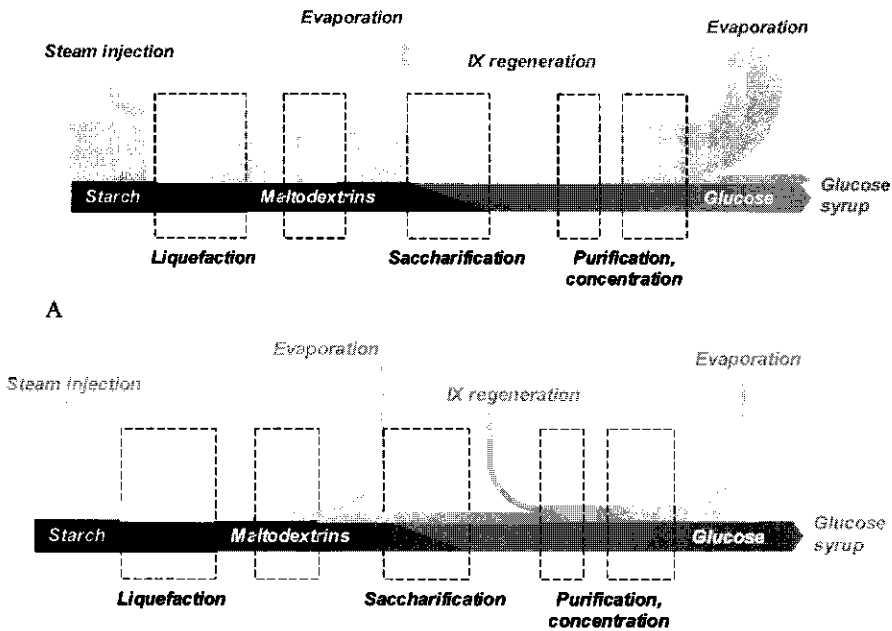
Figuur 1:Schematische weergave van de massa stromen van water en zetmeel met initieel 65% droge stof zetmeel (representatie geïnspireerd door Sankey diagrammen voor energie stromen)

Tot slot

Het doel van het onderzoek dat in dit proefschrift wordt beschreven was het onderzoeken van de mogelijkheid om de hoeveelheid water in het glucose productie proces te verminderen. De resultaten laten zien dat het waarschijnlijk mogelijk is het droge stof gehalte te verhogen tot rond 70% droge stof. Er is echter nog wel een aantal aandachtspunten voordat het proces succesvol geïntroduceerd kan worden. Het belangrijkste is dat het zetmeel geheel verstijfseld dient te worden bij lage vochtcondities. Aangezien de vorming van bijproducten sterker is bij hoge droge stof gehaltes, zal de ontwikkeling van een reactiesysteem dat de selectiviteit kan vergroten (bijvoorbeeld een membraanreactor of een meer selectief enzym) van belang zijn als de productkwaliteit te zeer onder druk komt te staan. Verder zullen de consequenties van het gebruik van hoge droge stof gehaltes gedurende de zuiveringsstappen onderzocht moeten worden. Het is echter wel duidelijk dat er potentieel is om de bestudeerde processen meer efficiënt te maken in termen van energie en watergebruik en zo bij te dragen een het effectiever en efficiënter gebruikmaken van de natuurlijke hulpbronnen.

Nawoord

Het zit er op! Hoewel de afrondende fase iets langer heeft geduurd dan gepland, is het nu klaar. Ik kijk terug op een periode waarin ik met veel plezier aan het onderzoek heb gewerkt en die voor mij synoniem staat voor leren, groei en vorming.

Echter, het uitvoeren van een promotieonderzoek is geen individueel project. Hierbij wil ik dan ook iedereen bedanken, die een bijdrage heeft geleverd aan het onderzoek en een paar mensen in het bijzonder. Allereerst Atze Jan, bedankt voor de mogelijkheid die je me hebt geboden om dit onderzoek te doen en de goede begeleiding; de vele inhoudelijke discussies en de persoonlijke gesprekken op de momenten dat het iets minder ging. Je hebt me gestimuleerd om te schrijven, me geleerd om dingen af te maken en mijn eigen onderzoek te waarderen. Samen met je enthousiasme en je gedrevenheid, maakt je dat tot een goede coach! Remko, je positieve benadering, enthousiasme en ideeën tijdens onze besprekingen waren voor mij erg motiverend en hebben ervoor gezorgd dat ik altijd weer vol inspiratie aan de slag kon en ging. Belangrijke dingen die ik van je heb geleerd zijn de filosofische kant van het onderzoek en de kracht van modellen om een systeem beter te leren begrijpen en doorgronden. Bedankt voor de fijne samenwerking.

Uiteraard is ook dank verschuldigd aan Cargill, de sponsor van dit project. Theo, geweldig dat je altijd actief meedacht en veel ideeën had, hoewel dat ons nog wel eens voor de uitdaging stelde om het gezamenlijke doel voor ogen te houden. Johan, als tegenpool van Theo hield altijd het wetenschappelijk doel van het project in het oog, wat ik als erg prettig heb ervaren. Sarah, bedankt voor de goede begeleiding en je kritische, opbouwende commentaar op de artikelen.

Ook binnen de universiteit zijn er een aantal mensen, die hun bijdrage geleverd hebben aan dit onderzoek. Allereerst Kees Vriezinga, Henk Schols en Rijkelt Beumer. Kees, je hebt ons geholpen om theoretisch inzicht te krijgen in de weerbarstige materie van de magnetron. Henk, bedankt voor de prettige en openhartige discussies over suikerchemie. Rijkelt, je hebt me een introductie gegeven in de wereld van de microbiologie. Helaas heeft onze samenwerking niet tot een publicatie geleid, maar desondanks heb ik veel van je geleerd. Pieter, de vele experimenten met de magnetron hebben ons geholpen om de link tussen theorie en praktijk te leggen. Ik hoop dat er een rustige periode voor je aanbreekt en wens jullie samen veel sterkte voor de toekomst. Jos en Maurice, bedankt voor jullie hulp tijdens het opstarten en onderhouden van de HPLC's. Bliksem Piebe, Gerrit, pc's maken jou niet gek! Gelukkig had je 2 assistenten op 615, waar je af en toe eens binnen kon lopen tijdens je kennismaking met Windows 2000...

Zonder de studenten, die hun afstudeeronderzoek bij mij hebben uitgevoerd, zou dit boekje niet geworden zijn wat het nu is. René, had je 4 jaar geleden gedacht dat je onderwijs geven leuk zou vinden? Marin, je enthousiasme straalde overal door. Julita, je bent ook AIO geworden op een erg interessant onderwerp. Veel succes met je onderzoek! Noortje, je had een lastig onderwerp, maar je hebt het goed opgepakt en je onderzoek heeft ons geïnspireerd voor hoofdstuk 2. Jasper, extruderen was je grote hobby en dat hebben we geweten. Daan, je had een lastige start, maar uiteindelijk hebben prachtige metingen de basis gelegd voor hoofdstuk 3.

Het sociale microklimaat op de kamer werd gevormd door Ed, Anneke, René en later Sandra. Ed, zoals je zelf schreef in je proefschrift, hebben we veel lol gehad. Maar je kan ook goed luisteren en relativeren en je was daardoor een goed klankbord hetgeen in hectische tijden erg prettig was. Ik heb veel van je geleerd en ben blij dat je mijn paraminf wilt zijn. Anneke, de combinatie sociaal en collegiaal maakt je tot een fijne collega en het was fijn om deze vier jaar met je te delen. René, zetmeel en lichte chaos zijn de dingen die als eerste bij me opkomen. Maar ik heb je leren kennen als iemand met veel humor en die toegewijd is aan zijn onderzoek. Het was prettig om met je samen te werken op het gebied van zetmeel en de afbraak daarvan. Sandra, ondanks de verschillen tussen onze onderwerpen was het altijd gezellig op de kamer. Veel succes met het laatste stuk van je onderzoek. Even verderop in de gang zat Jeroen. Jeroen, het is fijn om een collega te hebben die oprecht geïnteresseerd is in het onderzoek van zijn collega's en daarnaast ook om gewoon koffie te drinken met de bijbehorende niet-wetenschappelijk praat. We hebben een geweldige tijd gehad in Zuid-Afrika, veel gelachen en de gebruikelijke braai op z'n tijd. (Big-5 is een biertje!) Ik ben daarom blij dat ook jij mijn paranimf wilt zijn. Daarnaast wil ik alle andere collega's van de vakgroep bedanken voor de fijne periode die ik in Wageningen heb gehad, wat onder andere geleid heeft tot een geweldige sfeer tijdens de AIO-reizen naar Polen en Zuid-Afrika.

Uiteraard familie en vrienden; ik ben blij met de mensen in mijn omgeving, die geïnteresseerd zijn in datgene wat mij bezighoud. Met name pap en mam, bedankt voor jullie oprechte interesse en jullie luisterend oor tijdens de minder florissante tijden van het onderzoek.

Lieve Ingrid, als laatste wil ik jou bedanken voor je begrip en geduld als ik weer achter de pc kroop om de laatste stukken te schrijven, ten koste van onze spaarzame vrije tijd. Zonder jouw morele steun was het nooit gelukt om ook de laatste hobbels te nemen. Nu is het klaar en is het tijd om samen te genieten!

Mark

Curriculum vitae

Mark van der Veen werd geboren op 10 juni 1974 geboren te Groningen. In 1991 behaalde hij zijn HAVO diploma aan het Nienoordcollege te Leek. In datzelfde jaar begon hij zijn studie Chemische Technologie aan de Hanzehogeschool van Groningen. Hij liep stage bij Akzo Nobel Central Research te Arnhem en DSM-Andeno te Venlo. Hij studeerde in juni 1996 af op een afstudeeropdracht, uitgevoerd bij Gist-brocades (thans DSM) te Delft. Aansluitend, juli 1996 tot mei 1997 was hij werkzaam bij Gist-brocades te Delft. Van mei 1997 tot november 1999 was hij werkzaam bij Unilever Research te Vlaardingen. Van november 1999 tot december 2003 was hij werkzaam als Assistent In Opleiding bij de sectie proceskunde aan Wageningen Universiteit, waar het onderzoek, zoals beschreven in dit proefschrift, werd uitgevoerd. Vanaf april 2004 in Mark van der Veen werkzaam als proces modelleur bij Cargill B.V. te Bergen op Zoom.